

- 1 **CCSP Synthesis and Assessment Product 1.2**
- 2 **Past Climate Variability and Change in the Arctic and at High Latitudes**
- 3
- 4 **Chapter 5. Temperature and Precipitation History of the Arctic**
- 5
- 6 **Chapter Lead Authors:** Gifford H. Miller, University of Colorado and
- 7 Julie Brigham-Grette, University of Massachusetts
- 8 **Contributing Authors:**
- 9 Lesleigh Anderson, U.S.Geological Survey
- 10 Henning Bauch, GEOMAR, University of Kiel
- 11 Mary Anne Douglas, University of Alberta
- 12 Mary E. Edwards, University of Southampton
- 13 Scott Elias, Royal Holloway, University of London
- 14 Bruce Finney, University of Alaska-Fairbanks
- 15 Svend Funder, University of Copenhagen
- 16 Timothy Herbert, Brown University
- 17 Larry Hinzman, University of Alaska-Fairbanks
- 18 Darrell Kaufman, University of Northern Arizona
- 19 Glen MacDonald, University of California-Los Angeles
- 20 Alan Robock, Rutgers University
- 21 Mark Serreze, University of Colorado
- 22 John Smol, Queen's University
- 23 Robert Spielhagen, GEOMAR, University of Kiel

24 Alexander P. Wolfe, University of Alberta

25 Eric Wolff, British Antarctic Survey

26

26 **ABSTRACT**

27 The Arctic has undergone dramatic changes in temperature and precipitation during the
28 Cenozoic Era, the past 65 million years (Ma) of Earth history. Arctic temperature
29 changes during this time exceeded global average temperature changes during both warm
30 times and cold times, supporting the concept of Arctic amplification in which strong
31 positive feedbacks, processes that amplify a change caused by a change in the controls on
32 global temperature, produce larger changes in temperature across the Arctic. Warm times
33 in the past, those periods when the Arctic was either mildly or substantially warmer than
34 present, provide important constraints on future warming in the Arctic. Past warm times
35 are rarely ideal analogues of future warming because the forcings in the past that led to
36 exceptional warmth were often different than the forcings expected in the coming
37 decades. Nevertheless, paleoclimate records help to define the climate sensitivity of the
38 planet, and to quantify Arctic amplification.

39 At the start of the Cenozoic, 65 million years (Ma) ago, the planet was ice-free;
40 there was no Arctic Ocean sea ice, and neither a Greenland nor Antarctic ice sheet.
41 General cooling through the Cenozoic is attributed mainly to a slow decrease in
42 greenhouse gases in the atmosphere. As the Arctic cooled, high elevation mountain
43 glaciers formed as well as seasonal sea ice in the Arctic Ocean, but a detailed record of
44 changes in the Arctic is only available for the last few million years. A global warm
45 period in the middle Pliocene, about 3.5 Ma ago, is well represented in the Arctic, when
46 extensive deciduous forests occupied lands now only capable of supporting polar desert
47 tundra. A significant reorganization of global oceanic and atmospheric circulation
48 occurred between 3 and 2.5 Ma ago, accompanied by the development of the first

continental ice sheets over North America and Eurasia, with icebergs from these ice sheets delivering rock fragments into the central North Atlantic Ocean. This change marks the onset of the Quaternary Period (2.6 to 0 Ma ago), generally equated with “ice-age” time. From ~2.7 to ~0.8 Ma ago, the ice sheets came and went about every 41 thousand years (ka), the same timing as changes in the tilt of Earth’s axis, with ice sheets growing when Earth’s tilt was at a minimum, and melting when tilt was at a maximum. For the past 800 ka, ice sheets have grown larger and ice age times have been longer, lasting ~100 ka, separated by brief warm periods of ~10 ka duration. The cause of this shift remains debated. The relative warm times over which human civilization has developed is during the most recent of these 10 ka warm intervals, the Holocene (~11.5 to 0 ka ago). The penultimate warm interval, ~130 to 120 ka ago, occurred when solar energy in summer was greater than at any time in the current warm interval. As a consequence, the Arctic was ~5 °C warmer than at present, and almost all glaciers melted completely, except the Greenland Ice Sheet, which was reduced in size substantially from its present extent. Although sea ice is difficult to reconstruct, the available evidence suggests that the central Arctic Ocean retained a permanent ice cover, even though the flow of warm Atlantic water into the Arctic Ocean may have been greater than during the present warm interval.

The last glacial maximum peaked about 20 ka ago when the Arctic was ~20 °C colder than present. Ice recession was well underway by 16 ka ago, and most of the Northern Hemisphere ice sheets melted by 7 ka ago. Solar energy in summer rose steadily from 20 ka to a maximum (10% higher than at present) 11 ka ago, and has been decreasing since then, as the precession of the equinoxes has tilted the Northern

Hemisphere farther from the sun in summer. The extra energy received in summer in the early Holocene resulted in warmer summers throughout the Arctic, ranging from 1 to 3 °C above 20th Century averages, enough to completely melt many small glaciers throughout the Arctic, although Greenland was only slightly smaller than present. Summer sea ice limits were significantly less than their 20th Century average, and the flow of Atlantic water into the Arctic Ocean was substantially greater. As summer solar energy decreased in the second half of the Holocene, glaciers re-established or advanced, sea ice became more extensive, and the flow of warm Atlantic water into the Arctic Ocean became reduced. Late Holocene cooling reached its nadir during the Little Ice Age (~1250 to 1850 AD), when most Arctic glaciers reached their maximum Holocene extent. Warming over the past century has resulted in Arctic-wide glacier recession, the northward advance of terrestrial ecosystems, and the reduction of perennial Arctic Ocean sea ice.

Paleoclimate reconstructions of Arctic temperatures compared to global temperature changes during four key intervals over the past 4 Ma allows a quantitative estimate of Arctic amplification. These data suggest that Arctic temperature change is 3 to 4 times the global average temperature change during both cold and warm departures. This relation indicates that Arctic temperatures are likely to increase dramatically over the next century if global warming forecasts are correct.

5.1 Introduction

Recent instrumental records show that temperatures across much of the far north have risen more rapidly over the last few decades than in lower latitudes, and often about twice as fast

(Delworth and Knutson, 2000; Knutson et al., 2006). The remarkable reduction in Arctic Ocean summer sea ice in 2007 (**Fig. 5.1**) has outpaced the most recent predictions from available climate models (Stroeve et al., 2008), but is in concert with widespread reductions in glacier length, increased borehole temperatures, increased coastal erosion, changes in vegetation and wildlife habitats, the northward migration of marine life, and permafrost degradation. Based on the current trend of increasing greenhouse gases over the past century, climate models forecast continuing warming into the foreseeable future (**Fig. 5.2**) and a continuing amplification of global signals in the Arctic (Serreze and Francis, 2006). As outlined by the Arctic Climate Impact Assessment (ACIA, 2004), the sensitivity of the Arctic to changed forcing is due to strong positive feedbacks in the Arctic climate system (see Chapter 4.3). These feedbacks produce large amplification of changes to the climate of the Arctic, while also having impacts on the global climate system.

Because the strong Arctic feedbacks act on climate changes caused by nature or by humans, natural variability and human-caused changes are large in the Arctic, and separating them requires understanding and characterization of the natural variability. The short time interval over which instrumental data are available from the Arctic is not sufficient to characterize that natural variability, so a paleoclimatic perspective is required.

This chapter focuses primarily on the history of temperature and precipitation in the Arctic. These are important in their own right, and set the stage for understanding the histories of the Greenland ice sheet and the Arctic sea ice, which are described in chapters 7 and 8. Because of the great interest in rates of change, and because of some technical details in extracting rate of change from the broad history of temperature or precipitation, careful consideration of rates of change is deferred to chapter 6.

Before providing the history of temperature and precipitation in the Arctic, this chapter supplements the discussion in chapter 4 on forcings, feedbacks, and proxies by providing additional information on those aspects particularly relevant to the histories of temperature and precipitation in the Arctic. The climate history of the past 65 Ma is then summarized, focusing on temperature and precipitation changes that span the full range of the Arctic's natural climate variability and response under different forcings. Special emphasis has been placed on relevant intervals in the past with a mean climate state warmer than our own. Where possible, causes of the changes are discussed. From these summaries, it is possible to estimate the magnitude of polar amplification, and to characterize the response of the Arctic system to global warm times.

5.2 Feedbacks Influencing Arctic Temperature and Precipitation

The most commonly used measure of the climate is the mean surface air temperature (**Fig. 5.3**), which is influenced by climate forcings and climate feedbacks. As discussed with references in Chapter 4.3, important forcings over the past several millennia have been changes in the distribution of solar radiation that resulted from features of Earth's orbit, changes in solar irradiance, volcanism, and changes in atmospheric greenhouse-gas concentrations. On longer time scales (tens of millions of years), the long-term increase in the solar constant (30% increase in the past 4600 Ma) was important, and the redistribution of continental landmasses caused by plate tectonics also affected the planetary energy balance.

How much the temperature changes in response to a forcing of a given magnitude (or in response to the net magnitude of a set of forcings in combination) depends on the sum of all of the feedbacks. Feedbacks may act in days or less, or over millions of years. The focus here is on the faster ones. For example, a warming may have many causes (brighter sun, higher concentration of greenhouse gases in the atmosphere, less blocking of the sun by volcanoes, etc.). Whatever the cause, warmer air moving over the ocean tends to entrain more water vapor, which itself is a greenhouse gas, so having more water vapor in the atmosphere leads to a further rise in global mean surface temperature (Pierrehumbert et al., 2007). The discussion below focuses on those feedbacks that are especially linked to the Arctic. We include several processes linked to ice-age cycling here, because of the dominant role of northern land in supporting ice-sheet growth, although ice-age processes (like some of the other processes discussed below) clearly extend well beyond the Arctic.

5.2.1 Ice-albedo feedback

Ice and snow present highly reflective surfaces. The albedo of a surface is defined as the reflectivity of that surface to the wavelengths of solar radiation. Fresh ice and snow have the highest albedo of any widespread surfaces on the planet (**Fig. 5.4**), so it is apparent that changes in the seasonal and areal distribution of snow and ice will exert strong influences on the planetary energy balance (Peixoto and Oort, 1992). Open ocean, on the other hand, has a low albedo, absorbing almost all of the solar energy when the sun angle is high. Changes in albedo are most important in Arctic summer, when solar radiation is at a maximum, whereas changes in the winter albedo have little influence on

the energy balance because little solar radiation reaches the surface then. In general, warming reduces ice and snow whereas cooling allows them to be more extensive, so the changes in ice and snow act as positive feedbacks to amplify climate changes (e.g., Lemke et al., 2007).

5.2.2 Ice-insulation feedback

In addition to its effects on albedo, sea ice also causes a positive insulation feedback, primarily in the wintertime. Ice is effective at blocking heat transfer between relatively warm ocean (at or above the freezing point) and cold atmosphere (which, in the Arctic winter, averages -40 °C (Chapman and Walsh, 2007). If sea ice is removed by warming, then the ocean heats the overlying atmosphere in winter months, amplifying warming.

Feedbacks involving snow insulation of the ground may also be important, through their effects on vegetation and on permafrost temperature and its influence on storage or release of greenhouse gases, as described in the next subsections (e.g., Ling and Zhang, 2007).

5.2.3 Vegetation feedbacks

A related terrestrial feedback involves changing vegetation. A warming climate can result in a transition from tundra to shrub vegetation. However, the shrub vegetation has a lower albedo than tundra, causing further warming (**Fig. 5.5**) (Chapin et al., 2005; Goetz et al., 2007). Interactions involving the boreal forest and deciduous forest can also be important (Bonan et al., 1992; Rivers and Lynch, 2004).

5.2.4 Permafrost feedbacks

Additional but poorly understood feedbacks in the Arctic involve changes in cloud cover and the release of carbon dioxide from the land surface associated with changing extent of permafrost. Feedbacks between permafrost and climate became widely recognized only in recent decades, building on the works of Kvenvolden (1988; 1993), MacDonald (1990) and Haeberli et al. (1993). As permafrost thaws under a warmer climate (**Fig. 5.6**), CO₂ and methane trapped in permafrost can be released to the atmosphere (e.g., Vörösmarty, 2001; Smith et al. 2004, Thomas et al, 2002, Archer, 2007). Since CO₂ and methane are greenhouse gases, atmospheric temperature is likely to increase in turn, a positive feedback.

5.2.5 Freshwater balance feedbacks and thermohaline circulation

The Arctic Ocean is almost completely surrounded by continents (**Fig. 5.7**). Because precipitation is low over the ice-covered ocean (Serreze et al., 2006), the freshwater input is largely controlled by the runoff from large rivers in Eurasia and North America, and the inflow of relatively low-salinity Pacific water through the Bering Strait. The Yenisey, Ob, and Lena are among the nine largest rivers on Earth, and there are several other large rivers, including the Mackenzie, entering the Arctic Ocean (see Vörösmarty et al., 2008). The freshwater discharged by these rivers maintains low salinities on the broad, shallow, and seasonally ice-free seas bordering the Arctic Ocean. The largest of these border the Eurasian continent, where they serve as the dominant production areas of sea ice in the Arctic Ocean (for some fundamentals on Arctic sea ice,

see Barry et al., 1993). Sea ice formed along the Eurasian margin drifts toward Fram Strait, with a transit time of 2-3 years in the current regime. In the Amerasian part of the Arctic Ocean, the clockwise rotating Beaufort Gyre is the dominant ice-drift feature (see **Fig. 8.1**). However, the transport pathway for most of the freshwater entering the Arctic Ocean is the surface layer (the upper 50 m) of the Arctic Ocean (e.g., Schlosser et al., 2000). Low-salinity surface waters are exported from the Arctic Ocean to the northern North Atlantic (Nordic Seas) through western Fram Strait, after which they follow the east coast of Greenland and exit the Nordic Seas through Denmark Strait. A smaller outflow of freshwater occurs through the inter-island channels of the Canadian Arctic Archipelago, eventually reaching the North Atlantic via the Labrador Sea. The low-saline outflow from the Arctic Ocean is compensated by a relatively warm inflow of saline Atlantic water through eastern Fram Strait. Despite its warmth, Atlantic water has sufficient density due to its high salinity that it is forced to sink beneath the colder, but much fresher surface water upon entering the Arctic Ocean. North of Svalbard, Atlantic water spreads as a boundary current into the Arctic Basin, forming the Atlantic Water Layer (Morison et al. 2000). The strong vertical gradients of salinity and temperature in the Arctic Ocean result in a relatively stable stratification. However, recent observations have shown that in some areas in the Eurasian part of the Arctic Ocean, the warm Atlantic layer is in direct contact with the surface mixed layer (Rudels et al., 1996; Steele and Boyd, 1998; Schauer et al., 2002), thereby promoting vertical heat transfer to the Arctic atmosphere in winter. In recent decades circum-Arctic glaciers and ice sheets have been losing mass (more snow and ice melting in summer than accumulates as snow in winter; Dowdeswell et al., 1997; Rignot & Thomas, 2002; Meier et al., 2007), and river

runoff to the Arctic Ocean has been increasing since the 1930s (Peterson et al., 2002). These factors have led to increased freshwater export from the Arctic Ocean (Peterson et al., 2006). Recent studies suggest that changes in river runoff play an important role in the stability of Arctic Ocean stratification (Steele and Boyd, 1998; Martinson and Steele, 2001; Björk et al., 2002; Boyd et al., 2002; McLaughlin et al., 2002; Schlosser et al., 2002).

In the north Atlantic, primarily in the Nordic Seas and the Labrador Sea, wintertime cooling of the relatively warm and salty waters leads to density increase causing sinking of waters that then flow southward to participate in the global thermohaline circulation (“thermo” for temperature and “haline” for salt, the two components that determine density; this circulation system also is often referred to as the meridional overturning circulation or MOC). Continuing surface flow from the south replaces the water sinking in the Nordic and Labrador Seas, causing persistent open water rather than sea-ice cover in these regions. In turn, this lack of sea ice causes notably warmer conditions especially in wintertime over and near the North Atlantic and extending downwind across Europe and beyond (Seager et al., 2002). Salt rejected from sea ice growing nearby also may contribute to density increase and water sinking.

If the surface waters are made sufficiently less salty by an increase in freshwater from runoff, ice melt, or direct precipitation, the rate of sinking of those surface waters will diminish or stop (e.g., Broecker et al., 1985). Results of numerical models indicate that an increased freshwater runoff into the Arctic Ocean and the North Atlantic, along with a warming of surface waters in the northern high latitudes, will weaken the

thermohaline circulation in the north Atlantic, with consequences for marine ecosystems and energy transport (e.g., Rahmstorf, 1996, 2002; Marotzke, 2000; Schmittner, 2005).

Reducing the rate of North Atlantic thermohaline circulation may have global as well as regional effects (e.g., Obata, 2007). Oceanic overturning is an important mechanism for transferring atmospheric CO₂ to the deep ocean. Reducing the rate of deep convection in the ocean would result in a higher proportion of anthropogenic produced CO₂ remaining in the atmosphere. Similarly, a slowdown in thermohaline circulation would influence the turnover of nutrients from the deep ocean, with potential consequences across the Pacific Ocean.

5.2.6 Feedbacks over glacial-interglacial cycles

The growth and melting of immense ice sheets, which at their peak size covered ~30% of the modern land area including the modern sites of New York and Chicago, were paced by the orbital variations often called Milankovitch forcings (e.g., Imbrie et al., 1993), and described in chapter 4. There is little doubt that the orbital forcings drove this glacial-interglacial cycling, but there is a remarkably rich and varied literature on the detailed mechanisms (see, e.g., Roe, 1999).

The generally accepted explanation of the glacial-interglacial cycling is that ice sheets grew when limited summer sunshine at high northern latitudes allowed survival of accumulated snow, with melting when high summer sunshine in the north melted the ice. The north is more important than the south because the Antarctic has remained ice-covered during this cycling of the last million years and more, and there is no other high-latitude land in the south on which ice sheets could grow.

278 The increased reflectivity from expanded ice contributed to cooling. This is the
279 ice-albedo feedback as described above, but with slower response controlled by the flow
280 of the great ice sheets. The ice ages also experienced more atmospheric dust than did the
281 intervening warm interglacials, with the additional ice-age dust contributing to cooling by
282 blocking sunlight. Ice-sheet growth and the orbital changes led to complex changes in
283 the ocean-atmospheric system that shifted carbon dioxide from the air to the ocean,
284 lowering the atmospheric greenhouse effect. The carbon-dioxide changes lagged the
285 orbital forcing, and so carbon dioxide was clearly a feedback, but the large global cooling
286 of the ice ages has been successfully explained only if the reduced greenhouse effect is
287 included (Jansen et al., 2007.) By analogy, overspending a credit card induces debt,
288 which is made larger by interest payments on that debt. The interest payments clearly lag
289 the debt in time, did not cause the debt, but contribute to the size of the debt, and the debt
290 cannot be explained quantitatively unless the interest payments are included.

291 Abrupt climate changes have been associated with the ice-age cycles. The most-
292 prominent and best-known of these are linked to jumps in the wintertime extent of sea ice
293 in the north Atlantic, which in turn were linked to changes in the large-scale circulation
294 of the ocean (e.g., Alley, 2007), as described in the previous section. The associated
295 temperature changes were very large around the north Atlantic (to 10°C or more) but
296 much smaller in remote regions, and exhibited an opposite sign in the far south (so
297 northern cooling was accompanied by slight southern warming); hence, the globally
298 averaged temperature changes were small, probably linked primarily to ice-albedo
299 feedback and small changes in the strength of the greenhouse effect. As reviewed by
300 Alley (2007), the large ice-age ice sheets seem to have been important in these abrupt

swings both by triggering them, and by creating conditions under which triggering was easier; although such events may remain possible, they are less likely without the large ice sheet on Canada.

5.2.7 Arctic Amplification

The positive feedbacks outlined above amplify the Arctic response to climate forcings. The ice-albedo feedback is potentially strong in the Arctic because so much snow and ice occur there (see Serreze and Francis, 2006 for additional discussion); if conditions are too warm for any snow to form, there can be no ice-albedo feedback. Climate models initialized from modern or similar conditions and forced in various ways are in widespread agreement that global temperature trends are amplified in the Arctic, with the largest changes over the Arctic Ocean during the cold season (autumn through spring) (e.g., Manabe and Stouffer, 1980; Holland and Bitz, 2003; Meehl et al., 2007). Summer changes over the Arctic Ocean are relatively damped, although summer changes over Arctic lands may be substantial (Serreze and Francis, 2006). The strong wintertime changes over the Arctic Ocean are linked to the insulating character of sea ice.

Think first of an unperturbed climate. During summer, solar energy is used to melt the sea ice cover. As the ice cover melts, areas of open water are exposed. The albedo of the open water areas is much lower than that of sea ice, so the open water areas gain heat. Since much of the solar energy goes into ice melt and warming the ocean, the surface air temperature does not rise much, and indeed, over the melting ice, stays fairly close to the freezing point. Through autumn and winter, when there is little or no solar

energy, this ocean heat is released back to the atmosphere. There is a further release of heat back to the atmosphere from the formation of sea ice itself.

However, if the climate warms (e.g., through the effects of higher greenhouse gas concentrations) the summer melt season lengthens and intensifies, meaning more areas of low-albedo open water in summer to absorb solar radiation. With more heat gained in the upper ocean, more heat is released back to the atmosphere in autumn and winter, expressed as a rise in air temperature. Furthermore, with more heat in the ocean, the ice that forms in autumn and winter is thinner than before. This thinner ice is more easily melted in summer, meaning even more low-albedo open water areas to absorb solar radiation, meaning even larger releases of heat to the atmosphere in autumn, even thinner ice the next spring, and so on. The process can also work in reverse. An initial Arctic cooling means less summer melt and a smaller area covered by low-albedo open water. With a smaller summer heat gain in the ocean, there is less heat released back to the atmosphere in autumn and winter, meaning a further fall in air temperatures.

While the albedo feedback over the ocean seems to dominate, there is also an albedo feedback over land which is much more direct. Under a warming climate, one expects an earlier spring snowmelt period, meaning earlier exposure of low-albedo tundra, shrub, and forest cover, fostering further spring warming. Similarly, later formation of autumn snow cover will foster further autumn warming. With more snow-free days, there is a longer period for surface warming, implying warmer summers. Again, the process can work in reverse, where initial cooling leads to more snow cover, fostering further cooling. Collectively, these processes result in stronger net positive

feedbacks to forced temperature change (regardless of forcing mechanism) than typical globally, thereby producing “arctic amplification”.

Over longer times, growth of an ice sheet such as the Laurentide ice sheet on Canada, or melting of an ice sheet such as that on Greenland, can occur. This in turn can influence albedo, freshwater fluxes to the ocean, broad patterns of atmospheric circulation, greenhouse-gas storage or release in the ocean, and more.

5.3 Proxies of Arctic Temperature and Precipitation

Temperature and precipitation are especially important climate variables. Climate change is typically driven by changes in key forcing factors, which are then amplified or retarded by regional feedbacks that impact temperature and precipitation (section 5.2 and 4.2). Because feedbacks exhibit strong regional variability, spatially variable responses to hemispherically symmetric forcing are common across the Arctic (e.g., Kaufman et al., 2004). Consequently, spatial patterns of temperature and precipitation must be reconstructed regionally.

Reconstructing temperature and precipitation in pre-industrial times requires reliable proxies (see section 4.4 for a general discussion of proxies) that can be used to derive qualitative, or preferably, quantitative estimates of past climates. To capture the expected spatial variability, proxy climate reconstructions must be spatially distributed and span a wide range of geological time. In general, a multi-proxy approach to reconstructing past climates provides the most robust evidence for past changes in temperature and precipitation.

5.3.1 Proxies for Reconstruction of Temperature

5.3.1a Vegetation/pollen records

Estimates of past temperature from data that describe the distribution of vegetation (primarily fossil pollen assemblages but also plant macrofossils such as fruits and seeds) may be relative (warmer/colder) or quantitative (number of degrees of change). Most information pertains to the growing season, as plants are dormant in the winter and so less influenced by climate than during the growing season (but see below). For example, evidence of boreal forest vegetation (indicated by the presence of one or more boreal tree species) would be associated with warmer growing seasons than evidence of treeless tundra—and the general position of northern treeline approximates today to the location of the July 10 °C isotherm.

Indicator species are species with well-studied and relatively restricted modern climatic ranges. The appearance of these species in the fossil record indicates that a certain climatic milestone was reached, such as exceeding a minimum summer temperature threshold for successful growth or a winter minimum temperature of freezing tolerance (**Fig. 5.8**). This methodology was developed early for Scandinavia (Iversen, 1944); Matthews et al. (1990) used indicator species to constrain temperatures during the last interglaciation in northwest Canada, and Ritchie et al. (1983) used indicator species to highlight early Holocene warmth in northwest Canada. The technique has been used extensively with fossil insect assemblages.

Methodologies for the numerical estimation of past temperatures from pollen assemblages follow one of two approaches. The first is the inverse-modeling approach, in which fossil data from one or more localities are used to provide temperature estimates

for those localities (this approach also underlies the relative estimates of temperature described above). A modern ‘calibration set’ of data (in this case pollen assemblages) is related to observed modern temperature by equations, and the functions thus obtained are then applied to fossil data. This method has been developed and applied in Scandinavia (e.g., Seppä et al. 2004). A variant of the inverse approach is analogue analysis, in which a large modern dataset with assigned climate data forms the basis for comparison with fossil spectra. Good matches are derived statistically, and the resulting set of analogues provides an estimate of the past mean temperature and accompanying uncertainty (Anderson et al. 1989, 1991).

Inverse modeling relies upon observed modern relationships. In the past, some plant species occurred in abundances that are not observed today, and the fossil pollen spectra they produced may have no recognizable modern counterpart—so-called ‘no-analogue’ assemblages. Outside the envelope of modern observations, fossil pollen spectra, described in terms of pollen abundance, cannot be reliably related to past climate. This problem led to the adoption of a second approach to estimating past temperature (or other climate variables) called forward modeling. The pollen data are not used to develop numerical values but are used to test a ‘hypothesis’ about the status of past temperature (climate). The hypothesis may be a conceptual model of the status of past climate, but typically it is represented by a climate-model simulation for a time in the past. The climate simulation drives a vegetation model that assigns vegetation cover on the basis of bioclimatic rules (such as the winter minimums or required level of summer growing temperatures mentioned above). The resultant map is compared with a map of past vegetation developed from the fossil data. The philosophy of this approach is described

by Prentice and Webb (1998). Such data-model comparisons have been carried out for the Arctic by Kaplan et al (2003) and Wohlfahrt et al. (2004). The great advantage of this approach is that underlying the model simulation are hypothesized climatic mechanisms; this allows not only the description but also an explanation of past climate changes.

5.3.1b Marine Isotopic records The oxygen isotope composition of planktic foraminifera accurately record the oxygen isotope composition ($\delta^{18}\text{O}$: the proportion of the heavy isotope, ^{18}O , relative to the lighter, more abundant isotope, ^{16}O) of ambient seawater, modulated by the temperature at which the organisms build their calcareous shells (Epstein et al., 1953; Shackleton, 1967; Erez and Luz, 1982; **Fig. 5.9**). However, the low horizontal and vertical temperature variability found in Arctic Ocean surface waters ($<-1^{\circ}\text{C}$) has little effect on the oxygen isotope composition of *N. pachyderma* (sin.) (max. 0.2‰, according to Shackleton, 1974). Since meteoric waters, discharged into the ocean by precipitation and (indirectly) by river runoff, have considerably lower $\delta^{18}\text{O}$ values than do ocean waters, an excellent correlation exists between salinity and oxygen isotopic composition of Arctic surface waters (Bauch et al., 1995). Accordingly, the spatial variability of surface water salinity across the Arctic Ocean is recorded today by the $\delta^{18}\text{O}$ of planktic foraminifers (Spielhagen and Erlenkeuser, 1994; Bauch et al., 1997).

In paleorecords (sediment cores) from the deep Arctic Ocean, significant variability in the $\delta^{18}\text{O}$ values of planktic foraminifera is observed over millennial timescales (e.g., Aksu, 1985; Scott et al., 1989; Stein et al., 1994; Nørgaard-Pedersen et

al., 1998; 2003; 2007a, b; Polyak et al., 2004; Spielhagen et al., 2004; 2005). The observed variability in foraminifera $\delta^{18}\text{O}$ commonly exceeds the change in the isotopic composition of seawater resulting from just the storage of isotopically light freshwater in glacial ice sheets (ca. 1.3‰ $\delta^{18}\text{O}$) on glacial-interglacial time scales (Fairbanks, 1989). Changes over time in freshwater balance of the near-surface waters, and in temperature of those waters, are both recorded in the $\delta^{18}\text{O}$ values of foraminifera shells. Moreover, in cases where independent evidence of a regional warming of surface waters is available (e.g., in the eastern Fram Strait during the last glacial maximum; Nørgaard-Pedersen et al., 2003), this warming is thought to have been caused by a stronger influx of saline Atlantic Water. Because salinity influences $\delta^{18}\text{O}$ of foraminifera shells from the Arctic Ocean more than temperature does, reconstructing temperatures in the past from systematic variations in calcite $\delta^{18}\text{O}$ in Arctic Ocean sediment cores is difficult.

5.3.1c Lacustrine Isotopic Records Isotopic records preserved in lake sediment provide important paleoclimatic information on landscape change and hydrology. Lakes are common in high-latitude landscapes, and continuous sediment deposition provides uninterrupted, high-resolution records of past climate (**Fig. 5.10**).

Oxygen isotopic ratios of precipitation reflect climatic processes, and especially temperature (see 5.3.1d). The oxygen isotope ratios of shells and other materials in lakes primarily reflect ratios of the lake water. The isotopic ratios of the lake water are dominantly controlled by the isotopic ratios of precipitation, unless evaporation from the lake is sufficiently rapid compared to inflow of new water to shift the isotopic ratios towards heavier values by preferentially removing isotopically lighter water. Those lakes

with streams entering and leaving (open lakes) have isotopic ratios that are generally not affected very much by evaporation, as do some lakes supplied only by water flow through the ground (closed lakes), allowing isotopic ratios of shells and other materials in these lakes to be used in reconstructions of climate, especially temperature. However, some closed lakes are affected notably by evaporation, in which case the isotopic ratios of the lake are at least in part controlled by lake hydrology. Unless independent evidence is available on lake hydrology, quantitative interpretation of $\delta^{18}\text{O}$ is difficult. Consequently, $\delta^{18}\text{O}$ is normally combined with additional climate proxies to constrain other variables and strengthen interpretations. For example, in rare cases, ice core records are located near lakes and provide an oxygen isotope record for direct comparison (Fisher et al., 2004; Anderson and Leng, 2004). (**Fig. 5.11**). Oxygen-isotopic ratios are relatively easy to measure on carbonate shells or other carbonate materials. Greater difficulty, limiting accuracy or time-resolution of the records produced, is associated with analyses of oxygen isotopes in silica from diatom shells (Leng et al., 2004) and in organic matter (Sauer et al., 2001; Anderson et al., 2001). Additional uncertainty arises with organic matter because although some of it grew in the lake, some was also washed in and may have been stored on the landscape for some time previously.

5.3.1d Ice cores The most common way to deduce temperature from ice cores (**Fig. 5.12**) is through their water isotopic content, i.e. the ratio of $\text{H}_2^{18}\text{O}/\text{H}_2^{16}\text{O}$, or of $\text{HDO}/\text{H}_2\text{O}$ (where D is deuterium, ^2H). The ratios are expressed as $\delta^{18}\text{O}$ and δD respectively, relative to standard mean ocean water (SMOW). Pioneering studies (Dansgaard, 1964) showed how $\delta^{18}\text{O}$ is related to climatic variables in modern

precipitation. At high latitudes both $\delta^{18}\text{O}$ and δD are generally considered to represent the mean annual temperature at the core site, whereas the use of both measures together offers additional information about conditions at the source of the water vapor (e.g., Dansgaard et al., 1989).

The underlying idea is that an air mass loses water vapor by condensation as it travels from a warm source to a cold (polar) site (**Fig. 5.13**). Water containing the heavy isotopes has a lower vapor pressure, so the heavy isotope preferentially condenses and rains or snows out, causing the air to become progressively more depleted of the heavy isotope as the air mass moves to colder sites. It can easily be shown from spatial surveys (Johnsen et al., 1989) and indeed, from modeling studies using models enabled with water isotopes (e.g., Hoffmann et al., 1998; Mathieu et al., 2002) that a good spatial relationship between temperature and water isotope ratio exists,

$$\delta = aT + b$$

where T is mean annual surface temperature, and δ is annual mean $\delta^{18}\text{O}$ or δD value in precipitation in the polar regions, with the slope, a , having values typically around 0.6 for Greenland for $\delta^{18}\text{O}$.

Temperature is not the only factor that can affect isotopic ratios, however, with changes in the season when snow falls, in the source of the water vapor, and other things potentially important (Jouzel et al., 1997; **Fig. 5.14**). For this reason, it is common whenever possible to calibrate the isotopic ratios using additional paleothermometers. Over short times, instrumental records of temperature can be compared to isotopic ratios (e.g., Shuman et al., 1995). The few comparisons that have been done (summarized in Jouzel et al. (1997) tend to show slightly lower δ/T gradients than the spatial one.

Accurate reconstructions of past temperature, but with low time resolution, are obtained from the use of borehole thermometry. The center of the Greenland ice sheet has not finished warming from the ice age, and the remaining cold temperatures reveal how cold the ice age was (Cuffey et al., 1995; Johnsen et al., 1995). Additional paleothermometers are available using the thermal diffusion effect, whereby gas isotopes are separated slightly when an abrupt temperature change at the surface creates a temperature difference between the surface and the region a few tens of meters down where bubbles are pinched off from the interconnected pore spaces in old snow (called firn). The size of the gas-isotopic shift reveals the size of an abrupt warming, and the number of years between the indicators of an abrupt change in the ice and in the bubbles trapped in ice reveals the temperature before the abrupt change, if the snowfall rate before the abrupt change is known (Severinghaus et al., 1998; Huber et al., 2006; Severinghaus and Brook, 1999). These methods show that the value of the δ/T slope for many of the large changes recorded in Greenland ice cores was considerably less (typically by a factor of 2) than the spatial value, probably because of a relatively larger reduction in winter snowfall in colder times (Cuffey et al., 1995; Werner et al., 2000; Denton et al., 2005). The actual temperature changes were therefore larger than would be predicted from the standard calibration.

In summary, water isotopes in polar precipitation are a reliable proxy for mean annual air temperature, but for quantitative use, some means of calibrating them, either against instrumental data, by using an alternative estimate of temperature change, or through modeling, is always required for samples older than the Holocene.

5.3.1e Fossil Assemblages and Sea Surface Temperatures Different species live preferentially at different temperatures in the modern ocean, and this almost certainly was true in the past. Modern observations can be used to learn the preferences of species. The mathematical expression of these preferences plus the history of where the various species lived in the past can then be used to interpret past temperatures (Imbrie and Kipp, 1971; CLIMAP, 1981). This is primarily applied to near-surface (planktic) species, and especially to foraminifera, diatoms and dinoflagellates. Both the presence or absence, and the relative abundance, of species can be used. Such methods are now commonly supported by sea-surface temperature estimates using emerging biomarker techniques outline below.

5.3.1f Biogeochemistry Over the past decade, two new organic proxies for reconstructing past ocean surface temperature have emerged. Both measurements are based on quantifying the proportions of biomarkers—molecules produced by restricted groups of organisms—preserved in sediments. In the case of the “ $U^{k'}_{37}$ index” (Brassell et al., 1986 ; Prahl et al., 1988), a few closely related species of coccolithophorid algae are entirely responsible for producing the 37-carbon ketones (“alkenones”) used in the paleotemperature index, while crenarcheota (archaea) produce the tetra-ether lipids that make up the TEX_{86} index (Wuchter et al., 2004). Although the specific function that the alkenones and glycerol dialkyl tetraethers serve for these organisms is unclear, the relationship of the biomarker $U^{k'}_{37}$ index to temperature has been confirmed experimentally in the lab (Prahl et al., 1988) and with extensive calibrations of modern

surface sediments to overlying surface ocean temperatures (Muller et al., 1998, Conte et al., 2006, Wuchter et al., 2004).

Biomarker reconstructions have several advantages for reconstructing sea surface conditions in the Arctic. First, in contrast to $\delta^{18}\text{O}$ analyses of marine carbonates (*outlined above*), the confounding effects of salinity and ice volume do not compromise the utility of biomarkers as paleotemperature proxies (a brief discussion of caveats in the use of U^{k}_{37} is given below). Both the U^{k}_{37} and TEX_{86} proxies can be measured reproducibly to high precision (analytical errors corresponding to approximately 0.1°C for U^{k}_{37} and 0.5°C for TEX_{86}), and sediment extractions and gas/liquid chromatographic detections can be automated for high sampling rates. The abundances of biomarkers also provide insights into past ecosystem composition, so that links between the physical oceanography of the high latitudes and carbon cycling can be assessed. And lastly, organic biomarkers can often be recovered in Arctic sediments that do not preserve carbonate or siliceous microfossils. It should be noted, however, that the harsh conditions of the northern high latitudes mean that the organisms producing the alkenone and tetraethers may have been excluded at certain times and places; thus, continuous records cannot be guaranteed.

The principal caveats in using biomarkers for paleotemperature reconstructions come from ecological and evolutionary considerations. Alkenones are produced by algae that are restricted to the region with abundant light (the photic zone), so their paleotemperature estimates apply to this layer, which approximates the sea surface temperature. In the vast majority of the ocean, the alkenone signal recorded by sediments closely correlates with mean annual sea surface temperature (Muller et al., 1998; Conte et

al., 2006; **Fig. 5.15**). However, in the case of highly seasonal high-latitude oceans, the temperatures inferred from the alkenone $U^{k'}_{37}$ index may better approximate summer surface temperatures than mean annual sea-surface temperature. Furthermore, past changes in the season of production could bias long-term time series of past temperatures based on the $U^{k'}_{37}$ proxy. Depending on water column conditions, past production could have been highly focused toward a short (summer?) or a more diffuse (late Spring-early Fall?) productive season. A survey of modern surface sediments in the North Atlantic (Rosell-Mele et al., 1995) shows that the seasonal bias in alkenone unsaturation is not important except at high ($>65^\circ\text{N}$) latitudes (Rosell-Mele et al., 1995). A possible additional complication with the $U^{k'}_{37}$ proxy is that in the Nordic Seas an additional alkenone (of the 37:4 type) is common, although it is rare or absent in most of the world ocean including the Antarctic. The combination of the relatively fresh and cold waters of the Nordic Seas may be affecting alkenone production by the usual species, or may be affecting the mixture of species producing. Regardless, this oddity suggests caution in applying the otherwise robust global calibration of alkenone unsaturation to Nordic-Sea surface temperature (Rosell-Mele and Comes, 1999).

In contrast to the near-surface restriction of the algae producing the $U^{k'}_{37}$ proxy, the marine crenarcheota that produce the tetraether membrane lipids used in the TEX_{86} index can range widely through the water column. *In situ* analyses of particles suspended in the water column show that the tetraether lipids are most abundant in winter and spring months in many ocean provinces (Wuchter et al., 2005) and are present in large amounts below 100 m depth. However, it appears that the chemical basis for the TEX_{86} proxy is fixed by processes that occur in the upper lighted (photic) zone, so that the sedimentary

signal originates near the sea surface (Wuchter et al., 2005), just as for the $U^{k'}_{37}$ proxy. No studies have yet been conducted to assess how high latitude seasonality affects the TEX_{86} proxy.

As for many other proxies, use of these biomarker proxies involves the assumption that the modern relationship between organic proxies and temperature was the same in the past. The two modern (and genetically closely related) species producing the alkenones in the $U^{k'}_{37}$ proxy can be traced back in time in a continuous lineage to the Eocene (~50 Ma ago), and alkenone occurrences coincide with the fossil remains of the ancestral lineage in the same sediments (Marlowe et al., 1984). One might suppose that evolutionary past events in the broad group of algae that includes these species might have produced or eliminated other species generating these chemicals with a different relation to temperature; however, this would cause jumps in climate reconstructions at times of evolutionary events in the group, and no such jumps are observed. The TEX_{86} proxy can be applied to marine sediments 70 to 100 million years old. The working assumption is, therefore, that both organic proxies can be applied accurately to sediments containing the appropriate chemicals.

Because these biomarker proxies depend on changes in relative abundance of chemicals, it is important that natural processes after death of the producing organisms do not preferentially break down one chemical, changing the ratio. Fortunately, this appears to be the case (Prah et al., 1989; Grice et al., 1998; Teece et al., 1998; Herbert, 2003; Schouten et al., 2004). An additional complication is that sediments can be moved around by ocean currents, so that the material sampled at one place was produced in another place with different climatic conditions (Ohkouchi et al., 2002; Thomsen et al., 1998).

Ordinarily, transport of biomarkers to a place is small compared to the supply from the productive ocean above, so that the proxy records local climate. However, at some times and places, the Arctic has been comparatively nonproductive, so that transport from other parts of the ocean, or from land in the case of the TEX₈₆ proxy, may have been important (Weijers et al., 2006).

5.3.1g Biological Proxies in Lakes Lakes and ponds are common in most Arctic regions, and provide useful records of climate change (Schindler and Smol, 2006; Smol and Cumming, 2000; Cohen, 2003; Smol 2008). Many different biological climate proxies are preserved in Arctic lake and pond sediments (Pienitz et al., 2004). Diatom shells (Douglas et al., 2004) and remains of non-biting midge flies (chironomid head capsules; Bennike et al., 2004) are among the most commonly used biological indicators in Arctic paleoclimatic reconstructions (**Fig. 5.16**). The overall approach often used by those who study the history of lakes (paleolimnologists) is first to identify useful species. Then, the modern conditions are determined that are preferred by these indicator species, and the conditions beyond which these indicator species cannot survive (typically using surface sediment calibration sets or training sets, applying statistical approaches such as Canonical Correspondence Analysis and Weighted Averaging regression and calibration; see Birks, 1998). The resulting mathematical relations, or transfer functions (like those used in marine records) are then used to reconstruct the environmental variables of interest based on the distribution of indicator assemblages preserved in dated sediment cores (Smol, 2008). Where well-calibrated transfer functions are not available, including

in some parts of the Arctic, less-precise climate reconstructions are often based on the known ecological and life-history characteristics of the organisms.

Ideally, sedimentary characteristics would be linked directly to key climatic variables such as temperature (e.g., Bennike et al., 2004; Larocque and Hall, 2004; Barley et al., 2006; Pienitz and Smol, 1993; Joynt and Wolfe, 2001; Bigler and Hall, 2003; Weckström et al., 2006; Woller et al. 2004, Finney et al., 2004, and other chapters in Pienitz et al., 2004). However, the lake sediments typically record conditions in the lake which are only indirectly related to climate (Douglas and Smol, 1999). For example, lake ecosystems are strongly influenced by the length of the ice-free versus ice-covered season, by the sun-blocking effect of any snow cover on ice (**Fig. 5.17**) (e.g., Smol, 1988; Douglas et al., 1994; Douglas and Smol, 1999; Sorvari and Korhola, 1998; Sorvari et al., 2002; Rühland et al., 2003; Smol and Douglas, 2007a) and by the existence or absence of a seasonal layer of warm water near the lake surface that remains separate from colder waters beneath (**Fig. 5.18**). Shells and other features in the lake sediment record the species living in the lake and conditions under which they grew, which rather directly reflect the ice- and snow-cover and lake stratification, and only indirectly reflect the atmospheric temperature and precipitation that control the lake conditions.

5.3.1h. Insect proxies. Insects are common, and often are preserved well in Arctic sediment. Because many insect types live only within narrow ranges of temperature or other environmental conditions, the presence of particular insects in old sediments provides useful information on past climate.

Calibrating the observed insect data to climate involves extensive modern and recent studies, together with careful statistical analyses. For example, fossil beetles are often related to temperature using what is known as the Mutual Climatic Range method (Elias et al., 1999; Bray et al., 2006)). This method quantitatively assesses the relations between the modern geographical ranges of selected beetle species and modern meteorological data. A “climate envelope” is determined, within which a species can thrive. When used with paleodata, the method allows for the reconstruction of a range of parameters including mean temperatures of the warmest and coldest months of the year.

5.3.1i Sand Dunes When plant roots anchor the soil, sand cannot blow around to make dunes. In the modern Arctic, and especially in Alaska (**Fig. 5.19**) and Russia, sand dunes are forming and migrating in many places where dry, cold conditions restrict vegetation. During the last glacial interval and at some other times, dunes formed in places that now lack active dunes, indicating colder or drier conditions (Oswald et al., 1999; Carter, 1981; Beget, 2001; Mann et al., 2002). Some wind-blown mineral grains are deposited in lakes. The rate at which sand and silt are deposited in lakes increases as nearby vegetation is removed by cooling or drying, so analysis of the sand and silt in lake sediments provides additional information on the climate (e.g. Briner et al., 2006)

5.3.2 Proxies for Reconstruction of Precipitation

In the case of sand dunes described above, separating the effects of changing temperature versus changing precipitation may be difficult, but additional indicators such as insect

fossils in lake sediments may help by constraining the temperature. In general, precipitation is more difficult to estimate than is temperature, so reconstructions of changes in precipitation in the past are less common, and often less quantitative, than are reconstructions of past temperature changes.

5.3.2a Vegetation-Derived Precipitation Estimates Different plants live in wet and dry places, so indications of past vegetation provide estimates of past wetness. Plants do not respond primarily to rainfall, but instead to moisture availability. This is primarily controlled by the difference between precipitation and evaporation in most places, although some soils carry water downward so efficiently that dryness occurs even without much evaporation.

Much modern tundra vegetation occurs where precipitation exceeds evaporation. Plants such as *Sphagnum* (bog moss), cotton-grass (*Eriophorum*) and cloudberry (*Rubus chamaemorus*) indicate moist growing conditions. In contrast, grasses dominate dry tundra and polar semi-desert. Such differences are evident today (Oswald et al., 2003), and can be reconstructed from pollen and larger plant materials (macrofossils, or “macros”) in sediments. Regions of Alaska and Siberia with sand dunes that formed in the last glacial maximum but are not active today often are near regions which had grasses then but plants requiring greater moisture now (Colinvaux, 1964; Ager and Brubaker, 1985; Lozhkin et al. 1993; Goetcheus and Birks 2001, Zazula et al., 2003).

In arctic regions, snow cover may allow persistence of shrubs that would be killed if exposed during the harsh winter. For example, dwarf willow can survive if snow depths exceed 50 cm (Kaplan et al., 2003). Siberian stone pine requires considerable winter

snow to weigh down its branches and bury them (Lozhkin et al, 2007). The presence of these species therefore indicates certain minimum levels of winter precipitation.

Moisture levels can also be estimated quantitatively from pollen assemblages by means of formal techniques such as inverse and forward modeling, following techniques also used for estimation of past temperatures. Moisture-related transfer functions have been developed, in Scandinavia for example (Seppä and Hammarlund, 2000). Kaplan et al. (2003) compared pollen-derived vegetation with vegetation derived from model simulations for the present and key times in the past. The pollen data indicated that model simulations for the Last Glacial Maximum tended to be “too moist”—the simulations generated shrub-dominated biomes whereas the data indicated drier tundra dominated by grass.

5.3.2b Lake-level derived precipitation estimates In addition to their other uses in paleoclimatology as described above, lakes act as natural rain gauges. If precipitation increases relative to evaporation, lakes tend to rise, so records of past lake levels provide information on moisture availability.

Most of the water reaching a lake first soaked into the ground and flowed through spaces as groundwater, before either seeping directly into the lake or else coming back to the surface in a stream that flowed into the lake. Smaller amounts of water fall directly on the lake or flow over the land surface to the lake without first soaking in (e.g., MacDonald et al., 2000a). Lakes lose water in streams (“overflow”), as outflow into groundwater, and by evaporation. If water supply to a lake increases, the lake level will rise and the lake will spread. This will increase water loss from the lake, by increasing

the area for evaporation, by increasing the area through which groundwater is leaving and the “push” (hydraulic head) causing that outflow, and perhaps by forming a new outgoing stream or increasing the size of an existing stream. Thus, the level of a lake adjusts in response to changes in the balance between precipitation and evaporation in the region feeding water to the lake (the catchment). Because either a rise in precipitation or a drop in evaporation will cause a rise in lake level, an independent estimate of either precipitation or evaporation is required to allow estimation of the other from a history of lake levels (Barber and Finney, 2000).

Former lake levels can be identified by deposits including the fossil shoreline they leave (**Fig. 5.20**), and sometimes these are preserved underwater and can be recognized in sonar surveys or other data, and these deposits can often be dated. Furthermore, the sediments of the lake may retain a signature of lake-level fluctuations, because coarse-grained material generally occurs near the shore with finer-grained materials offshore (Digerfeldt, 1988), and these too can be identified, sampled and dated (Abbott et al. 2000).

For a given lake, modern values of the major inputs and outputs can be obtained empirically, allowing construction of a model that simulates lake-level changes in response to changing precipitation and evaporation. Allowable pairs of precipitation and evaporation can then be estimated for any past lake level. Particularly in cases where precipitation is the primary control of water depth, it is possible to model lake level responses to past changes in precipitation (e.g., Vassiljev, 1998; Vassiljev et al., 1998). For two lakes in interior Alaska, this technique suggested that precipitation was as much

as 50% lower than present at the Last Glacial Maximum (ca. 20ka) (Barber and Finney, 2000).

Biological groups living within lakes also leave fossil assemblages that can be interpreted in terms of lake level by comparison with modern assemblages. In all cases, factors other than water depth likely influence the assemblages (MacDonald et al., 2000a), but these may themselves be indirectly related to water depth (e.g., conductivity and salinity). Aquatic plants, which are represented by pollen and macrofossils, tend to dominate from nearshore to moderate depths, and shifts in the abundance of pollen or seeds in one of more sediment profiles can indicate relative water-level changes (Hannon and Gaillard, 1997; Edwards et al., 2000). Diatom and chironomid (midge) assemblages may also be related quantitatively to lake depth by means of inverse modeling and transfer functions used to reconstruct past lake levels (Korhola et al., 2000; Ilyashuk et al., 2005).

The great variety of lakes, and the corresponding range of sedimentary indicators, require that field scientists be broadly knowledgeable in selecting which lakes to study and which techniques to use in reconstructions. For some important case studies, see Abbott et al., (2000), Edwards et al., (2000), Pienitz et al., (2000), Anderson et al., (2005), Hannon and Gaillard, 1997; Korhola et al., 2000; and Ilyashuk et al., 2005).

5.3.2c Precipitation estimates from ice cores. Ice cores provide a direct way of recording the net accumulation rate at sites with permanent ice. The initial thickness of an annual layer in an ice core (after mathematically squeezing the air out based on the measured density so that the thickness of ice is considered) is the annual accumulation.

Most ice cores are drilled in cold regions where little meltwater production and runoff occur. Furthermore, sublimation/condensation and snow-drift are generally relatively small terms in the accumulation, so that accumulation is not too different from the precipitation (e.g., Box et al., 2006). The layer thickness deeper in the core must be corrected for the thinning that has occurred as the ice-sheet pile spreads and thins under its own weight, but this correction can be made with much accuracy for most samples using simple ice flow models (e.g., Alley et al., 1993; Cuffey and Clow, 1997).

The annual-layer thickness can be recorded using any component that varies regularly with a defined seasonal cycle. Suitable components include visible layering (e.g. **Fig. 5.12a**), which responds to changes in snow density or impurities (Alley et al., 1997), the seasonal cycle of water isotopes (Vinther et al., 2006), and seasonal cycles in different chemical species (e.g. Rasmussen et al., 2006). Using more than one component gives extra security to the combined output of counted years and layer thicknesses.

Although the correction for strain (layer thinning) increases the uncertainty in estimating absolute precipitation rate deeper in ice cores, estimates of changes in relative accumulation rate along an ice core can be considered reliable (e.g., Kapsner et al., 1995). Because the accumulation rate combines with the temperature to control the rate at which snow is transformed to ice, and because the isotopic composition of the trapped air (Sowers et al., 1989) and the number of trapped bubbles in a sample (Spencer et al., 2006), record the results of that transformation, accumulation rates can also be estimated from measurements of these parameters plus independent estimation of past temperature using techniques described above.

5.4 Arctic Climate over the past 65 Ma

Over the past 65 Ma (the Cenozoic), the Arctic has experienced a greater change in temperature, vegetation and ocean surface characteristics than any other Northern Hemisphere latitudinal band (e.g., Sewall and Sloan, 2001; Bice et al., 2006; and see results presented below). Those times when the Arctic was unusually warm offer insights into the feedbacks within the Arctic system that can amplify changes imposed from outside the Arctic regions. Below we summarize the evidence for Cenozoic history of climate in the Arctic, focusing especially on warm times, using climate and environmental proxies outlined in section 5.3.

5.4.1. Early Cenozoic and Pliocene Warm Times

Records of the $\delta^{18}\text{O}$ composition of bottom-dwelling foraminifera from the global ocean document a long-term cooling of the deep sea over the past 70 Ma (**Fig. 4.8**; Zachos et al., 2001), with the development of large Northern Hemisphere continental ice sheets 2.6 to 2.9 Ma ago (Duk-Rodkin et al., 2004). As discussed below and in chapter 6, Arctic climate history is broadly consistent with the global data reported by Zachos et al. (2001), with general cooling and increase in ice punctuated by short-lived and longer-lived reversals, variations in cooling rate, and additional features related to growth and shrinkage of ice once ice became well-established. A detailed Arctic Ocean record equivalent to the global results of Zachos et al., (2001) is not yet available, and because the Arctic Ocean is geographically somewhat isolated from the world ocean (e.g., Jakobsson and MacNab, 2006), the possibility exists that some differences would be found. Emerging paleoclimate reconstructions from the Arctic Ocean derived from

recently recovered sediment cores from the Lomonosov Ridge (Moran et al., 2006, Backman et al., 2006) shed new light on the Cenozoic evolution of the Arctic Basin, but the data have yet to be fully integrated with the evidence from terrestrial records or with the sketchy records from elsewhere in the Arctic Ocean (see Chapter 8).

Data clearly show warm Arctic conditions during the Cretaceous and early Cenozoic. For example, late-Cretaceous (70 Ma ago) Arctic Ocean temperatures of 15°C (compared to near-freezing today) are indicated by TEX₈₆-based estimates (Jenkyns et al., 2004). The same indicator shows that peak Arctic Ocean temperatures near the North Pole rose from ~18°C to more than 23°C during the short-lived Paleocene-Eocene thermal maximum ~55 Ma ago (**Fig. 5.21**; Sluijs et al., 2006; 2008; also see Moran et al., 2006), synchronous with warming on nearby land from pre-event temperature of ~17°C to peak temperature during the event of ~25°C (Weijers et al., 2007). By ~50 Ma ago, Arctic Ocean temperatures of ~10°C occurred with relatively fresh surface waters dominated by aquatic ferns (Brinkhuis et al., 2006). Restricted connections to the world ocean allowed the fern-dominated interval to persist for ~800,000 years; return of more-vigorous interchange was accompanied by a warming in the central Arctic Ocean of ~3°C (Brinkhuis et al., 2006). On Arctic lands during the Eocene (55 to 34 Ma ago), forests of *Metasequoia* dominated a landscape characterized by organic-rich floodplains and wetlands quite different from the modern tundra (Francis, 1988; McKenna, 1980; Williams et al. 2003).

Terrestrial evidence shows that warm conditions persisted into the early Miocene from 23 to 16 Ma ago, when the central Canadian Arctic Islands were covered in mixed conifer-hardwood forests similar to those of southern Maritime Canada and New England

today (Whitlock and Dawson, 1990); *Metasequoia* was still present, although less abundant than in the Eocene. Still younger, deposits known as the Beaufort Formation and tentatively dated to ~8 to 3 Ma ago (and thus within Miocene to Pliocene times) record an extensive riverside forest of pine, birch and spruce, which lived across the Canadian Arctic Archipelago before geologic processes formed many of the channels that now divide the islands.

The transition from relatively warm climates of the earlier Cenozoic to the colder times of the Quaternary ice age with cyclic growth and shrinkage of extensive land ice, occurred during the Pliocene (5 to 1.8 Ma ago). This change occurred while continental configurations remained similar to those of the present, and most Pliocene plant and animal species were similar to those that remain today. A well-documented warm period in the middle Pliocene (~3 Ma ago), just before the planet transitioned into the Quaternary Ice Age, included forests covering large regions near the Arctic Ocean that are currently polar deserts. The presence of *Arctica islandica*, a marine bivalve that does not live where there is seasonal sea ice, in marine deposits as young as 3.2 Ma on Meighen Island at 80 °N, likely records the peak of Pliocene warmth of the ocean (Fyles et al. 1991). Widespread indications are available of warmer conditions than recently (Dowsett et al., 1994), including one site on Ellesmere Island where application of a novel technique for paleoclimatic reconstruction based on ring-width and isotopic measurements of wood suggests mean-annual temperatures 14 °C warmer than recently (Ballantyne et al., 2006). Additional data from records of beetles and plants indicate mid-Pliocene conditions as much as 10°C warmer than recently for mean summer

conditions, with even larger wintertime changes to a maximum of 15°C or more (Elias and Matthews, 2002).

Much attention has been focused on learning the cause(s) for the slow, bumpy slide in temperatures from the Cretaceous hothouse to the recent ice age. As discussed below, changes in greenhouse-gas concentrations appear to have played the dominant role, with contributions from changes in continental positions, in sea level, and in oceanic circulation linked to these.

Based on climate modeling, Barron et al. (1993) found that continental position had little effect on temperature difference between Cretaceous and modern temperatures (also see Poulsen et al., 1999 and references therein). Donnadieu et al. (2006), also using climate modeling, found that continental motions and their effects on atmospheric and oceanic circulation caused a change in global average temperature of almost 4°C between early and late Cretaceous; this is not a direct comparison to modern, but is suggestive that continental motions can have a notable effect on climate. However, there are as yet no indications from modeling, despite much effort, that the motion of continents by itself can explain most or all of the long-term cooling trend from the Cretaceous to the ice age, or the “wiggles” during that cooling.

The direct paleoclimatic data provide one interesting perspective on the role of oceanic circulation in the warmth of the latter Eocene. When the Arctic Ocean was filled with water ferns living in “brackish” water (less salty than normal marine water) in an ocean that was ice-free or nearly so, the oceanic currents reaching the near-surface Arctic Ocean must have been greatly weakened relative to today to allow the fresh water to persist. Thus, the Arctic-Ocean warmth of that time cannot be explained by heat

transport by oceanic currents. The resumption of stronger currents and normal salinity was accompanied by a warming of $\sim 3^{\circ}\text{C}$ (Brinkhuis et al., 2006), important but not dominant in the temperature difference between then and now.

As discussed in section 4.2.4, the atmospheric CO_2 concentration has changed over tens of millions of years in response to many processes, and especially to those processes linked to plate tectonics (continental drift) and perhaps also to biological evolution. Many lines of proxy evidence (see Royer, 2006) show that the warm Cretaceous had higher atmospheric CO_2 than recently, and that the subsequent fall in CO_2 occurred in parallel with the cooling (**Fig. 5.22**). Furthermore, models find that the changing CO_2 concentration is sufficient to explain much of the cooling (e.g., Bice et al., 2006; Donnadieu et al., 2006).

A persistent difficulty is that models driven by reconstructed CO_2 tend to underestimate Arctic warmth (e.g., Sloan and Barron, 1992). Many possible explanations have been offered for this, including underestimation of CO_2 levels (Shellito et al., 2003; Bice et al., 2006), an enhanced greenhouse effect from polar stratospheric clouds during warm times (Sloan and Pollard, 1998; Kirk-Davidoff et al., 2002), changed planetary obliquity (Sewall and Sloan, 2004), reduced biological productivity providing fewer cloud-condensation nuclei and thus fewer reflective clouds (Kump and Pollard, 2008), and enhanced heat transport by tropical cyclones (Korty et al., 2008). Several of these involve feedbacks not normally represented in climate models and serving to amplify warming in the Arctic; consideration of the literature cited above and of additional materials points to some combination of stronger greenhouse-gas forcing (see Alley,

2003 for a review) and stronger long-term feedbacks than typically included in models, rather than to major orbital change, although that cannot be excluded.

An important role for greenhouse gases in providing the primary control on Arctic temperature changes is indicated by the warmth of the Paleocene-Eocene Thermal Maximum. As described above (see Sluijs et al., 2008 for an extensively referenced summary of the event together with new data pertaining to the Arctic), this thermal maximum involved a rapid (over a few centuries or less), widespread warming coincident with a large increase in atmospheric greenhouse-gas concentrations from a biological source (whether from sea-floor methane, living biomass, soils, or other sources remains debated), followed by a slower decay of the anomalous warmth and removal of the extra greenhouse gases over tens of thousands of years to roughly 100,000 years. The event in the Arctic seems to have occurred within a longer interval of restricted oceanic circulation into the Arctic Ocean (Sluijs et al., 2008), and was too fast for any notable effect of drifting continents or evolving life. The reconstructed CO₂ change thus is strongly implicated in the warming (e.g., Zachos et al., 2008).

Taken very broadly, the Arctic changes parallel the global ones over the Cenozoic, except with larger changes in the Arctic than globally averaged (e.g., Sluijs et al., 2008). The global changes parallel changing atmospheric carbon-dioxide concentrations, with changing CO₂ the likely cause of most of the temperature change (e.g., Royer, 2006; Royer et al., 2007).

The well-documented warmth of the Pliocene is not fully explained. This interval is recent enough that continental positions were substantially the same as today. As reviewed by Jansen et al. (2007), many reconstructions show notable Arctic warmth but

little low-latitude change; however, recent work suggests the possibility of low-latitude warmth as well (Haywood et al., 2005). Reconstructions of Pliocene atmospheric CO₂ concentration (reviewed by Royer, 2006) generally agree with each other within the considerable uncertainties, but allow values above, similar to, or even below the typical levels just prior to major human influence. Data remain equivocal on whether oceanic heat transports were enhanced during Pliocene warmth (reviewed by Jansen et al., 2007). The high-latitude warmth thus may have originated primarily from changes in greenhouse-gas concentrations in the atmosphere, or from changes in oceanic or atmospheric circulation, or some combination, perhaps with a slight possibility that other processes also contributed.

5.4.2. The Early Quaternary: Ice-Age Warm Times

A major reorganization of the climate system occurred between 3.0 and 2.5 Ma ago, resulting in the development of the first continental ice sheets over the North American and Eurasian Arctic, marking the onset of the Quaternary Ice Ages (Raymo, 1994). For the first 1.5 – 2.0 Ma, ice age cycles occurred on a 41 ka rhythm, with the climate oscillating between glacial and interglacial states (**Fig. 5.23**). A prominent but apparently short-lived interglacial (warm interval) occurred ~2.4 Ma ago. This is recorded especially in the Kap København Formation, a 100-m-thick sequence of estuarine sediments covering an extensive lowland area near the northern tip of Greenland (Funder et al., 2001).

The rich and well-preserved fossil fauna and flora in the Kap København Formation (**Fig. 5.24**) record warming from cold conditions into an interglacial and

subsequent cooling, over 10,000 to 20,000 years. During the peak warmth, forest trees reached the Arctic Ocean coast, 1,000 km north of the northernmost trees today. Based on this warmth, Funder et al. (2001) suggested that the Greenland Ice Sheet must have been reduced to local ice caps over mountain areas (**Fig. 5.24a**) (see Chapter 7). Although high-time-resolution records are not available across the Arctic Ocean at that time, by analogy with present faunas along the Russian coast, the coastal zone would have been ice-free for 2 to 3 months in summer. Today this coast of Greenland experiences year-round sea ice, and models for diminishing sea ice in a warming world generally indicate long-term persistence of summertime sea ice off these shores (e.g., Holland et al., 2006). Thus, the reduced sea ice off northern Greenland during deposition of the Kap København Formation suggests a widespread warm time with reduced Arctic sea ice.

During Kap København times, precipitation was higher and temperatures were warmer than at the peak of the current interglacial about 7 ka ago, with the temperature difference larger during winter than during summer. Higher temperatures during deposition of the Kap København were not caused by notably greater solar insolation, owing to the relative repeatability of the Milankovitch variations over millions of years (e.g., Berger et al., 1992). As discussed above, uncertainties in estimation of atmospheric carbon-dioxide concentration, ocean heat transport, and perhaps other factors are sufficiently large for the time of the Kap København Formation to preclude strong conclusions about the cause(s) of the unusual warmth.

Potentially correlative records of warm interglacial conditions are found in deposits on coastal plains along the northern and western shores of Alaska. High sea

levels during interglaciations repeatedly flooded the Bering Strait, rapidly changing the configuration of the coastlines, altering regional continentality, and reinvigorating the exchange of water masses between the North Pacific, Arctic and North Atlantic oceans. Since the first submergence of the Bering Strait about 5.5 to 5 Ma ago (Marincovich and Gladenkov, 2001), this marine gateway has allowed relatively warm Pacific water masses from as far south as northern Japan to reach as far north as the Beaufort Sea (Brigham-Grette and Carter, 1992). The Gubik Formation of Northern Alaska records at least three warm high sea stands in the early Quaternary (**Fig. 5.25**). During the Colvillian transgression, ~2.7 Ma ago, the Alaskan Coastal Plain supported open boreal forest or spruce-birch woodland with scattered pine and rare fir and hemlock (Nelson and Carter, 1991). Warm marine conditions are confirmed by the general character of the ostracode fauna, which includes *Pterygocythereis vannieuwenhuisi* (Brouwers, 1987), an extinct species of a genus whose modern northern limit is the Norwegian Sea, but in the northwestern Atlantic Ocean does not occur north of the southern cold-temperate zone (Brouwers, 1987). Despite the high sea level and relative warmth indicated by the Colvillian transgression, erratics (rocks not of local origin) in Colvillian deposits southwest of Barrow, Alaska, indicate that glaciers were terminating in the Arctic Ocean and producing icebergs large enough to reach NW Alaska at this time.

Subsequently, the Bigbendian transgression (~2.5 Ma ago) was also warm, as indicated by rich molluscan faunas including the gastropod *Littorina squalida* and the bivalve *Clinocardium californiense* (Carter et al., 1986). The modern northern limit of both of these mollusk species is well to the south (Norton Sound, Alaska). The presence of sea otter bones suggests that the limit of seasonal ice on the Beaufort Sea was

restricted during the Bigbendian interval to positions north of the Colville River and thus well north of typical 20th-century positions (Carter et al., 1986); modern sea otters cannot tolerate severe seasonal sea-ice conditions (Schneider and Faro, 1975).

The youngest of these early-Quaternary events of high sea level is the Fishcreekian transgression (~2.1 to ~2.4 Ma ago), suggested to be correlative to the Kap Kobenhavn Formation on Greenland (Brigham-Grette and Carter, 1992). However, age control is not complete, and Brigham (1985) and Goodfriend et al. (1996) suggested that the Fishcreekian could be as young as 1.4 Ma. This deposit contains several mollusk species that currently are found only to the south. Moreover, sea otter remains and the intertidal gastropod *Littorina squalida* at Fish Creek suggest that perennial sea ice was absent or severely restricted during the Fishcreekian transgression (Carter et al., 1986b). Correlative deposits rich in mollusk species currently living only well to the south are reported from the coastal plain at Nome, Alaska (Kaufman and Brigham-Grette, 1993).

The available data clearly indicate episodes of relatively warm conditions correlative with high sea levels and reduced sea ice in the early Quaternary. The high sea levels suggest melting of land ice (see Chapter 7), so the correlation of warmth and reduced land and sea ice (see Chapter 8) indicated by recent instrumental observations, model results, and data from other time intervals is also found for this time interval. Improved time resolution of histories of forcing and response will be required to assess cause(s) of the changes, but the available estimates of forcings indicate that they were relatively moderate, and thus that the strong Arctic amplification of climate change was active in these early Quaternary events.

1029 **5.4.3 The Mid-Pleistocene Transition: 41 ka and 100 ka worlds**

1030 Since the late Pliocene, the cyclical waxing and waning of continental ice sheets
1031 have dominated global climate variability. The variations in sunshine caused by features
1032 of Earth's orbit have been very important in these ice-sheet changes, as described in
1033 Chapter 4.

1034 After the onset of glaciation in North America ~2.7 Ma ago (Raymo, 1994), ice
1035 grew and shrank as the Earth's obliquity (tilt) varied in its 41 ka cycle. But between 1.2
1036 and 0.7 Ma ago, the variations in ice volume became larger and slower, with a ~100-ka
1037 period dominating especially over the last ~700 ka (**Fig. 5.23**) Although the Earth's
1038 eccentricity varies with a ~100-ka period, this does not cause as much change in sunshine
1039 in the key regions of ice growth as do the faster cycles, so the reasons for the dominant
1040 ~100-ka period in ice volume remain obscure. Roe and Allen (1999) assessed six
1041 different models for this behavior, and found that all fit the data rather well, with the
1042 record still too short to allow the data to demonstrate superiority of any one model.

1043 Models for the 100-ka variability often assign a major role to the ice sheets
1044 themselves, and especially to the Laurentide Ice Sheet on North America, which
1045 dominated the total global change in ice volume (e.g., Marchant and Denton, 1996). For
1046 example, Marshall and Clark (2002) modeled the growth and shrinkage of the Laurentide
1047 ice sheet, and found that during growth the ice was frozen to the bed beneath and unable
1048 to move rapidly. After many tens of thousands of years, trapping of the Earth's heat led
1049 to thawing of the bed, allowing faster flow. Faster flow of the ice sheet lowers the upper
1050 surface, allowing warming and melting (see Chapter 7). Behavior such as this could
1051 cause the main variations of ice volume to be slower than the main variations in sunshine

caused by the Earth's orbital features, with the slow-flowing ice partially ignoring the faster variations in sunshine, until the shift to faster flow allows faster response. Note that this remains an hypothesis, and other possibilities also exist.

The cause of the switch from ~41ka to ~100-ka climate variability, known as the mid-Pleistocene transition, also remains obscure. This transition is of particular interest because it does not seem to have been caused by any major change in the Earth's orbital behavior, and so the transition may reflect some fundamental threshold within the climate system.

The mid-Pleistocene transition may be related to continuation of the gradual global cooling from the Cretaceous, as described above (Raymo et al., 1997; 2006; Ruddiman, 2003). If, for example, the 100-ka cycling requires that the Laurentide ice sheet grow sufficiently large to trap enough of the Earth's heat to thaw the ice-sheet bed (Marshall and Clark, 2002), then the long-term cooling may have reached the threshold at which the ice sheet became large enough.

However, such a cooling model does not explain the key observation (Clark et al., 2006) that the ice sheets of the last 700 ka have reached larger volume (Clark et al., 2006) but smaller area (Boellstorff, 1978; Balco et al., 2005a,b) than the earlier ice sheets. Clark and Pollard (1998) used this observation to argue that the early Laurentide Ice Sheet must have been substantially lower in elevation than in the late Pleistocene, possibly by as much as 1 km. Clark and Pollard (1998) suggested that the tens of millions of warm years back to the Cretaceous and beyond had produced thick soils and broken-up rocks below the soil. When glaciations began, the ice advanced over these water-saturated soils, which deformed easily. Just as grease on a griddle allows batter

poured on top to spread easily into a wide, thin pancake, deformation of the soils beneath the growing ice (Alley, 1991) would have produced an extensive ice sheet that did not contain a large volume of ice. As successive ice ages swept the loose materials to the edges of the ice sheet, with rivers removing most of the materials to the sea, hard bedrock was exposed in the central region. And, just as the bumps and friction of an ungreased waffle iron slow spreading of the batter to give a thicker, not-as-wide breakfast than on a greased griddle, the hard, bumpy bedrock produced an ice sheet that did not spread as far but contained more ice.

Other hypotheses also exist for these changes. A complete explanation of the onset of extensive glaciation on North America and Eurasia as well as Greenland about 2.8 Ma ago, or of the transition from 41 ka to 100 ka ice age cycles, remains the object of ongoing investigations.

5.4.4 A link between ice volume, atmospheric temperature and greenhouse gases

The average global-average temperature change across one of the large 100-ka ice-age cycles was about 5-6°C (Jansen et al., 2007), with larger changes in the Arctic and close to the ice sheets, including changes of 21-23°C atop the Greenland ice sheet (Cuffey et al., 1995). The total change in sunshine reaching the planet over these cycles was near zero, with the orbital features serving primarily to move sunshine from north to south and back, or from equator to poles and back, depending on the cycle considered (see Chapter 4).

As discussed by Jansen et al. (2007), and in section 5.2.6, above, many factors probably contributed to the large temperature change despite very small global change in total sunshine. Cooling produced growth of reflective ice that lowered the amount of sunshine absorbed by the planet. Complex changes especially in the ocean lowered atmospheric carbon dioxide, and both oceanic and terrestrial changes lowered atmospheric methane and nitrous oxide, all greenhouse gases, with the changes in carbon dioxide most important. Various changes produced additional dust that blocked sunshine from reaching the planet. Cooling caused expansion of more-reflective grasslands or tundra into regions formerly forested, also reflecting more sunshine. While the orbital features drove the ice-age cycling, these feedbacks are required to provide quantitatively accurate explanations of the changes.

The relation between climate and carbon dioxide has been relatively constant back at least 650,000 years (Siegenthaler et al., 2005), with the growth and shrinkage of ice, cooling and warming of the globe, and other changes repeating along similar although not identical paths. However, some of the small differences between successive cycles are of interest, as discussed next.

5.4.5 Marine Isotopic Stage 11 – a long interglaciation

Following the mid-Pleistocene Transition, the growth and decay of ice sheets followed a 100 ka cycle, with brief, warm interglaciations of about 10 ka duration, then progressively more extensive ice coverage, terminated rapidly by the transition into the next warm interglaciation (e.g., Kellogg, 1977; Ruddiman et al., 1986; Jansen et al., 1988; Bauch and Erlenkeuser, 2003; Henrich and Baumann, 1994). As discussed above,

1120 this 100 ka cycle may be linked to the 100 ka variation of the eccentricity, or out-of-
1121 roundness, of the Earth's orbit about the sun, although other explanations are possible.

1122 The eccentricity exhibits an additional cycle of just over 400,000 years, such that
1123 the orbit goes from almost round to more eccentric to almost round over 100,000 years,
1124 but the maximum eccentricity reached in this 100,000-year cycle increases and decreases
1125 with a 400,000-year cycle (Berger and Loutre, 1991; Loutre, 2003). When the orbit is
1126 almost round, there is little effect from Earth's precession, which determines whether the
1127 Earth is closer to the sun or farther from the sun during a particular season such as
1128 northern summer. About 400,000 years ago, during MIS 11, the 400,000-year cycle
1129 caused persistence of a nearly round orbit. The interglacial of MIS 11 lasted longer than
1130 previous or subsequent interglacials (see Droxler et al., 2003 and references therein;
1131 Kandiano and Bauch, 2007; Jouzel et al., 2007), perhaps because the summer sunshine at
1132 high northern latitudes did not become low enough at the end of the first 10,000 years of
1133 the interglacial to allow ice growth at high northern latitudes, because the persistently
1134 nearly round orbit prevented northern summer from occurring at a great distance from the
1135 sun (**Fig. 5.26**).

1136 As discussed in chapter 7, indications of Arctic and subarctic temperatures at this
1137 time versus more-recent interglacials are inconsistent (also see Stanton-Frazee et al.,
1138 1999; Bauch et al., 2000; Droxler and Farrell, 2000; Helmke and Bauch, 2003). Sea level
1139 seems to have been higher at this time than at any time since, and data from Greenland
1140 are consistent with notable shrinkage or loss of the ice sheet accompanying notable
1141 warmth, although the age of this shrinkage is not constrained well enough to be sure that
1142 the warm time recorded was indeed MIS 11 (chapter 7).

5.4.6 Marine Isotopic Stage (MIS) 5e: The Last Interglaciation

The warmest millennia of at least the past 250,000 years occurred during MIS 5, and especially during the warmest part of that interglaciation, MIS 5e (e.g., McManus et al., 1994; Fronval and Jansen, 1997; Bauch et al., 1999; Kukla, 2000), when global ice volumes were smaller than today and Earth's orbital parameters aligned to produce a strong positive anomaly in solar radiation during summer throughout the Northern Hemisphere (Berger and Loutre, 1991). The average solar radiation during the key summer months (May, June, July) was ~11% above present across the Northern Hemisphere between 130 and 127 ka ago, with a slightly greater anomaly, 13%, over the Arctic. Greater solar energy in summer, melting of the large northern hemisphere ice sheets, and intensification of the North Atlantic Drift (Chapman et al., 2000; Bauch and Kandiano, 2007), combined to reduce Arctic Ocean sea ice, allow expansion of boreal forest to the Arctic Ocean shore across large regions, reduce permafrost, and melt almost all glaciers in the Northern Hemisphere (CAPE Project Members, 2006).

High solar radiation in summer during MIS 5e, amplified by key boundary condition feedbacks (especially sea ice, seasonal snow cover, and atmospheric water vapor; see above), collectively produced summer temperature anomalies 4 to 5 °C above present over most Arctic lands, significantly above the average Northern Hemisphere summer temperature anomaly (0–2 °C above present; CLIMAP Project Members, 1984; Bauch and Erlenkeuser, 2003). MIS 5e demonstrates the strength of positive feedbacks on Arctic warming (CAPE Project Members, 2006; Otto Bleisner et al 2006).

5.4.6a Terrestrial MIS 5e records At high northern latitudes, summer temperatures exert the dominant control on glacier mass balance, unless accompanied by dramatic precipitation changes (e.g., Oerlemans, 2001; Denton et al., 2005; Koerner, 2005). Summer temperature is also the most effective predictor for most biological processes, although seasonality and moisture availability may influence some biological such as dominance by evergreen versus deciduous vegetation (Kaplan et al., 2003). For these reasons, most studies of conditions during MIS 5e have focused on reconstructing summer temperatures. Terrestrial MIS 5e climate especially has been reconstructed from diagnostic assemblages of biotic proxies preserved in lake, peat, river, and shallow marine archives, and from isotopic changes preserved in ice cores and lake carbonates. Estimated winter temperatures as well as summer temperatures, and hence seasonality, are well constrained for Europe, but poorly known for most sectors; likewise, precipitation reconstructions are limited to qualitative estimates in most cases where available, and are not available for most regions.

All sectors of the Arctic had summers warmer than present during MIS 5e, but the magnitude of warming exhibited spatial variability (**Fig. 5.27**; CAPE Last Interglacial Project Members, 2006). The greatest positive summer temperature anomalies occurred around the Atlantic sector, where summer warming was typically 4 to 6 °C. This anomaly extended into Siberia, but decreased from Siberia westward to the European sector (0 to 2 °C), and eastward toward Beringia (2 to 4 °C). The Arctic coast of Alaska had sea-surface temperatures 3 °C above recent values, and considerably less summer sea ice than recently, but much of interior Alaska had smaller anomalies (0 to 2 °C) that probably extended into western Canada. In contrast, northeastern Canada and parts of

Greenland had summer temperature anomalies of ~5 °C, and perhaps more (see chapter 7 for a discussion of Greenland).

Precipitation and winter temperatures are more difficult to reconstruct for MIS 5e than are summer temperatures. In northeastern Europe, the latter part of MIS 5e was characterized by a marked increase in winter temperatures. A large positive winter temperature anomaly also occurred in Russia and western Siberia, although the timing is not as well constrained (Troitsky, 1964; Gudina et al., 1983; Funder et al., 2002). Most other sectors that have qualitative precipitation estimates indicate wetter conditions than in the Holocene.

5.4.6b Marine MIS 5e records Low sedimentation rates and the rare preservation of carbonate fossils limit the number of sites at which MIS 5e can be reliably identified in sediment cores from the central Arctic Ocean. MIS 5e sediments from the central Arctic Ocean usually contain high concentrations of planktonic (surface-dwelling) foraminifera and coccoliths, indicative of a reduction in summer sea-ice coverage that permitted enhanced biological productivity (Gard, 1993; Spielhagen et al., 1997; 2004; Jakobsson et al. 2000; Backman et al., 2004; Polyak et al., 2004; Nørgaard-Pedersen et al., 2007a,b). However, occasional dissolution of carbonate fossils complicates the interpretation of microfossil concentrations. Also, marine sediments from MIS 5a, slightly younger and cooler than MIS 5e, sometimes have higher microfossil concentrations than do MIS 5e sediments (Gard, 1986; 1987).

Arctic Ocean sediment cores recently recovered from the Lomonosov Ridge, north of Greenland, have revived the discussion of MIS 5e conditions in the Arctic Ocean.

Unusually high concentrations of a subpolar foraminifera species that usually dwells in waters with temperatures well above the freezing point were found in MIS 5e levels and interpreted to indicate warm interglacial conditions and much reduced sea-ice cover in the interior Arctic Ocean (Nørgaard-Pedersen et al., 2007a,b). Interpretation of these and other microfossils is complicated by the strong vertical stratification in the Arctic Ocean; today, the warm Atlantic water (temperatures $>1^{\circ}\text{C}$) is in most areas isolated from the atmosphere by a relatively thin layer of cold ($<1^{\circ}\text{C}$) fresher water that limits the transfer of heat to the atmosphere. It is not always possible to determine whether warm-water foraminifera found in marine sediment from the Arctic Ocean lived in warm waters that remained isolated from the atmosphere below the cold surface layer, or whether the warm Atlantic water had displaced the cold surface layer and was interacting with the atmosphere to affect its energy balance.

Landforms and fossils from the western Arctic and Bering Strait indicate vastly reduced sea ice during MIS 5 (**Fig. 5.28**). The winter sea-ice limit is estimated to have been as much as 800 km farther north than its average 20th-century position, and summer sea ice may have been absent at times (Brigham-Grette and Hopkins, 1995). These reconstructions are consistent with the northward migration of treeline across much of Alaska and nearby Chukotka by hundreds of kilometers, with the elimination of tundra across Chukotka to the Arctic Ocean coast (Lozhkin and Anderson, 1995).

Sufficient data are not yet available to allow unambiguous reconstruction of MIS 5e conditions in the central Arctic Ocean. Key uncertainties are related to the extent and duration of Arctic Ocean sea ice. The vertical structure of the upper 500 m of the water column is also climatically important but poorly known, in particular whether the strong

vertical stratification characteristic of the modern regime persisted throughout MIS 5e, or whether reduced sea ice and changes in the hydrologic cycle and winds broke down this stratification and allowed Atlantic water to reside at the surface over larger portions of the Arctic Ocean.

5.4.7 MIS 3 warm intervals

The temperature and precipitation history of MIS 3 (~70 ka to 30 ka ago) is difficult to reconstruct because of the paucity of continuous records and the difficulty in providing a secure time frame. The $\delta^{18}\text{O}$ record of temperature change over the Greenland ice sheet and other ice-core data show that the North Atlantic region experienced repeated episodes of rapid, high-magnitude climate change, with rapid increases in temperature of up to 15°C (reviewed by Alley, 2007 and references therein), with each warm period lasting several hundred to a few thousand years. These brief climate excursions not only found in the Greenland Ice Sheet, but are also recorded in cave sediments from China (Wang et al., 2001; Dykoski, et al., 2005) and high-resolution marine records off California (Behl and Kennett, et al., 1996), the Caribbean Sea's Cariaco Basin (Hughen et al., 1996.), the Arabian Sea (Schultz et al., 1998) and the Sea of Okhotsk (Nürnberg and Tiedmann, 2004), among many other sites. The ice-core records from Greenland include indications of climate change in many regions on the same time scale (for example, the methane trapped in ice-core bubbles was in part produced in tropical wetlands and was essentially 100% produced beyond the Greenland ice sheet; Severinghaus et al., 1998). These ice-core records demonstrate clearly that the climate-change events were synchronous across widespread areas; the ages of events

from many regions agreeing within the stated uncertainties, in good agreement. These events were thus hemispheric to global in nature (see review by Alley, 2007), and are considered a “fingerprint” of large-scale ocean-atmosphere coupling (Bard, 2002). The cause(s) for these events is still debated. However, Broecker and Hemming (2001) and Bard (2002) among others suggested they were likely the result of major and abrupt reorganizations of the ocean’s thermohaline circulation probably related to ice sheet instabilities that introduced large quantities of fresh water into the North Atlantic (Alley, 2007). Such large and abrupt oscillations linked to changes in North Atlantic surface conditions and probably to the large-scale oceanic circulation persisted into the Holocene (MIS 1), with the youngest having occurred about 8.2 ka ago (Alley and Ágústsson, 2005). However, it appears that the abrupt cooling at that time reflects an ice-age-linked cause, a catastrophic flood from a very large lake dammed by the melting Laurentide ice sheet.

Within MIS 3, land ice was somewhat reduced compared to the colder times of MIS 2 and MIS 4, but Arctic temperatures generally were much lower and ice more extensive than in MIS 1, with certain exceptions. Sea level was lower at that time, the coastline well offshore in many places, and the increased continentality (isolation from the moderating influence of the sea) may have contributed to warmer summertime temperatures, presumably offset by colder wintertime temperatures.

For example, on the New Siberian Islands in the East Siberian Sea, Andreev et al (2001) documented the existence of graminoid-rich tundra thought to have covered wide areas of the emergent shelf, with summer temperatures perhaps as much as 2°C warmer than during the 20th century. At Elikchan 4 Lake in the upper Kolyma drainage, the

sediment record contains at least three intervals (especially one ~38 ka ago) when summer temperatures and treeline reached late Holocene conditions (Anderson and Lozhkin, 2001). Insect faunas nearby in the lower Kolyma are thought to have reached 1-4.5°C warmer than recently for similar intervals (Alfimov et al., 2003). In general, variable paleoenvironmental conditions were typical of the traditional Karaginskii/MIS 3 period across arctic Russia; however, stratigraphic confusion within the limits of radiocarbon-dating precludes widespread correlation of events .

Relative warmth during MIS 3 appears to have been strongest in Eastern Beringia with some evidence of temperatures between 45 and 33 ka only 1 to 2 °C lower than present (Elias, 2007). The warmest interval across interior Alaska is known as the Fox Thermal Event, dated ~40-35 ka ago, marked by the establishment of spruce forest tundra (Anderson and Lozhkin, 2001). Yet forests were most dense a little earlier across the Yukon, ~43-39 ka ago. In general (Anderson and Lozhkin, 2001), the warmest interstadial interval for all of Beringia possibly occurred between 44-35 ka ago, with strong signals from interior sites and little to no vegetation response in areas closest to Bering Strait. Climatic conditions in eastern Beringia appear to have been harsher than modern for all of MIS 3. In contrast, MIS 3 climates of western Beringia achieved modern or near modern levels during several intervals. Moreover, while the transition from MIS 3 to MIS 2 was clearly marked by a transition from warm/moist to cold/dry conditions across western Beringia, this transition is absent or subtle in all but a few records from Alaska (Anderson and Lozhkin, 2001).

5.4.8 MIS 2, the last glacial maximum (30 to 15 ka ago)

The last glacial maximum was particularly cold in both the Arctic and globally, and provides useful constraints on the magnitude of Arctic amplification (see below). During peak cooling of the last glacial maximum, planetary temperatures were ~5-6 °C lower than present (Farrera et al., 1999; Braconnot et al., 2007, Jansen et al., 2007), whereas Arctic temperatures in central Greenland were more than 20°C lower (Cuffey et al., 1995; Dahl-Jensen et al., 1998), with similar temperature depressions over Beringia (Elias et al., 1996a).

5.4.9 MIS 1, The Holocene: the present interglaciation

In the face of rising solar energy in summer tied to orbital features, and rising greenhouse gases, Northern Hemisphere ice sheets began to recede from near their largest extent shortly after 20 ka ago, and at a noticeable increasing rate of recession after ~16 ka ago (see, e.g., Alley et al., 2002 for the timing of various events during the deglaciation). Most coastlines became ice-free before 12 ka ago, and ice continued to melt rapidly as summer insolation reached a peak (~9% above modern) ~11 ka ago. The MIS 2/MIS 1 transition, which marks the start of the Holocene interglaciation, is often placed at the abrupt termination of the cold event called the Younger Dryas, which recently was estimated as ~11.7 ka ago (Rasmussen et al., 2006).

A wide variety of evidence from terrestrial and marine archives indicates that peak Arctic summertime warmth was achieved during the early Holocene, when most regions of the Arctic experienced sustained temperatures that exceeded observed 20th century values. This period of peak warmth, which is geographically variable in its timing, is generally referred to as the Holocene Thermal Maximum (HTM). The ultimate

driver of the warming was orbital forcing, which produced increased summer solar radiation across the Northern Hemisphere. At 70°N, insolation in June now is near a local minimum, with a maximum ~11-12 ka ago; June insolation was ~15 W m⁻² larger than recently about 4 ka ago, and ~45 W at m⁻² the Holocene peak, for a total change of ~10% (**Fig. 5.29**; Berger and Loutre, 1991). Winter (January) insolation was only slightly lower than today ~11 ka ago, in large part because there is almost zero insolation so far north in January.

By 6 ka ago, sea level and ice volumes were close to those observed more recently, and climate forcings such as atmospheric carbon-dioxide concentration differed little from pre-industrial conditions (e.g., Jansen et al., 2007), except for the steady decrease in far-northern summer insolation that occurred throughout the Holocene. High-resolution archives (decades to centuries) containing multiple climate proxies are available for most of the Holocene across the Arctic. Consequently, the mid- to late-Holocene allows evaluation of the range of natural climate variability, and the magnitude of climate change in response to relatively small forcings.

5.4.9.a The Holocene Thermal Maximum (HTM) Many of the Arctic paleoenvironmental records for the HTM appear to have recorded primarily summertime conditions. Many different proxies have been exploited to derive these reconstructions, including: biological indicators such as pollen, diatoms, chironomids, dinoflagellate cysts and other microfossils; elemental and isotopic geochemical indexes from lacustrine sediments, marine sediments, and ice cores; borehole temperatures; and, age distributions

of radiocarbon-dated tree stumps north of/above current treeline, marine mollusks and whale bones (Kaufman et al., 2004).

A recent synthesis of 140 Arctic paleoclimatic and paleoenvironmental records extending from Beringia westward to Iceland by Kaufman et al. (2004) provides insights into the nature of the HTM in the western Arctic (**Fig. 5.30**). Fully 85% of the sites included in the synthesis contained evidence of a HTM. The average duration of the HTM extended from 2100 years in Beringia to 3500 years in Greenland. The period 10 ka to 4 ka ago includes the greatest number of sites recording HTM conditions and the greatest spatial extent of the HTM in the western Arctic (**Fig. 5.31b**). There is a strong geographic gradient in the timing of HTM initiation and termination in the western Arctic (**Fig. 5.31c**). The earliest initiation of the HTM occurred in Beringia, where warmer-than-present conditions became established 14 to 13 ka ago. Intermediate ages for initiation of the HTM (10 ka to 8 ka ago) are apparent in the Canadian Arctic islands and extending across central Greenland, although the HTM on Iceland occurred a bit later, from 8 to 6 ka ago. The onset of the HTM on Svalbard was earlier, by 10.8 ka ago (Svendsen and Mangerud, 1997). The continental portions of central and eastern Canada experienced the latest general onset of HTM conditions (7 to 4 ka ago). Similarly, the earliest termination of the HTM occurred in Beringia, although most regions reflect cooling by 5 ka ago. Much of the pattern of the onset of the HTM can be explained at least in part by proximity to the cold winds from the melting Laurentide ice sheet in Canada, which depressed temperatures nearby until the ice melted back.

Records for sea-ice conditions in the Arctic Ocean and adjacent channels have been developed by radiocarbon-dating indicators including the remains of open-water

proxies such as whales and walrus, warm-water marine mollusks, and changes in microfauna preserved in marine sediments. These reconstructions, presented in more detail in Chapter 8 (Sea Ice), parallel the terrestrial record for the most part. The data demonstrate an increased flux of warm Atlantic water into the Arctic Ocean beginning ~11.5 ka ago, but peaking between about 8 and 5 ka ago, which, coupled with increased summer insolation, resulted in a decrease in the area of perennial sea-ice cover during the early Holocene. Decreased sea-ice cover in the western Arctic during the early Holocene also may be indicated by changes in sea-salt sodium concentrations in the Penny Ice Cap (Eastern Canadian Arctic; Fisher et al., 1998) and the Greenland Ice Sheet (Mayewski et al., 1997). In most regions, perennial sea ice increased in the late Holocene, although it has been suggested that the Chukchi Sea experienced decreasing sea ice (de Vernal et al., 2005), possibly in response to changing rates of Atlantic water inflow in Fram Strait.

In North America, treeline expanded northward into regions formerly mantled by tundra as summer temperatures increased through the early Holocene, although the northward extent of treeline advance appears to have been limited to perhaps a few tens of kilometers beyond the recent position (Seppä et al., 2003; Gajewski and MacDonald, 2004). In contrast, treeline change across the Eurasian Arctic was much greater. Tree macrofossils (Kremenetski et al., 1998; MacDonald et al., 2000a,b, 2007) collected at and/or beyond the current treeline indicate that tree genera such as a birch (*Betula*) and larch (*Larix*) advanced to beyond the modern limits of treeline across most of northern Eurasia between 11 and 10 ka ago (**Figs. 5.31 and 5.32**). Spruce (*Picea*) advanced slightly later than the other two genera. Interestingly, pine (*Pinus*), which forms the conifer treeline in Fennoscandia and the Kola Peninsula, does not appear to have

established appreciable forest cover at or beyond the present treeline in those regions at the far west of Europe until around 7 ka ago (MacDonald et al. 2000b). However, quantitative reconstructions of temperature from the Kola Peninsula and adjacent Fennoscandia suggest that summer temperatures were warmer than modern temperatures by 9 ka ago (Seppä and Birks, 2001; 2002; Hammarlund et al., 2002; Solovieva et al., 2005), and the development of extensive pine cover at and north of the present treeline appears to have been delayed relative to this warming. In the Taimyr Peninsula of Siberia and across nearby regions, the most northerly limit reached by trees during the Holocene was over 200 km north of the current treeline. The treeline appears to have begun to retreat across northern Eurasia ~4 ka ago. The timing of the HTM across the Eurasian Arctic overlaps the widest expression of the HTM in the western Arctic (**Fig. 5.31**), and it differs in that the timing of onset and termination show dramatically less variability across Eurasia than across North America, and the magnitude of the treeline expansion and retreat is far greater in the Eurasian Arctic. Fossil pollen and other indicators of vegetation or temperature from the northern Eurasian margin also support the contention of a prolonged warming and northern extension of treeline during the early through middle Holocene (see for example Hyvärinen, 1975; Clayden et al., 1997; Velichko et al., 1997; Kaakinen and Eronen, 2000; Seppä, 1996; Pisaric et al., 2001; Seppä and Birks, 2001, 2002; Gervais et al., 2002; Hammarlund et al., 2002; Solovieva et al., 2005).

Changes in landforms suggest that the early to middle Holocene was associated with permafrost degradation in Siberia. A synthesis of available Russian data by Astakhov (1995) suggests that melting permafrost was apparent north of the Arctic Circle

during the early through middle Holocene. Areas south of the Arctic Circle appear to have experienced deep thawing (100 to 200 m depth) from the early Holocene until about 4 ka to 3 ka ago, when cooler conditions led to renewed permafrost development. The deep thawing and subsequent renewal of surface permafrost produced an extensive thawed layer sandwiched between the shallow, more recently frozen ground, and deeper Pleistocene permafrost across much of northwestern Siberia.

Quantitative estimates of the HTM summer temperature anomaly along the northern margins of Eurasia and adjacent islands typically range from 1 to 3°C. The geographic position of northern treeline across Eurasia is largely controlled by summer temperature and the length of the growing season (MacDonald et al., 2007), and in some areas the magnitude of treeline displacement there suggests a summer warming equivalent in impact to 2.5 to 7.0°C (see for example Birks, 1991; Wohlfarth et al., 1995; MacDonald et al., 2000b; Seppä and Birks, 2001, 2002; Hammarlund et al., 2002; Solovieva et al., 2005). Sea-surface temperature anomalies during the Holocene HTM ranged up to 4 to 5°C higher than the late Holocene for the eastern North Atlantic Sector and adjacent Arctic Ocean (Salvigsen, 1992; Koç et al., 1993). HTM summer temperature anomalies in the western Arctic ranged from 0.5 to 3°C with a mean of 1.65°C, and with the largest anomalies in the North Atlantic sector (Kerwin et al., 1999; Kaufman et al., 2004; Flowers et al., in press).

5.4.9.b Neoglaciation A broad array of climate proxies is available to characterize the overall pattern of Late Holocene climate change. Following the HTM, most proxy summer temperature records from the Arctic indicate an overall cooling trend

through the late Holocene. Cooling is first recognized between 6 and 3 ka ago, depending on the threshold for change of each particular proxy. Records that exhibit a shift by 6 to 5 ka ago typically reflect intensified cooling about 3 ka ago (**Fig. 5.32**).

Cooling during the second half of the Holocene led to the expansion of mountain glaciers and ice caps around the Arctic. The term “Neoglaciation” is widely applied to this episode of glacier growth, and in some cases re-formation, following their maximum retreat during the HTM (Porter and Denton, 1967). The former extent of glaciers is inferred from dated moraines and proglacial sediments deposited in lakes and marine settings. For example, ice-rafted detritus (Andrews et al., 1997) and the glacial geologic record (Funder, 1989) indicate that outlet glaciers of the Greenland Ice Sheet advanced between 6 and 4 ka (see Chapter 7). Multiproxy records from ten glaciers or glaciated areas in Norway show evidence for increased activity by 5 ka ago (Nesje et al., 2001; Nesje et al., 2008). Major advances of outlet glaciers of northern Icelandic ice caps begin by 5 ka ago (Stötter et al., 1999; Geirsdottir et al., in press). In the European Arctic, glaciers expanded on Franz Josef Land (Lubinski et al., 1999) and Svalbard (Svendsen and Mangerud, 1997) by 4 ka ago, although sustained growth primarily began around 3 ka ago. An early Neoglacial advance of mountain glaciers is registered in Alaska, most prominently in the Brooks Range, the highest-latitude mountains in the state (Ellis and Calkin, 1984; Calkin, 1988). In southwest Alaska, mountain glaciers in the Ahklun Mountains did not reform until about 3 ka ago (Levy et al., 2003). Neoglacial advances began in Arctic Canada by 5 ka ago (Miller et al., 2005)

Additional evidence of Neoglacial cooling comes from: a reduction in melt layers in the Agassiz Ice Cap (Koerner and Fisher, 1990) and in Greenland (Alley and

Anandakrishnan, 1995); the decrease in $\delta^{18}\text{O}$ values in ice cores including those from the Devon Island (Fisher, 1979) and Greenland (Johnsen et al., 1992) together with indications of cooling from borehole thermometry (Cuffey et al., 1995); the retreat of large marine mammals and warm-water-dependent mollusks from the Canadian Arctic (Dyke and Savelle, 2001); the southward migration of the northern tree line across central Canada (MacDonald et al., 1993), Eurasia (MacDonald et al., 2000a), and Scandinavia (Barnekow and Sandgren, 2001); the expansion of sea-ice cover along the shores of the Arctic Ocean on Ellesmere Island (Bradley, 1990), over Baffin Bay (Levac et al., 2001), and the Bering Sea (Cockford and Frederick, 2007); and the shift in vegetation communities inferred from plant macrofossils and pollen around the Arctic (Bigelow et al., 2003). The assemblage of microfossils and the stable isotope ratios of foraminifera indicate a shift toward colder, lower-salinity conditions about 5 ka ago along the East Greenland Shelf (Jennings et al., 2002) and the western Nordic seas (Koç and Jansen, 1994), suggesting increased influx of sea ice from the Arctic. Where quantitative estimates of temperature change are available, they generally indicate that summer temperature decreased by 1-2°C during this initial phase of cooling.

The general pattern of an early- to middle-Holocene thermal maximum followed by Neoglacial cooling forms a multi-millennial trend that, in most places, culminated in the 19th century. Superposed on the long-term cooling trend were multiple centennial-scale warmer and colder intervals, which are expressed to a varying extent and are interpreted with various levels of confidence in different proxy records. In northern Scandinavia, evidence for notable late Holocene cold intervals prior to the 16th century

includes narrow tree-ring widths (Gr Rudd et al., 2002), lowered tree line (Eronen et al., 2002), and major glacier advances (Karlén, 1988) between 2.6 and 2.0 ka ago.

5.4.9.c The Medieval Warm Period (MWP) Probably the most oft-cited warm interval of the late Holocene is the Medieval Warm Period (MWP). The term originated based on multiple lines of evidence from Western Europe, but is often applied to other regions to refer to any of the relatively warm intervals of various magnitudes that occurred at different times between about 950 and 1200 AD (Lamb, 1977) (**Fig. 5.33**). In the Arctic, evidence for climate variability, including relative warmth, during this interval is based on glacier extents, marine sediments, speleothems, ice cores, borehole temperatures, tree rings, and archaeology. The most consistent records of an Arctic MWP come from the North Atlantic sector of the Arctic. The summit of Greenland (Dahl-Jensen et al., 1998), western Greenland (Crowley and Lowery, 2000), Swedish Lapland (Gr Rudd et al., 2002), northern Siberia (Naurzbaev et al., 2002), and Arctic Canada (Anderson et al., 2008) were all relatively warm around 1000 AD. During Medieval time, Inuit populations moved out of Alaska into the Eastern Canadian Arctic, hunting whale from skin boats in regions perennially ice-covered through the 20th century (McGhee, 2004).

The evidence for Medieval warmth throughout the rest of the Arctic is less clear. However, there are at least some indications of Medieval warmth, including general retreat of glaciers in southeastern Alaska (Reyes et al., 2006; Wiles et al., 2008), and enhanced growth in some high-latitude tree-ring records from Asia and North America (D'Arrigo et al., 2006). However, Hughes and Diaz (1994) argued that the Arctic as a

whole was not anomalously warm throughout Medieval time (also see Bradley et al., 2003a, and National Research Council, 2006). Warmth during the Medieval interval is generally ascribed to lack of explosive volcanoes that produce particles to block the sun, and perhaps to enhanced brightness of the sun (Crowley, 2000; Goosse et al., 2005; also see Jansen et al., 2007); warming around the North Atlantic and adjacent regions may have been linked to changes in oceanic circulation as well (Broecker, 2001).

5.4.9d Climate of the past millennium and the Little Ice Age

Given the importance of understanding climate of the most recent past, and the richness of the available evidence, an intensive scientific effort has resulted in numerous temperature reconstructions for the past millennium (Jones, et al., 1998; Mann et al., 1998; Esper et al., 2002; Crowley et al., 2003; Mann and Jones, 2003; Moberg et al., 2005; Briffa et al., 2001; National Research Council, 2006; Jansen et al., 2007), and especially the last 500 years (Bradley and Jones, 1992; Overpeck et al., 1997). Most of these reconstructions are based on annually resolved proxy records, primarily from tree rings, and are aimed at extracting a record of air temperature change over large regions, or entire hemispheres. Data from Greenland ice cores and a few annually laminated lake sediment records are typically included in these compilations, but few other records of quantitative temperature changes spanning the last millennium are available from the Arctic. In general, the temperature records exhibit broad similarities showing modest warmth during Medieval times, a variable, but cooling climate from about 1250 to 1850 AD, followed by warming as shown by both paleoclimate proxies and the instrumental record.

Less is known about changes in precipitation, which is spatially and temporally more variable than temperature.

The trend toward colder summers after about 1250 AD coincides with the onset of the Little Ice Age (LIA), which persisted until about 1850 AD, although the timing and magnitude of specific cold intervals were different in different places. Proxy climate records, both glacial and non-glacial, from around the Arctic and for the Northern Hemisphere as a whole, show that the coldest sustained interval of the Holocene occurred sometime between about 1500 and 1900 AD (Bradley et al., 2003b). Recent evidence from the Canadian Arctic indicates that the onset of expanding glaciers and ice sheets following recession in Medieval times occurred between 1250 and 1300 AD, with further amplification ~1450 AD (Anderson et al., 2008).

Glacier mass balances across most of the Northern Hemisphere during the Holocene are closely correlated with summer temperature (Koerner, 2005), and the widespread evidence of glacier readvances across the Arctic during the LIA is consistent with estimates from tree rings of summer cooling. The climate history of the LIA has been extensively studied in natural and historical archives, and is well documented in Europe and North America (Grove, 1988). Historical evidence from the Arctic is relatively sparse, but generally agrees with historical records from NW Europe (Grove, 1988). Icelandic written records indicate that the duration and extent of sea ice in the Nordic Seas were high during the LIA (Ogilvie and Jónsson, 2001).

The average temperature of the Northern Hemisphere during the Little Ice Age was less than 1°C lower than the late 20th century (Bradley and Jones, 1992; Hughes and Diaz, 1994; Crowley and Lowery, 2000), but regional effects resulted in variable

temperature anomalies. Little Ice Age cooling appears to have been stronger in the Atlantic sector of the Arctic than in the Pacific (Kaufman et al., 2004), perhaps because ocean circulation promoted the development of sea ice in the north Atlantic, which further amplified LIA cooling there (Broecker, 2001; Miller et al., 2005).

The Little Ice Age also shows evidence of multi-decadal climatic variability, including widespread warming during the mid through late 18th century (e.g., Cronin et al., 2003). Although the initiation of the Little Ice Age and the structure of climate fluctuations during the multi-centennial interval vary around the Arctic, most records show warming beginning in the late 19th century (Overpeck et al., 1997). The end of the Little Ice Age was apparently more uniform both spatially and temporally than its initiation (Overpeck et al., 1997).

The climate change that led to the Little Ice Age is manifested in proxy records other than those that reflect temperature. For example, the LIA was associated with a shift in transport of dust and other chemicals to the summit of Greenland (O'Brien et al., 1995), perhaps related to deepening of the Icelandic low-pressure system (Meeker and Mayewski, 2002). The negative phase of the North Atlantic Oscillation was amplified during the Little Ice Age (Shindell et al., 2001), while in the North Pacific, the Aleutian low was significantly weakened during the Little Ice Age (Anderson et al., 2005; Fisher et al., 2004).

The cooling into the Little Ice Age resulted from the orbital changes as described above, together with increased explosive volcanism, and probably also decreased solar luminosity as recorded by sunspot numbers as far back as 1600 AD (Renssen et al., 2005; Ammann et al., 2007; Jansen et al., 2007).

1577

1578 **5.4.10 Placing 20th Century warming in the Arctic in a millennial**
1579 **perspective**

1580 Much scientific effort has been devoted to learning how 20th-century and
1581 21st-century warmth compares to earlier times (e.g., National Research Council, 2006;
1582 Jansen et al., 2007). Owing to the orbital changes affecting midsummer sunshine (a drop
1583 in June insolation of $\sim 1 \text{ W/m}^2$ at 75°N and 2 W/m^2 at 90°N over the last 1000 years;
1584 Berger and Loutre, 1991), additional forcing was needed in the 20th century to give the
1585 same summertime temperatures as achieved in the Medieval Warm Period.

1586 Globally or even hemispherically averaged, the National Research Council (2006)
1587 found that “Presently available proxy evidence indicates that temperatures at many, but
1588 not all, individual locations were higher during the past 25 years than during any period
1589 of comparable length since A.D. 900.” (p. 3); greater uncertainties for hemispheric or
1590 global reconstructions were identified in assessing older comparisons. As reviewed next,
1591 some similar results are available for the Arctic.

1592 Thin, cold ice caps in the Eastern Canadian Arctic preserve intact the vegetation
1593 beneath them that was killed during ice-cap inception. As these ice caps melt, they
1594 expose this dead vegetation, which can be dated by radiocarbon with a precision of a few
1595 decades. A recent compilation of over 50 radiocarbon dates on dead vegetation emerging
1596 beneath thin ice caps on northern Baffin Island shows that some ice caps formed more
1597 than 1600 years ago and persisted through Medieval times before melting early in the 21st
1598 century (Anderson et al., 2008).

Melt records from ice caps offer another clear record by which 20th Century warmth can be placed in a millennial perspective. The most detailed record comes from the Agassiz Ice Cap in the Canadian High Arctic, for which the percentage of summer melting of each season's snowfall is reconstructed for the past 10 ka (Fisher and Koerner, 2003). The percent melt follows the general trend of decreasing summer insolation from orbital changes, with some significant brief departures. Of particular note, is the significant increase in melt percent over the past century, with the current values above any other melt intensity since at least 1700 years ago, and more melting than any sustained interval since 4 to 5 ka ago.

As reviewed by Smol and Douglas (2007b), changes in lake sediments record climatic and other changes in the lakes. Extensive changes especially in the post-1850 interval are most easily interpreted in terms of warming above the Medieval warmth on Ellesmere Island and probably in other regions, although other explanations cannot be excluded (also see Douglas et al., 1994). D'Arrigo et al. (2006) show tree-ring evidence from a few North American and Eurasian records pointing to the Medieval Warm Period being cooler than the late 20th century, although the statistical confidence is not extraordinarily high.

Whole-Arctic reconstructions are not yet available to allow confident comparison of late-20th-century warmth to Medieval levels, nor has the work been done to correct for the orbital influence and thus to allow accurate comparison of the remaining forcings.

5.5 Summary

5.5.1 Major features of Arctic Climate over the past 65 Ma

Section 5.4 summarized some of the extensive evidence for changes in Arctic temperatures, and to a lesser extent in Arctic precipitation, over the last 65 million years, together with some discussion of “attribution”—what is the best scientific understanding of the causes of the climate changes. In this subsection, a brief synopsis is provided; for citations, the reader is referred to the extensive discussion just above.

At the start of the Cenozoic, 65 Ma ago, the Arctic was much warmer than recently, with forests growing in all land regions, and no perennial sea ice or Greenland Ice Sheet. Gradual but bumpy cooling has dominated most of the last 65 million years, with falling atmospheric CO₂ concentration apparently the most important contributor to the cooling, although with possible additional contributions from changing continental positions and their effect on atmospheric or oceanic circulation. One especially prominent “bump”, the Paleocene-Eocene Thermal Maximum about 55 Ma ago, caused warming of >5°C in the Arctic Ocean and ~8°C on land, probably in a few centuries to a millennium or so, followed by cooling over ~100 ka; warming from release of much CO₂ (possibly initially as sea-floor methane that was then oxidized to CO₂) is the most-likely explanation. A modest warming in the middle Pliocene (~3 Ma ago) resulted in sufficient warmth that deciduous trees occurred on Arctic land that supports only High Arctic polar desert vegetation at present; whether this was from circulation changes, CO₂, or some other cause remains unclear.

The cooling reached the threshold ~2.7 Ma ago for extensive development of continental ice sheets over the North American and Eurasian Arctic, marking the onset of the Quaternary Ice Age. Initially, the growth and shrinkage of the ice ages were directly controlled by changes in northern sunshine caused by features of Earth’s orbit,

and with the 41-ka cycling of sunshine tied to the obliquity (tilt) of the North Pole especially prominent. More recently, this cycling has continued by a 100 ka cycle has become more prominent, perhaps because the ice sheets became large enough that their behavior became important. Short, warm interglacials (usually lasting 10,000 years, although the one about 440,000 years ago lasted longer) have alternated with longer glacials. Recent work suggests that, in the absence of human influence, the current interglacial would continue for a few tens of thousands of years before start of a new ice age. Although driven by the orbital cycles, the large temperature differences between glacials and interglacials, and the globally synchronous response, reflect the effects of strong positive feedbacks, including changes in atmospheric CO₂ and other greenhouse gases, and in the extent of reflective snow and ice.

Interactions among the various orbital cycles have caused small differences between successive interglacials. The interglacial about 130-120 ka ago had more summer sunshine in the Arctic than in the current interglacial, with temperatures in many places ~4 to 6 °C warmer than recently, leading to reduced ice on Greenland (chapter 7), higher sea level, and widespread loss of small glaciers and ice caps.

The cooling into and warming out of the most recent glacial were punctuated by numerous abrupt climate changes, with millennial persistence of conditions between jumps requiring years to decades. These events were very large around the North Atlantic, with a much smaller effect on temperature elsewhere in the Arctic, and with changes extending to equatorial regions and causing see-saw response in the far south (i.e., warming when the north cooled). Large changes in extent of sea ice in the North

Atlantic were probably responsible, linked to changes in regional to global patterns of ocean circulation; freshening of the North Atlantic favored sea-ice formation.

These abrupt changes also occurred in the current interglacial, the Holocene, but ended as the Laurentide Ice Sheet on Canada melted away. Arctic temperatures in the Holocene broadly responded to orbital changes, with warmer temperatures during the middle Holocene when there was more summer sunshine. Warming generally led to northward migration of vegetation and to shrinkage of ice on land and sea. Small oscillations in climate during the Holocene, including the so-called Medieval Warm Period and the Little Ice Age, were linked to variations in the sun-blocking effect of particles from explosive volcanoes, and perhaps to small variations in solar output or in ocean circulation or other factors. The warming from the Little Ice Age began for largely natural reasons but appears to have been accelerated by human contributions, and especially by increasing CO₂ (Jansen, 2007).

5.5.2. Arctic Amplification

The scientific understanding of climatic processes shows that the Arctic experiences many strong positive feedbacks (Serreze and Francis, 2006; Serreze et al., 2007a). As outlined in section 5.2, these especially involve the interactions of snow and ice with sunlight, the ocean, and the land surface including vegetation. For example, higher temperature tends to remove reflective ice and snow, allowing absorption of more sunshine to cause further warming (ice-albedo feedback). Also, higher temperature tends to remove sea ice that insulates the cold wintertime air from the warmer ocean beneath, further warming the air (ice-insulation feedback). Furthermore, higher temperature tends

to allow dark shrubs to replace low-growing tundra that is easily covered by snow, enhancing the ice-albedo feedback. Similarly strong negative feedbacks are not known to stabilize Arctic climate, so physical understanding indicates that climate changes should be amplified in the Arctic compared to lower-latitude sites. This expectation is confirmed by the available data, as shown in **Figure 5.34**.

In considering Arctic amplification, account must be taken of the forcing. For the three younger time intervals shown in the figure, the Holocene Thermal Maximum (HTM, ~ 6 ka ago), the Last Glacial Maximum (LGM, ~20 ka ago) and marine isotope stage 5e, also known as the last interglacial (LIG, ~130-125 ka ago), the climate changes were primarily forced by the Milankovitch features of Earth's orbit. The anomalies of incoming solar radiation (insolation) averaged over the whole planet and a year are very small for all times considered, with the orbital changes serving primarily to shift sunlight around on the planet. However, during these intervals the insolation forcing was relatively uniform across the Northern Hemisphere, with insolation anomalies north of 60 °N typically only 10 to 20% greater than the anomalies for corresponding times averaged over the Northern Hemisphere. For example, at the peak of the LIG (130-125 ka), the Arctic (60-90 °N) summer (May-June-July) insolation anomaly was 12.7% above present, while the NH anomaly was 11.4% above present (Berger and Loutre, 1991).

To assess the geographic distribution of climate response, we compare Arctic and Northern Hemisphere summer temperature anomalies for the three younger time periods because of the similar forcing for the Arctic and Northern Hemisphere. During the Pliocene (and during earlier warm times discussed below but not plotted in the figure), warmth persisted much longer than the cycling time of insolation changes resulting from

Earth's orbital irregularities (~20 and ~40 ka). Consequently, we compare global temperature anomalies with Arctic anomalies.

A difficulty is that for some of those younger times, global and Arctic estimates of temperature anomalies are available but hemispheric estimates are not. (The global estimates clearly include hemispheric data, but those data have not been summarized in anomaly maps or hemispheric anomaly estimates that were published in the refereed scientific literature.) To obtain hemispheric estimates here, we note (as described in more detail below) that climate models driven by the known forcings show considerable fidelity in reproducing the global anomalies shown by the data for the relevant times, and hemispheric anomalies can be assessed within these models. The hemispheric anomalies so produced are consistent with our understanding of the available data, and so are used here.

The Palaeoclimate Modelling Intercomparison Project (PMIP2; Harrison et al., 2002, and see <http://pmip2.lsce.ipsl.fr/>) coordinates an international effort to intercompare paleoclimate simulations produced by a range of climate models, and to compare these climate model simulations with data-based paleoclimate reconstructions, for a middle Holocene warm time (6 ka ago), and for the last glacial maximum (LGM; 21 ka ago). A comparison of simulations for 6 and 21 ka ago by PMIP is reported by Braconnot et al. (2007).

As part of this PMIP effort, Harrison et al. (1998) compared global (mostly Northern Hemisphere) vegetation patterns simulated using the output of 10 different climate model simulations for 6 ka ago and found close agreement with the vegetation reconstructed from paleoclimatic records. Similar comparisons on a regional basis for

the Northern Hemisphere north of 55 °N (Kaplan et al., 2003), the Arctic (CAPE Project Members, 2001), Europe (Brewer et al., 2007) and North America (Bartlein et al., 1998) also showed close matches between data and models for the early Holocene. Data-model comparisons for the LGM (Bartlein et al., 1998; Kaplan et al., 2003), and Last Interglaciation (CAPE Last Interglacial Project Members, 2006; Otto-Bliesner et al., 2006) reached similar conclusions. (Also see Pollard and Thompson, 1997; Pinot et al., 1999; Farrera et al., 1999; Kageyama et al., 2001.) The close correspondence of paleoclimate data with model simulations of HTM and LIG warmth and LGM cold provides confidence that we can compare climate model simulations of past times with paleoclimate-based reconstructions of summer temperatures for the Arctic to evaluate the magnitude of Arctic amplification. This is done in Figure 5.34, with the details explained in the figure caption. Clearly, however, additional data plus analysis of existing as well as new data would improve confidence in the results and perhaps reduce the error bars.

The forcing of the warmth of the middle Pliocene remains unclear. Orbital oscillations have continued throughout Earth history, but the Pliocene warmth persisted long enough to cross many orbital oscillations, which thus cannot have been responsible for the warmth.

As shown in Figure 5.34, the available data indicate that Arctic temperature anomalies were much larger than global ones. The regression line through the four data points has a slope of 3.6 ± 0.6 , suggesting that the change in Arctic summer temperatures tends to be 3 to 4 times larger than globally.

This trend of larger Arctic anomalies was already well established during the greater warmth of the early Cenozoic peak warming and the Cretaceous before.

Somewhat greater uncertainty is attached to these older times with different continental configurations, so these data are not plotted in Figure 5.34, but the leading result is fully consistent with the regression. Barron et al. (1995) estimated global-average Cretaceous temperatures $\sim 6^{\circ}\text{C}$ warmer than recently. As reviewed by Alley (2003) (also see Bice et al., 2006), subsequent work suggests upward revision of tropical sea-surface temperatures by up to a few degrees. The Cretaceous peak warmth seems to have been somewhat higher than early-Cenozoic values, or perhaps similar (Zachos et al., 2001). In the Arctic, as discussed in section 5.4.1, the early Cenozoic (late Paleocene) included temperatures probably mostly recording summertime conditions of $\sim 18^{\circ}\text{C}$ in the ocean and $\sim 17^{\circ}\text{C}$ on land, followed by warming during the short-lived Paleocene-Eocene Thermal Maximum to $\sim 23^{\circ}\text{C}$ in the ocean and 25°C on land (Sluijs et al., 2006; 2008; Moran et al., 2006; Weijers et al., 2007), with no evidence of wintertime ice, and with indications that temperatures remained higher than during the mid-Pliocene. Recently, the oceanic site has remained ice-covered and near or below freezing during the summer, with much colder temperatures in winter; hence, changes in the Arctic were much larger than for the globally averaged change.

We have not included quantitative estimates in Figure 5.34 for the pre-Pliocene warm times, but a 3-fold Arctic amplification is consistent with the data within the broad uncertainties. The forcing of the Cretaceous and early-Cenozoic warmth seems to have been primarily from increased greenhouse-gas concentration, as discussed above, so the Arctic amplification seems to be independent of the forcing. This is expected; many of the strong Arctic feedbacks serve to amplify temperature change without regard to causation—warmer summer temperatures melt reflective snow and ice, regardless of

whether the warmth came from changing solar output, orbital configuration, greenhouse-gas concentrations, or other causes.

Targeted studies designed to quantitatively assess Arctic amplification of climate change remain relatively rare, and additional clarity could be added. The available data, as assessed here, point to three-fold to four-fold Arctic amplification, such that, in response to the same forcing, Arctic temperature changes are three-fold to four-fold larger than hemispheric-average changes, which are dominated by changes in the much larger lower-latitude regions.

5.5.3 Implications for the future

Paleoclimatology shows that climate has changed greatly in the Arctic over time, and that the changes typically have been much larger in the Arctic than in lower latitudes. Strong feedbacks have been important in these Arctic changes, including the ice-albedo feedback in which cooling grows reflective snow and ice that amplify cooling, or warming causes melting that amplifies warming. Changes in sea-ice coverage of the Arctic Ocean have also been critical—open water cannot fall below the freezing point, but air over ice-covered water can become very cold in the dark Arctic winter, allowing changes in sea-ice coverage to cause perhaps the largest temperature changes observed on the planet (see, e.g., Denton et al., 2005).

Importantly, these feedbacks have served to amplify climate changes with different causes, including those forced primarily by greenhouse-gas changes, consistent with physical understanding of the nature of the feedbacks. Simple analogy, together with physical understanding, then indicate that climate changes will continue to be

1805 amplified in the Arctic. In turn, this indicates that continuing greenhouse-gas forcing of
1806 global climate or other human influences will change climate more in the Arctic than in
1807 lower-latitude regions.
1808

FIGURE CAPTIONS

Figure 5.1 Sea ice median extent for September, 2007, compared to averaged intervals over recent decades including 1953-2000 (red curve). 1979 to 2000 (orange curve) and for September 2005 (green curve). Sea ice extent time series plotted in square kilometers shown from 1953 to 2007 in the graph below (Stroeve et al, 2008). The reduction in Arctic Ocean summer sea ice in 2007 outpaced the most recent predictions from available climate models.

Figure 5.2 Projected surface temperature changes for the last decade of the 21st century (2090-2099) relative to the period 1980-1999. The map shows the IPCC multi-AOGCM average projection for the A1B (balanced emphasis on all energy resources) scenario. The most significant warming is projected to occur in the Arctic. (IPCC, 2007; Figure SPM6)

Figure 5.3 Global mean observed near-surface air temperatures for the month of January, 2003 derived from the Atmospheric Infrared Sounder (AIRS) data. Contrast between equatorial and Arctic temperatures is greatest during the northern hemisphere winter. The transfer of heat from the tropics to the polar regions is a primary feature of the Earth's climate system.

(Source: http://www-airs.jpl.nasa.gov/graphics/features/airs_surface_temp1_full.jpg, 0°C=273.15 Kelvin)

Figure 5.4 Albedo values in the Arctic

5a. AVHRR-derived Arctic albedo values in June, 1982-2004 multi-year average, showing the strong contrast between snow and ice covered areas (green through red) and open water or land (blue). (Courtesy of X. Wang, University of Wisconsin-Madison, CIMSS/NOAA)

5b. Cartoon illustrating albedo feedbacks. Albedo is a fraction of the incident sunlight that is reflected back. Snow, ice, and glaciers have high albedo. Dark objects like the open ocean has low albedo (about 0,06), absorbing some 93% of the suns energy. Bare

ice has an albedo of 0.5 however sea ice covered with snow has an albedo of nearly 90%
(Source: <http://nsidc.org/seaice/processes/albedo.html>).

Figure 5.5 Changes in vegetation cover across the Arctic region can influence albedo, altering the onset of snow melt in the shoulder seasons of spring and fall. A) Progression of the melt season in Northern Alaska in May 2001 (top) and May 2002 (bottom) demonstrates how areas with exposed shrubs show earlier snow melt. B) Example of the altered albedo showing dark branches against reflective snow surface (Sturm et al., 2005; picture courtesy of Matt Sturm).

Figure 5.6 Permafrost, or permanently frozen ground, shows a clear warming trend over recent decades in sites throughout the Arctic, however, local effects can cause perturbations in this trend. Shown here are selective sites in the Northern Hemisphere, including: A. Alaska: WD-West Dock; DH-Deadhorse; FB-Franklin Bluffs; HV-Happy Valley; LG-Livengood; GK-Gulkana; BL-Birch Lake; OM-Old Man. B. Northwest Canada: WG-Wrigley; NW-Norman Wells; NA-Northern Alberta; FS-Fort Simpson. C. European Russia: VT-Vorkuta; RG-Rogovoi; KT-Karataikha; MB-Mys Bolvansky. D. Northwest Siberia: UR-Urengoi; ND-Nadym. E. Yakutia: TK-Tiksi; YK-Yakutsk. F. Central Asia: KZ-Kazakhstan; MG-Mongolia (Brown and Romanovsky, in press)

Figure 5.7 Inflows and outflows of water in the Arctic Ocean. Red lines show the components and paths of the surface and Atlantic Water layer in the Arctic. Black arrows show the pathways of Pacific water inflow from 50-200 m depth. Blue arrows denote surface water circulation; major river inflow is shown in green. Red arrows show the movements of the density driven Atlantic water and intermediate water masses into the Arctic.. (AMAP, 1998).

Figure 5.8 Fossil pollen assemblages can be used to reconstruct habitats based on the modern climatic range of the collective species. This change can then be used to estimate past temperatures or the seasonality of a particular site. Correlation of global sea level

curve (Lambeck et al., 2002), northern hemisphere summer insolation (Berger and Loutre, 1991,) and the Greenland Ice Sheet (GISP2) $\delta^{18}\text{O}$ record (Grootes et al., 1993), ages all given in calendar years. The GISP2 record also shows the timing of Heinrich events (H1, H2 etc.) and numbered Dansgaard/Oschege events. The bottom panel shows temporal changes in the percentages of the main taxa of trees and shrubs, herbs and spores at Elikchan 4 Lake in the Magadan region of Chukotka, Russia. The base of this core is roughly 60 ka BP (Lozhkin and Anderson, 1996) but the record shows that during the period from roughly 27 ka to nearly 55 ka, vegetation, especially treeline recovered over short intervals to nearly Holocene conditions at the same time the isotopic record in Greenland suggests repeated warm cold cycles of change. Note that lake core axis is depth, and not time (Brigham-Grette et al., 2004)

Figure 5.9 14 Microscopic marine plankton known as foraminifera (inset example) grow a shell of calcium carbonate (CaCO_3) in isotopic equilibrium or near equilibrium with ambient sea water. The oxygen isotopic ratio measured in these shells (expressed in $\delta^{18}\text{O}$ parts per million (ppm) = $10^3[(R_{\text{sample}}/R_{\text{standard}})-1]$, where $R_x = (^{18}\text{O})/(^{16}\text{O})$ is the ratio of isotopic composition of a sample compared to that of an established standard, such as ocean water), can be used to determine the temperature of the surrounding waters. However a number of factors, other than temperature, can influence the ratio of ^{18}O to ^{16}O . While warmer temperatures will produce a more negative (lighter) $\delta^{18}\text{O}$ ratio, glacial meltwater and river runoff with depleted values will also produce lighter values. On the other hand, cooler temperatures or higher salinity waters will drive the ratio up, making it heavier, or more positive. The growth of large continental ice sheets selectively removes the lighter isotope (^{16}O), leaving the ocean enriched in the heavier isotope (^{18}O).

Figure 5.10 Open and closed lake systems across the arctic regions differ hydrologically according to the balance between inflow, outflow and the ratio of precipitation to evaporation. These parameters dominate factors influencing lake stable isotopic chemistry as well as the depositional character of the sediments and organic matter. Lake El'gygytyn in the arctic Far East of Russia is annually open and flows to the Bering Sea

during July and August, but the outlet closes by early September as lake level drops and storms move beach gravels to choke the outlet. (Brigham-Grette photo).

Figure 5.11 Locations of Arctic and sub-Arctic lakes (blue) and ice cores (green) for which oxygen isotope records documenting Holocene paleoclimate have been constructed. Map adapted from the Atlas of Canada, © 2002. Her Majesty the Queen in Right of Canada, Natural Resources Canada. / Sa Majesté la Reine du chef du Canada, Ressources naturelles Canada.

Figure 5.12 a) One meter section of the Greenland Ice Core Project core from a depth of 1837 meters showing annual layers. (Source: Courtesy of Eric Cravens, Assistant Curator, U.S. National Ice Core Laboratory). b) Field site of Summit Station on the top of the Greenland Ice sheet (photo by Michael Morrison, GISP2 SMO, University of New Hampshire; NOAA Paleoslide Set)

Figure 5.13 Relationship between the isotopic composition of precipitation and temperature in the colder parts of the world where ice sheets exist. Data from the International Atomic Energy Agency (IAEA) network (Fricke and O'Neil, 1999; calculated as the means of the summer and winter data of their Table 1 for all sites with complete data), and from Greenland (x; Johnsen et al., 1989) and Antarctica (+; Dahe et al., 1994). For the IAEA data, open squares are poleward of 60° latitude (but with no inland ice-sheet sites), open circles from 45° to 60°, and filled circles equatorward of 45°. About 71% of the Earth's surface area is equatorward of 45°, where dependence of $\delta^{18}\text{O}$ on temperature is weak to nonexistent. Only 16% of Earth's surface falls in the 45° to 60° band, with only 13% poleward of 60°. The linear array is clearly dominated by data from the ice sheets.

Figure 5.14 Paleotemperature estimates of site and source waters from Greenland: GRIP and NorthGrip Masson-Delmotte et al., 2005). GRIP (left) and NorthGRIP (right) site(top) and source (bottom) temperatures derived from GRIP and NorthGRIP $\delta^{18}\text{O}$ and

deuterium excess corrected for seawater $\delta^{18}\text{O}$ (until 6000 BP). Shaded lines show an estimate of the uncertainties due to the tuning of the isotopic model and the analytical precision. Solid line is GRIP temperature derived from the borehole temperature profile (Dahl-Jensen et al., 1998).

Figure 5.15 Biomarker alkenone. U_{37}^K versus measured water temperature for surface mixed layer (0–30 m) samples. (a) Atlantic region. The empirical 3rd order polynomial regression for samples collected in $>4^\circ\text{C}$ waters, excluding outlier data from the southwest Atlantic margin and northeast Atlantic upwelling regime, is $U_{37}^K = 1.004 \times 10^{-4}T^3 + 5.744 \times 10^{-3}T^2 - 6.207 \times 10^{-2}T + 0.407$ ($r^2 = 0.98$, $n = 413$). (b) Pacific, Indian, and Southern Ocean regions. The empirical linear regression of Pacific samples is $U_{37}^K = 0.0391T - 0.1364$ ($r^2 = 0.97$, $n = 131$). Pacific regression does not include the Indian and Southern Ocean data. (c) Global data. The empirical 3rd order polynomial regression, excluding anomalous southwest Atlantic margin data, is $U_{37}^K = 5.256 \times 10^{-5}T^3 + 2.884 \times 10^{-3}T^2 - 8.4933 \times 10^{-2}T + 9.898$ ($r^2 = 0.97$, $n = 588$). Samples excluded from the regressions are shown by crosses. (Conte et al, 2006)

Figure 5.16 Diatom assemblages reflect a variety of environmental conditions in Arctic lake systems. Transitions, especially rapid change from one assemblage to another can reflect large changes in light conditions, nutrient availability and/or temperature, for example. Biogenic silica, dominated by the silica skeletal framework constructed by diatoms, is commonly measured in lake sediments as a measure of past changes in aquatic primary productivity.

Figure 5.17 Ice and snow cover often play an important role in influencing the physical, chemical, and biological characteristic of Arctic lakes. This schematic shows changing ice and snow conditions on an Arctic lake during relatively (a) cold, (b) moderate, and (c) warm conditions. During colder years, a permanent raft of ice may persist throughout the short summer, precluding the development of large populations of phytoplankton, and restricting much of the primary production to the shallow, open water moat. Many other

physical, chemical and biological changes occur in lakes that are either directly or indirectly affected by snow and ice cover (see Table 1; Douglas and Smol 1999). Modified from Smol (1988).

Figure 5.18 Lake ice melts as it continues to warm (A – D). Eventually, in deeper lakes (vs ponds) thermal stratification may also occur (or be prolonged) during the summer months (D), further altering the limnological characteristics of the lake. Modified from Douglas (2007).

Figure 5.19 The form and distribution of wind-blown silt (loess), wind-blown sand (dunes), and other deposits of wind-blown sediment in Alaska, have been use to infer both Holocene and last-glacial past wind directions. (Compiled from multiple sources by Muhs and Budahn, 2006).

Figure 5.20 At this unnamed, hydrologically closed lake in the Yukon Flats Wildlife Refuge in Alaska, concentric rings of vegetation have developed progressively inward as water levels lowered due to a negative change in the lake's overall water balance. Historic Landsat imagery and air photographs indicate that these shorelines formed during the last ~40 years. (Photo by Lesleigh Anderson)

Figure 5.21 Recovered sections and palynological and geochemical results across the Paleocene-Eocene Thermal Maximum ~55 million yrs ago of IODP Hole 302-4A (87° 52.00' N; 136° 10.64' E; 1,288 m water depth, in the central Arctic Ocean basin). Mean annual surface water temperatures (as indicated in the TEX₈₆' column) are estimated to have reached 23°C similar to waters in the tropics today. [Error bars for Core 31X show the uncertainty of its stratigraphic position. Orange bars indicate intervals affected by drilling disturbance.] Stable carbon isotopes are expressed relative to the PeeDee Belemnite standard. Low-salinity-tolerant dinocysts comprise *Senegalinium* spp., *Cerodinium* spp., and *Polysphaeridium* spp., while *Membranosphaera* spp., *Spiniferites ramosus* complex, and *Areoligera-Glaphyrocysta* cpx. represent the typical

normal marine species. Arrows and *A. aug* (second column) indicate the first and last occurrences of dinocyst *Apectodinium augustum* – a diagnostic indicator of PETM warm conditions. (Sluijs et al., 2006)

Figure 5.22 Atmospheric CO₂ and continental glaciation 400 Ma to present. Vertical blue bars mark the timing and palaeolatitudinal extent of ice sheets (after Crowley, 1998). Plotted CO₂ records represent five-point running averages from each of the four major proxies (see Royer, 2006 for details of compilation). Also plotted are the plausible ranges of CO₂ from the geochemical carbon cycle model GEOCARB III (Berner and Kothavala, 2001). All data have been adjusted to the Gradstein et al. (2004) time scale. Extensive growth of continental ice sheets occurs when CO₂ is low. (source: Jansen, 2007: Figure 6.1)

Figure 5.23 The average isotopic composition ($\delta^{18}\text{O}$) of bottom-dwelling foraminifera from a globally distributed set of 57 sediment cores covering the last 5.3 Ma (modified from Lisiecki and Raymo, 2005). The $\delta^{18}\text{O}$ is controlled primarily by global ice volume and deep-ocean temperature, with less ice and/or warmer temperatures upward. The influences of all the Milankovitch frequencies of Earth's orbital variation are present throughout, but the increase in glaciation about 2.7 Ma ago occurred with establishment of a strong 41 ka variability linked to Earth's obliquity (changes in tilt of Earth's spin axis), and the additional increase in glaciation about 1.2-0.7 Ma involved a shift to stronger 100 ka variability. Dashed lines are used because the changes seem to have been somewhat gradual. The general trend toward higher $\delta^{18}\text{O}$ that runs through this series reflects the long-term drift toward a colder Earth that began in the early Cenozoic (see Fig. 4.8).

Figure 5.24 a) Greenland without ice for the last time? Dark green: boreal forest, light green: deciduous forest; brown: tundra and alpine heaths; white: ice caps. The north-south temperature gradient is constructed from a comparison between North Greenland and NW European temperatures, using standard lapse rate, and assuming precipitation

distribution after the same pattern as known from the Holocene. The topographical base comes from the model by Letreguilly et al. 1991 of Greenland's sub-ice topography after isostatic recovery. b) Upper part of the Kap København Formation, North Greenland. The sand was deposited in an estuary 2.4 Ma ago, and contain abundant well preserved leaves, seeds, twigs, and insect remains. (Photograph of S.V. Funder).

Figure 5.25 The largely marine Gubik Formation on the North Slope of Alaska contains three superposed lower units recording relative sea level as high +30-+40 m. Pollen in these same deposits suggest that borderland vegetation at each of these times was less forested with boreal forests or spruce-birch woodlands at 2.7 Ma giving way to larch and spruce forests at about 2.6 and open tundra by ca. 2.4 Ma (see photos with oldest at the top from Robert Nelson, Colby College who did the pollen work). Isotopic reference time series of Lisecki and Raymo (2005) suggests best as assignments for these sea level events (Brigham and Carter, 1992).

Figure 5.26 Glacial cycles over the past 800ka derived from marine-sediment and ice cores (McManus, 2004). The history of deep-ocean temperatures and global ice volume is inferred from $\delta^{18}\text{O}$ measured in bottom-dwelling foraminifera shells preserved in Atlantic Ocean sediments. Air temperatures over Antarctica are inferred from the ratio of deuterium to hydrogen in ice from central Antarctica (EPICA, 2004). Marine Isotope Stage 11 (MIS 11) is an interglacial with similar orbital parameters to the Holocene, yet lasted about twice as long as most interglacials. Note the smaller magnitude and less-pronounced interglacial warmth of the glacial cycles that preceded MIS 11.

Interglaciations older than MIS 11 were less warm than subsequent interglaciations.

Figure. 5.27 Polar projection from CAPE Last Interglacial Project Members (2006) showing regional maximum LIG summer temperature anomalies relative to present derived from paleotemperature proxies (see tables 1 and 2 in from CAPE Last Interglacial Project Members, 2006). Terrestrial sites in circles, marine sites in squares.

Figure 5.28 Fossiliferous paleoshorelines and marine sediments were used by Brigham-Grette and Hopkins (1995) to evaluate the seasonality of coastal sea ice on both sides of

the Bering Strait during the Last Interglaciation. The winter sea limit is estimated to have been north of the narrowest section of the strait, 800 km north of modern limits. Lozhkin and Anderson (1995) suggest from pollen data derived from Last Interglacial lake sediments that tundra was nearly eliminated from the Russian coast at this time. More open water resulted in an increase in some taxa tolerant of deeper winter snows in Chukotka during the warm interglaciation. (Map of William Manley <http://instaar.colorado.edu/QGISL/>).

Figure 5.29 The Arctic Holocene Thermal Maximum (HTM) as expressed in a comparison of seasonal insolation patterns at 70° N (Berger & Loutre 1991), reconstructed Greenland air temperature from the GISP2 drilling project (Alley 2000), the age distribution of radiocarbon-dated fossil remains of different tree genera from north of present treeline (MacDonald et al., 2007), and the frequency of Western Arctic sites experiencing HTM conditions. (Kaufman et al. 2004)

Figure. 5.30 The timing of initiation and termination of the HTM in the Western Arctic (Kaufman et al., 2004).

- a. Regions reviewed in Kaufman et al. 2004
- b. Initiation of the Holocene thermal maximum in the western Arctic. Longitudinal distribution (left) and frequency distribution (right)
- c. Spatio-temporal pattern of the Holocene thermal maximum (HTM) in the western Arctic. Initiation (upper) and termination (lower) of the HTM. Gray dots indicate equivocal evidence for the HTM. Dot colors indicate bracketing ages of the HTM, which are contoured using the same color scheme

Figure. 5.31 The northward extension of larch (*Larix*) across the Eurasian Arctic during the HTM compared to present treeline larch forest distribution and anticipated (Arctic Climate Impact Assessment, 2005) northern forest limits due to climate warming (MacDonald et al., 2007).

Fig. 5.32 Upper panel: The record of summer melting on the Agassiz Ice Cap, northern Ellesmere Island, Canada over the course of the Holocene. Melt indicates the fraction of each core section containing evidence of melting (from Koerner and Fisher, 1990). Middle panel: Summer temperature anomalies estimated from the elevation of ^{14}C dated sub-fossil pine wood samples (*Pinus sylvestris* L.) in the Scandes mountains, central Sweden (black bars) relative to temperatures at the modern pine limit in the region. Upper limit of pine growth is indicated by the dashed line. Changes in temperature were estimated by assuming a lapse rate of $6\text{ }^{\circ}\text{C km}^{-1}$ (from Dahl and Nesje 1996, based on samples collected by L. Kullman and G. and J. Lundqvist). Lower panel: Paleotemperature reconstruction from oxygen isotopes in calcite sampled along the growth axis of a stalagmite from a cave at Mo i Rana, in northern Norway. Growth ceased around A.D. 1750. (from Lauritzen 1996; Lauritzen and Lundberg 1998; 2002). Figure from Bradley (2000).

Figure 5.33 Schematic diagrams of temperature variations over the past thousand years. The dotted line nominally represents conditions near the beginning of the twentieth century. From the IPCC AR1 (Fig. 7.1; 1990). Recent reviews (e.g. Bradley et al., 2003) suggest that this curve probably is most representative of the northern North Atlantic region rather than a reflection of global temperature.

Figure 5.34 Paleoclimate data quantify the magnitude of Arctic amplification. Shown are paleoclimate estimates of Arctic summer temperature anomalies relative to recent, and the appropriate northern-hemisphere or global summer temperature anomalies, together with their uncertainties, for the last glacial maximum (LGM; ~20 ka ago), Holocene thermal maximum (HTM; ~8 ka ago), last interglaciation (LIG; 130-125 ka ago) and middle Pliocene (~3.5-3.0 Ma ago). The trend line suggests that summer temperature changes are amplified 3 to 4 times in the Arctic. Explanation of data sources follows, for the different times considered beginning with the most recent.

Holocene Thermal Maximum (HTM): Arctic $\Delta T = 1.7 \pm 0.8\text{ }^{\circ}\text{C}$; NH $\Delta T = 0.5 \pm 0.3\text{ }^{\circ}\text{C}$; Global $\Delta T = 0 \pm 0.5\text{ }^{\circ}\text{C}$.

A recent summary of summer temperature anomalies for the western Arctic (Kaufman et al., 2004) built on earlier summaries (Kerwin et al., 1999; Cape Project Members, 2001), and is consistent with more-recent reconstructions (Kaplan and Wolfe, 2006; Flowers et al., 2007). Although the Kaufman et al. (2004) summary covered only the western half of the Arctic, the earlier summaries by Kerwin et al., (1999) and Cape Project Members (2001) indicated that similar anomalies characterized the Eastern Arctic, with all syntheses reporting the largest anomalies in the North Atlantic sector. Few data are available for the central Arctic Ocean; we assume that the circumpolar dataset provides an adequate reflection of air temperatures across the Arctic Ocean as well.

Climate models suggest that the average planetary anomaly was concentrated over the Northern Hemisphere. Braconnot et al. (2007) summarized the simulations from 10 different climate model contributions to the PMIP2 project that compare simulated summer temperatures 6 ka ago with recent values. The global average summer temperature anomaly 6 ka ago was 0 ± 0.5 °C, whereas the Northern Hemisphere anomaly was 0.5 ± 0.3 °C. These patterns are similar to model results described by Hewitt and Mitchell (1998) and Kitoh and Murakami (2002) for 6 ka ago, and a global simulation for 9 ka (Renssen et al., 2006), that simulate little summer temperature difference outside the Arctic when compared to pre-industrial temperatures.

Last Glacial Maximum (LGM): Arctic $\Delta T = -20 \pm 5$ °C; Global and Northern Hemisphere $\Delta T = -5 \pm 1$ °C

Quantitative estimates of temperature reductions during the peak of the LGM are less widespread in the Arctic than during warm times. Ice-core borehole temperatures offer the most compelling evidence (Cuffey et al., 1995; Dahl-Jensen et al., 1998), with additional support from biological proxies in the North Pacific sector (Elias et al., 1996a), where no ice cores are available that extend back to the LGM. Because of the limited datasets for the LGM temperature reduction in the Arctic, we incorporate a large uncertainty. The global-average temperature decrease during peak glaciations based on paleoclimate proxy data was 5 to 6 °C, with little difference between the two hemispheres (Jansen et al., 2007; Farrera et al., 1999; Braconnot et al., 2007). A similar temperature

anomaly is derived from climate model simulations (Otto-Bliesner et al., 2007).

Last Interglaciation (LIG): Arctic $\Delta T = 5 \pm 1$ °C; Global and NH $\Delta T = 1 \pm 1$ °C)

A recent summary of all available quantitative reconstructions of summer temperature anomalies for the Arctic during peak LIG warmth shows a spatial pattern similar to the HTM reconstructions, with the largest anomalies in the North Atlantic sector and the smallest anomalies in the North Pacific sector, but with substantially larger anomalies (5 ± 1 °C) than during the HTM (CAPE Last Interglacial Project Members, 2006). A similar pattern of LIG summer temperature anomalies is apparent in climate model simulations (Otto-Bliesner et al., 2006). Global and Northern Hemisphere summer temperature anomalies are derived from summaries in CLIMAP Project Members (1984), Crowley (1990), Montoya et al. (2000) and Bauch and Erlenkeuser (2003).

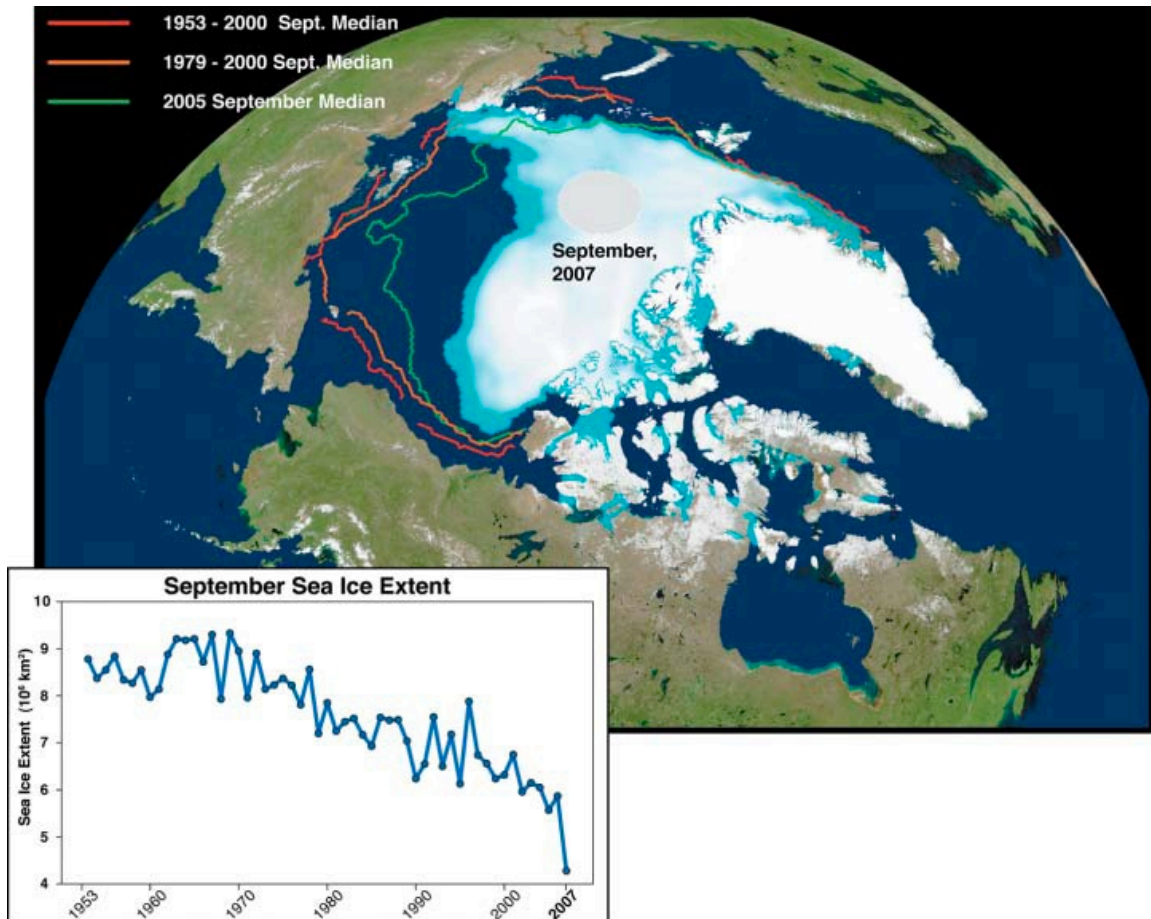
Middle Pliocene: Arctic $\Delta T = 12 \pm 3$ °C; Global $\Delta T = 4 \pm 2$ °C)

The widespread occurrence of forests throughout the Arctic in the middle Pliocene offers a glimpse into a notably warm time in the Arctic, with essentially modern continental configurations and connections between the Arctic Ocean and the global ocean. Reconstructed Arctic temperature anomalies are available from several sites that show much warmth with no summer sea ice in the Arctic Ocean basin. These sites include the Canadian Arctic Archipelago (Dowsett et al., 1994; Elias and Matthews, 2002; Ballantyne et al., 2006), Iceland (Buchardt and Símónarson, 2003), and the North Pacific (Heusser and Morley, 1996). A global summary of mid-Pliocene biomes by Salzmann et al. (2008) concluded that Arctic mean-annual-temperature anomalies were in excess of 10 °C; some sites indicate temperature anomalies up to 15 °C. Estimates of global sea-surface temperature anomalies are from Dowsett (2007).

Global reconstructions of mid-Pliocene temperature anomalies from proxy data and general circulation models show modest warming across low to mid-latitudes, averaging 4 ± 1 °C (Dowsett et al., 1999; Raymo et al., 1996; Sloan et al., 1996; Budyko et al.,

2171 1985; Haywood and Valdes, 2004; Jiang et al. 2005; Haywood and Valdes, 2006;
2172 Salzmann et al., 2008).
2173

2173
2174
2175



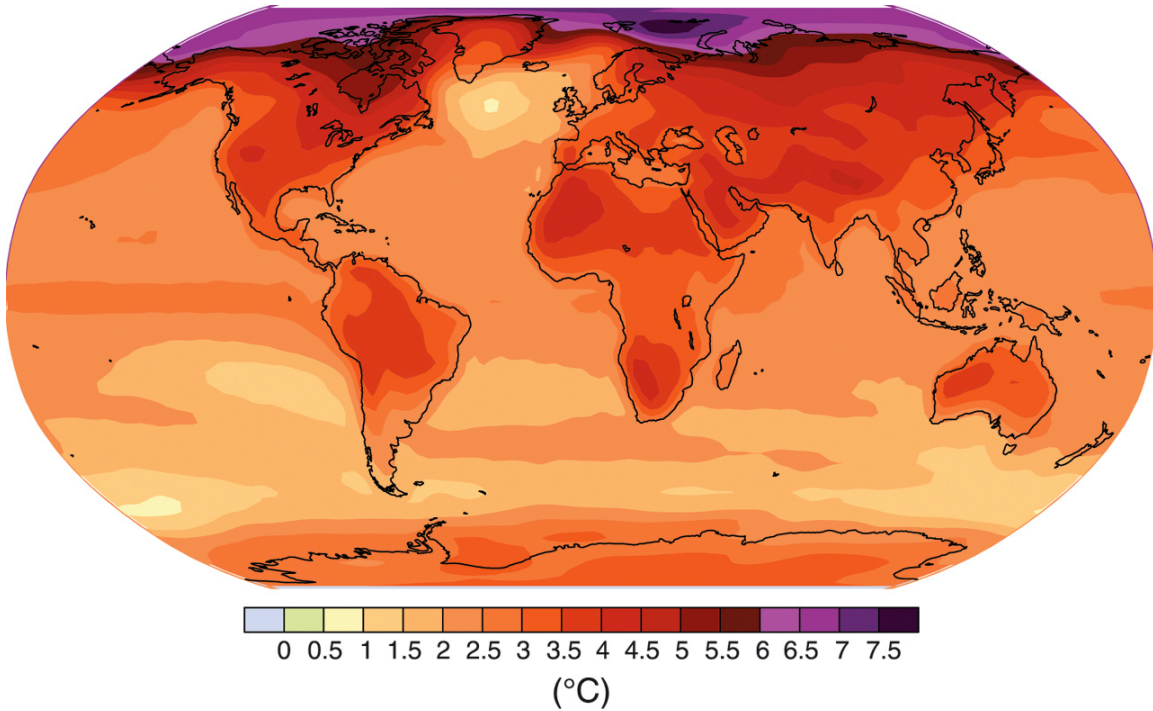
2176
2177
2178
2179
2180
2181
2182
2183

Figure 5.1 Sea ice median extent for September, 2007, compared to averaged intervals over recent decades including 1953-2000 (red curve). 1979 to 2000 (orange curve) and for September 2005 (green curve). Sea ice extent time series plotted in square kilometers shown from 1953 to 2007 in the graph below (Stroeve et al, 2008). The reduction in Arctic Ocean summer sea ice in 2007 outpaced the most recent predictions from available climate models.

2183

2184

Geographical pattern of surface warming

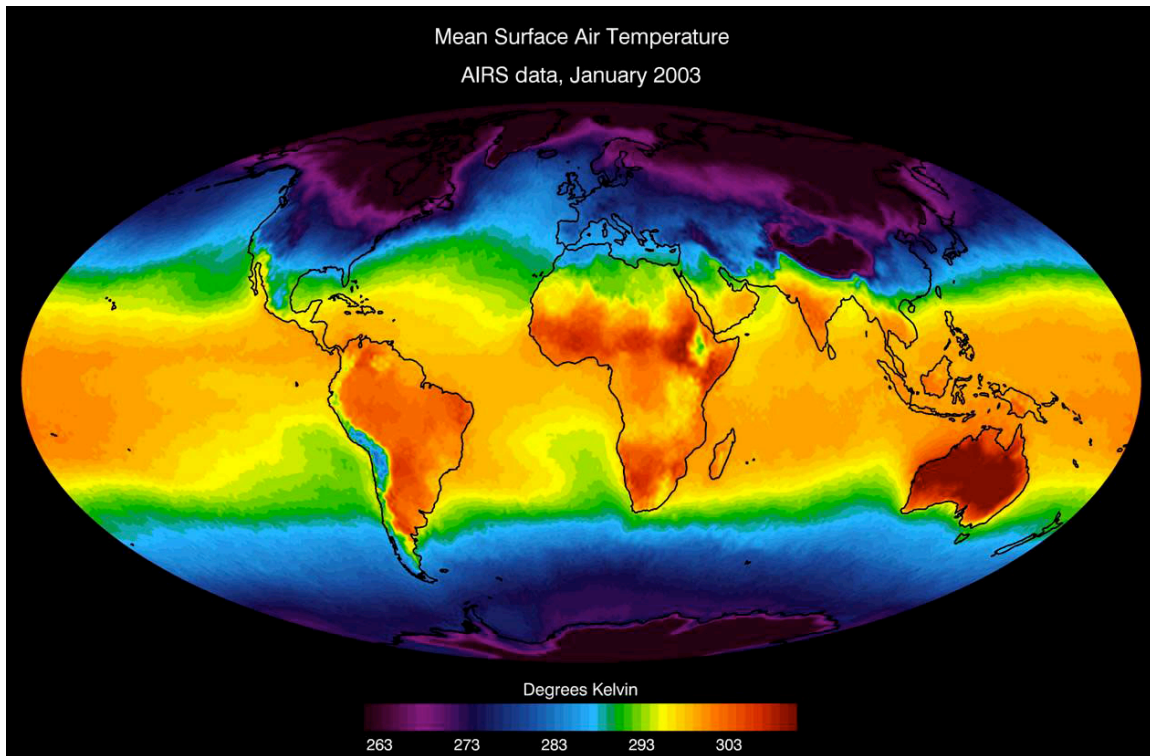


2185

2186 **Figure 5.2** Projected surface temperature changes for the last decade of the 21st century
2187 (2090-2099) relative to the period 1980-1999. The map shows the IPCC multi-AOGCM
2188 average projection for the A1B (balanced emphasis on all energy resources) scenario.
2189 The most significant warming is projected to occur in the Arctic. (IPCC, 2007; Figure
2190 SPM6)

2191

2191



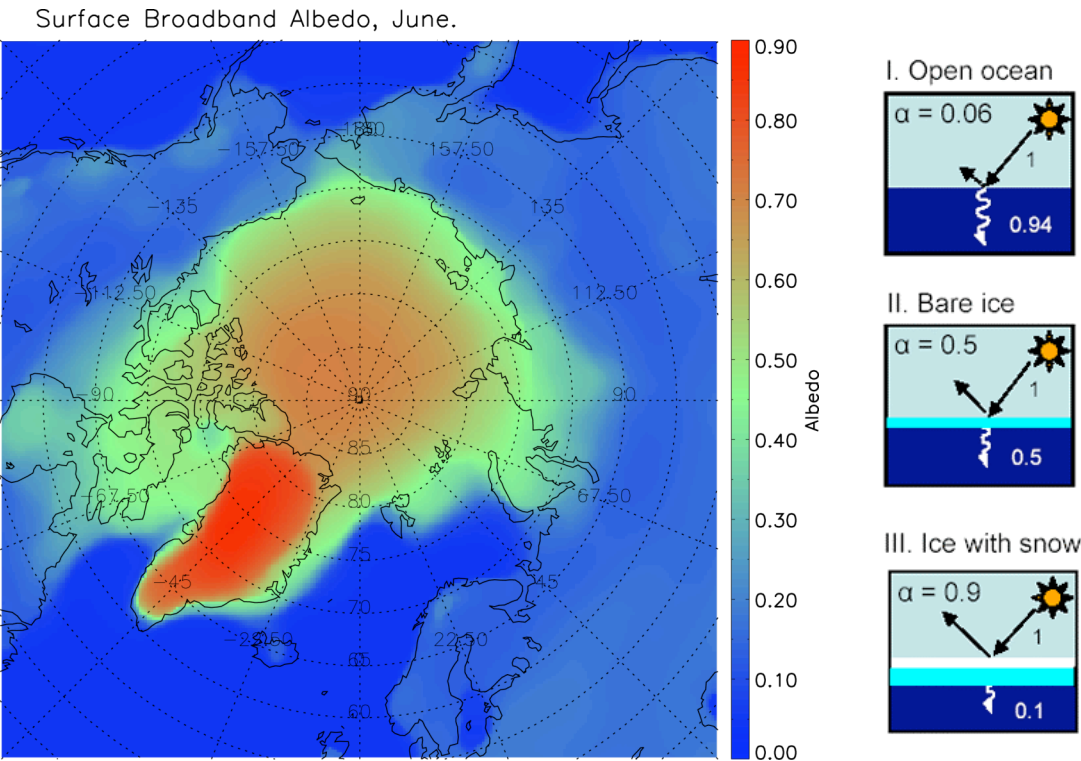
2192

2193 **Figure 5.3** Global mean observed near-surface air temperatures for the month of
2194 January, 2003 derived from the Atmospheric Infrared Sounder (AIRS) data. Contrast
2195 between equatorial and Arctic temperatures is greatest during the northern hemisphere
2196 winter. The transfer of heat from the tropics to the polar regions is a primary feature of
2197 the Earth's climate system ($0^{\circ}\text{C}=273.15$ Kelvin)

2198 (Source: http://www-airs.jpl.nasa.gov/graphics/features/airs_surface_temp1_full.jpg)

2199

2199



2200

2201

a

2202

Figure 5.4 Albedo values in the Arctic

2203

5a. AVHRR-derived Arctic albedo values in June, 1982-2004 multi-year average, showing the strong contrast between snow and ice covered areas (green through red) and open water or land (blue). (Courtesy of X. Wang, University of Wisconsin-Madison, CIMSS/NOAA)

2207

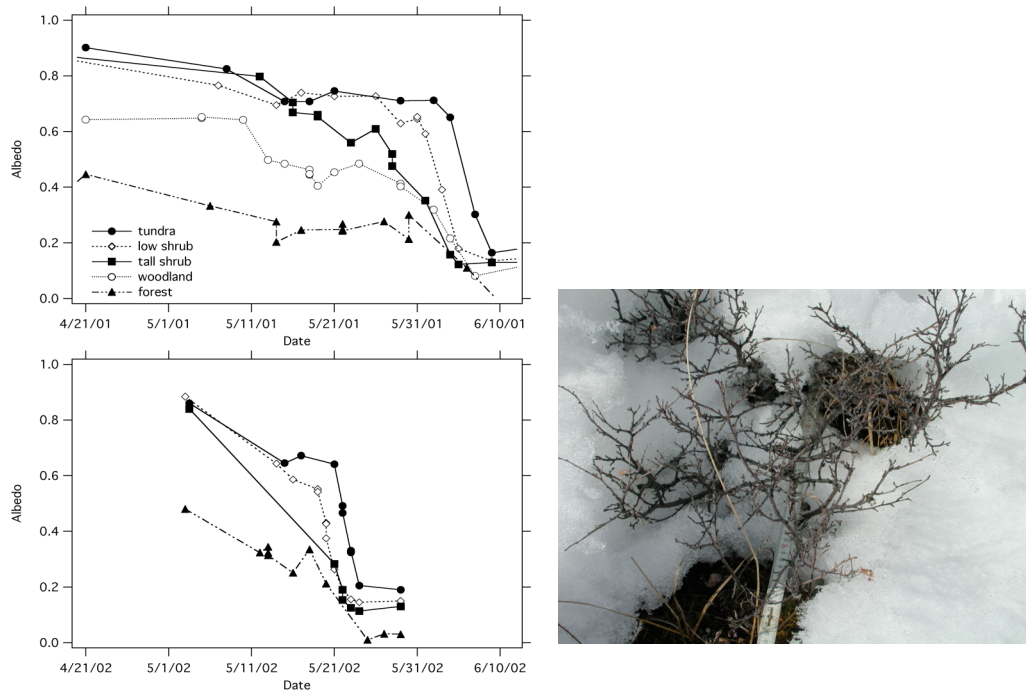
5b. Relative albedo (solar reflectance) of open water, bare ice, and ice covered with snow. The areal distribution and percentages these surfaces at high latitudes exerts a strong influence on the planetary energy balance through the ice-albedo feedback mechanism.

2210

2211

b

2211



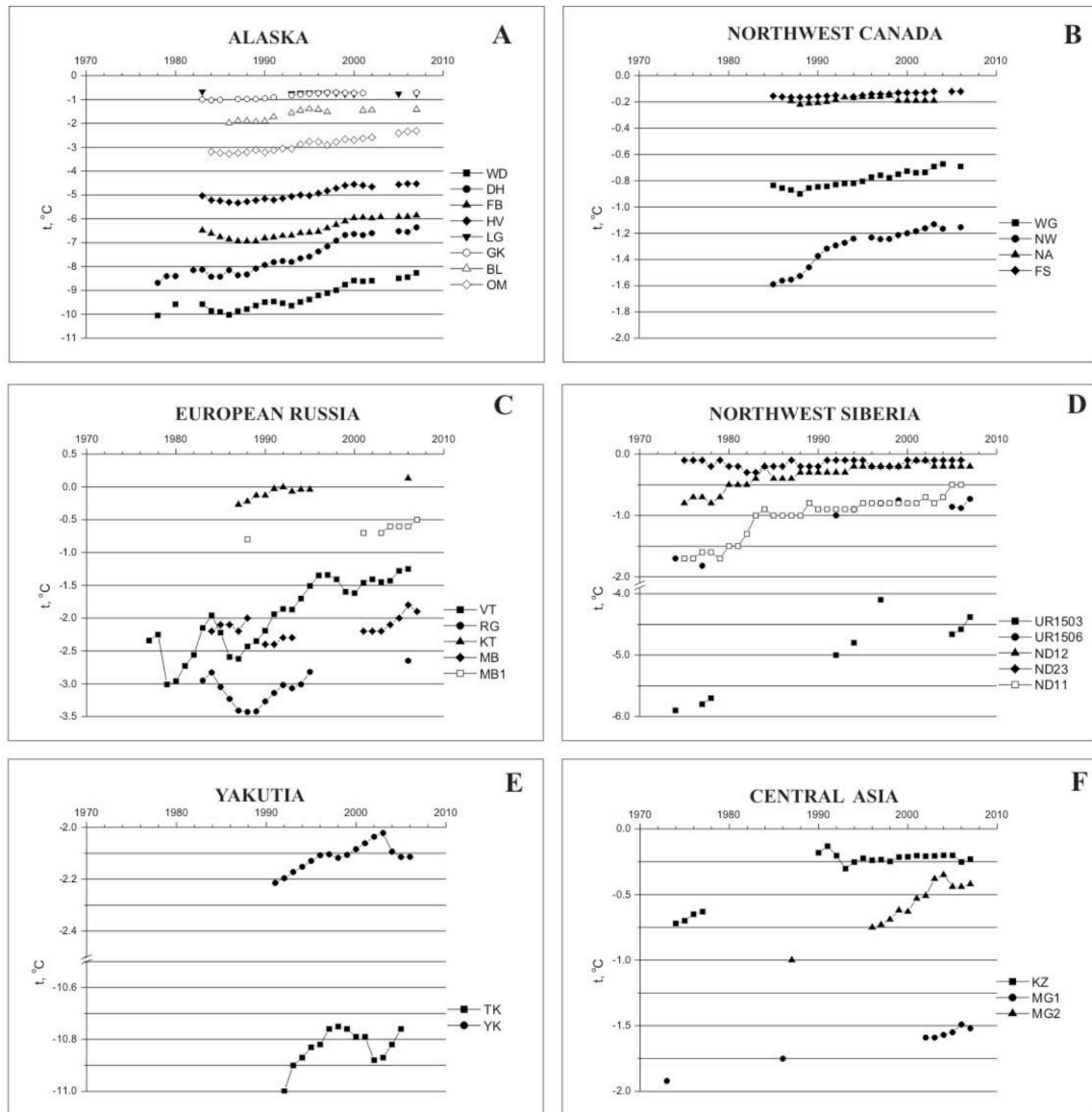
2212

2213

2214 **Figure 5.5** Changes in vegetation cover across the Arctic region can influence albedo,
 2215 altering the onset of snow melt in the shoulder seasons of spring and fall. a) Progression
 2216 of the melt season in Northern Alaska in May 2001 (top) and May 2002 (bottom)
 2217 demonstrates how areas with exposed shrubs show earlier snow melt. b) Example of the
 2218 altered albedo showing dark branches against reflective snow surface (Sturm et al., 2005;
 2219 picture courtesy of Matt Sturm).

2220

2220



2221

2222 **Figure 5.6** Permafrost, or permanently frozen ground, shows a clear warming trend over
 2223 recent decades in sites throughout the Arctic, however, local effects can cause
 2224 perturbations in this trend. Shown here are selective sites in the Northern Hemisphere,
 2225 including: A. Alaska: WD-West Dock; DH-Deadhorse; FB-Franklin Bluffs; HV-Happy
 2226 Valley; LG-Livengood; GK-Gulkana; BL-Birch Lake; OM-Old Man. B. Northwest
 2227 Canada: WG-Wrigley; NW-Norman Wells; NA-Northern Alberta; FS-Fort Simpson. C.

- 2228 European Russia: VT-Vorkuta; RG-Rogovoi; KT-Karataikha; MB-Mys Bolvansky. D.
2229 Northwest Siberia: UR-Urengoi; ND-Nadym. E. Yakutia: TK-Tiksi; YK-Yakutsk. F.
2230 Central Asia: KZ-Kazakhstan; MG-Mongolia (Brown and Romanovsky, in press)
2231

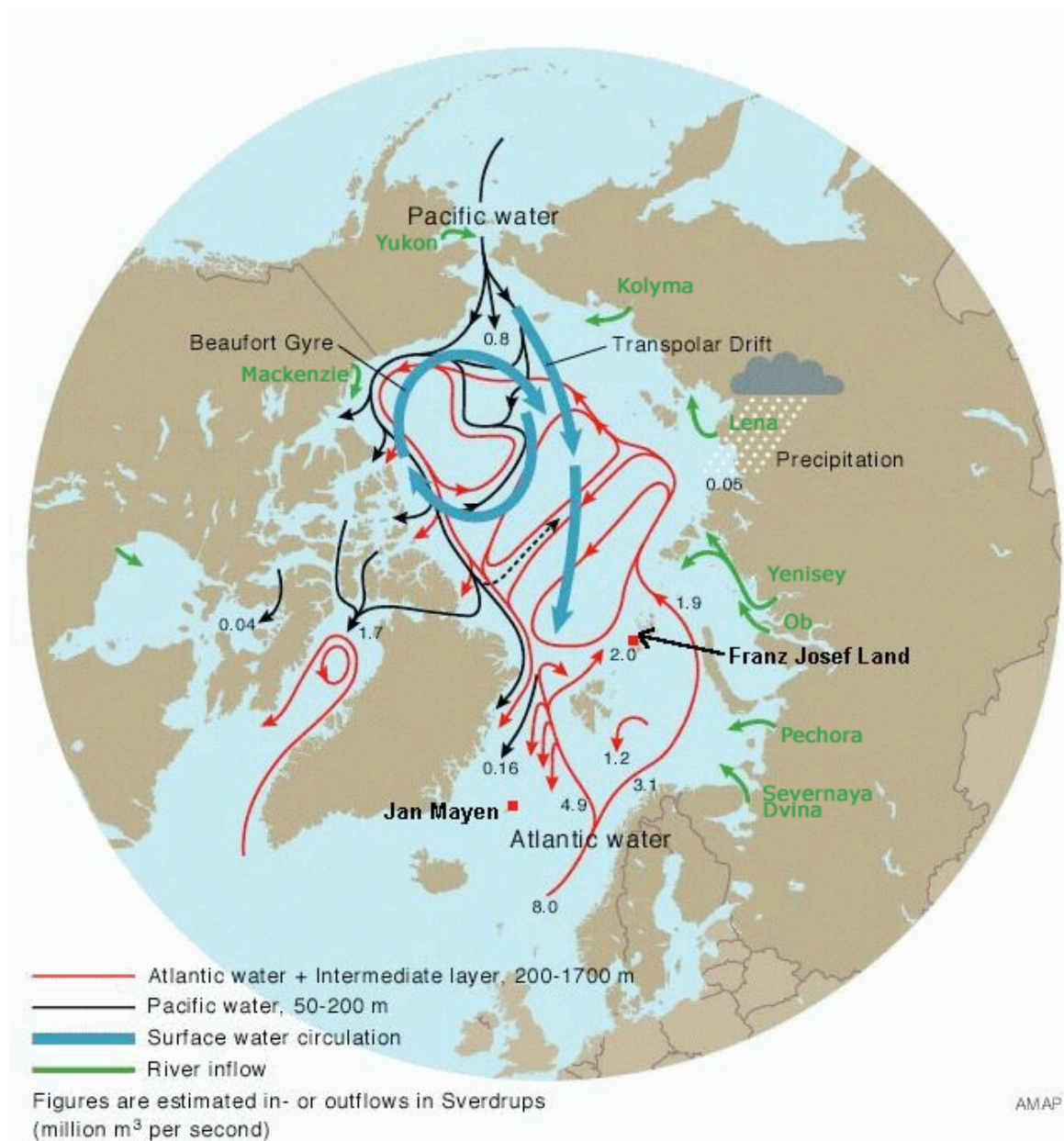
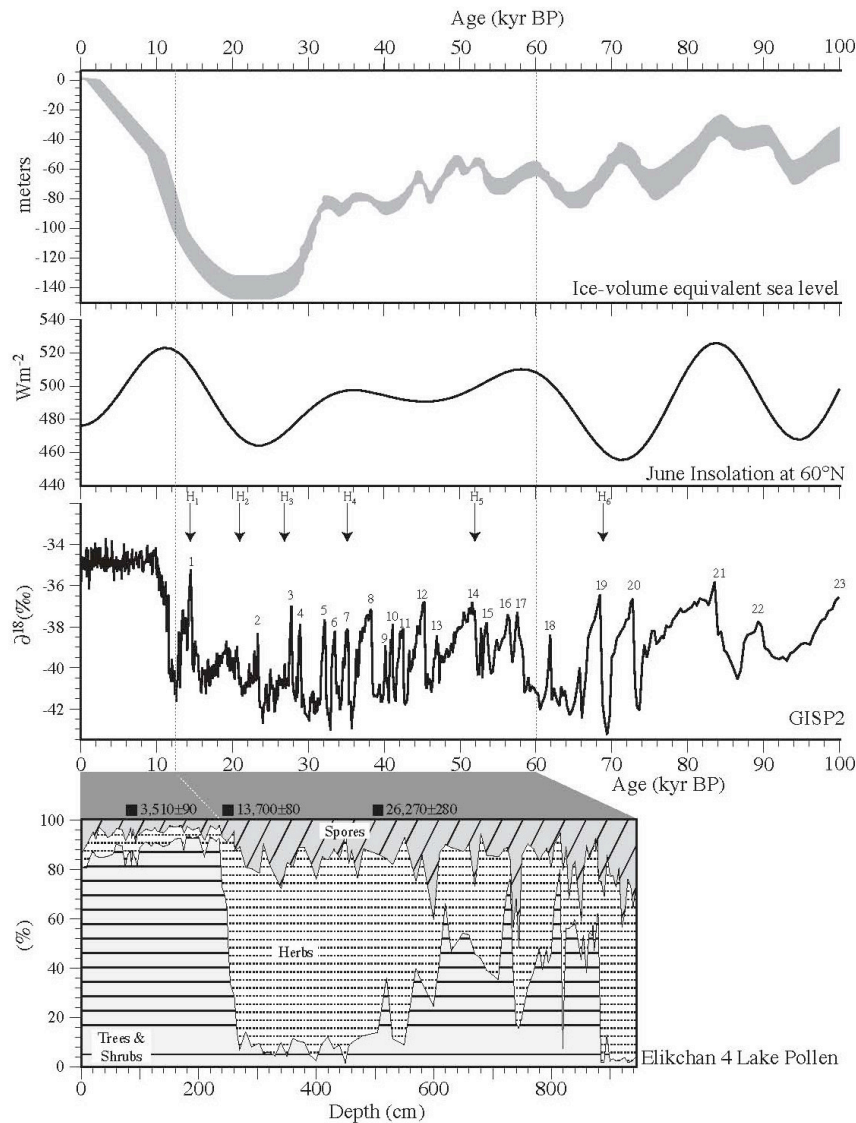


Figure 5.7 Inflows and outflows of water in the Arctic Ocean. Red lines show the components and paths of the surface and Atlantic Water layer in the Arctic. Black arrows show the pathways of Pacific water inflow from 50-200 m depth. Blue arrows denote surface water circulation; major river inflow is shown in green. Red arrows show the movements of the density driven Atlantic water and intermediate water masses into the Arctic. (Source: AMAP, 1998; Macdonald, R.W. and J.M. Bowers, 1996).

2239



2240

2241 **Figure 5.8** Fossil pollen assemblages can be used to reconstruct habitats based on the
 2242 modern climatic range of the collective species. This change can then be used to estimate
 2243 past temperatures or the seasonality of a particular site. Correlation of global sea level
 2244 curve (Lambeck et al., 2002), northern hemisphere summer insolation (Berger and
 2245 Loutre, 1991,) and the Greenland Ice Sheet (GISP2) $\delta^{18}O$ record (Grootes et al., 1993),
 2246 ages all given in calendar years. The GISP2 record also shows the timing of Heinrich
 2247 events (H1, H2 etc.) and numbered Dansgaard/Oscheger events. The bottom panel shows

2248 temporal changes in the percentages of the main taxa of trees and shrubs, herbs and
2249 spores at Elikchan 4 Lake in the Magadan region of Chukotka, Russia. The base of this
2250 core is roughly 60 ka BP (Lozhkin and Anderson, 1996) but the record shows that during
2251 the period from roughly 27 ka to nearly 55 ka, vegetation, especially treeline recovered
2252 over short intervals to nearly Holocene conditions at the same time the isotopic record in
2253 Greenland suggests repeated warm cold cycles of change. Note that lake core axis is
2254 depth, and not time (Brigham-Grette et al., 2004)
2255

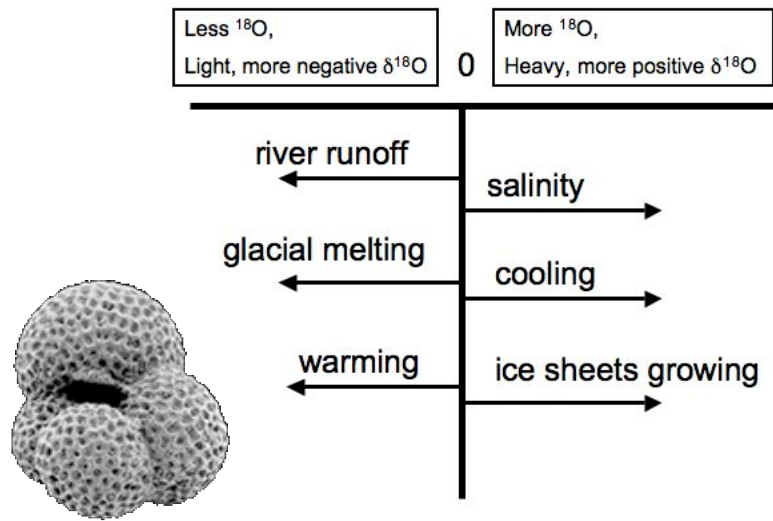


Figure 5.9 14 Microscopic marine plankton known as foraminifera (inset example) grow a shell of calcium carbonate (CaCO_3) in isotopic equilibrium or near equilibrium with ambient sea water. The oxygen isotopic ratio measured in these shells (expressed in $\delta^{18}\text{O}$ parts per million (ppm) = $10^3[(R_{\text{sample}}/R_{\text{standard}})-1]$, where $R_x = (^{18}\text{O})/(^{16}\text{O})$ is the ratio of isotopic composition of a sample compared to that of an established standard, such as ocean water), can be used to determine the temperature of the surrounding waters. However a number of factors, other than temperature, can influence the ratio of ^{18}O to ^{16}O . While warmer temperatures will produce a more negative (lighter) $\delta^{18}\text{O}$ ratio, glacial meltwater and river runoff with depleted values will also produce lighter values. On the other hand, cooler temperatures or higher salinity waters will drive the ratio up, making it heavier, or more positive. The growth of large continental ice sheets selectively removes the lighter isotope (^{16}O), leaving the ocean enriched in the heavier isotope (^{18}O).

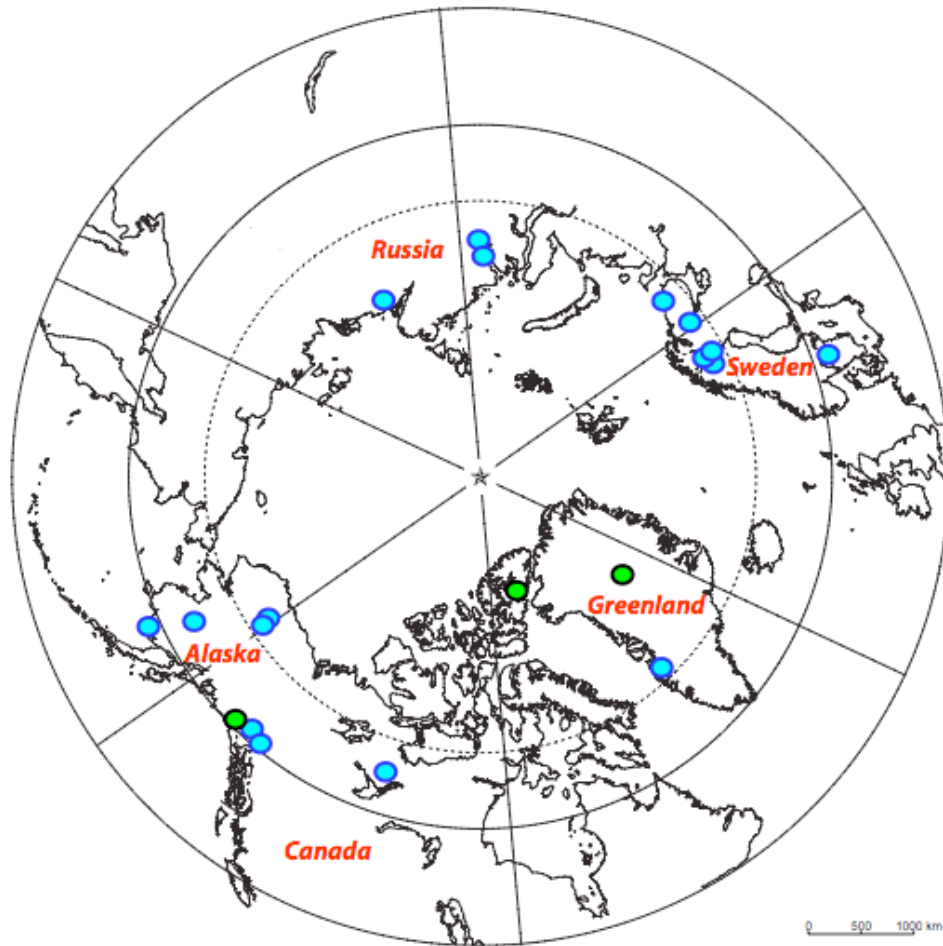
2270



2271

2272 **Figure 5.10** Open and closed lake systems across the arctic regions differ hydrologically
2273 according to the balance between inflow, outflow and the ratio of precipitation to
2274 evaporation. These parameters dominate factors influencing lake stable isotopic
2275 chemistry as well as the depositional character of the sediments and organic matter. Lake
2276 El'gygytgyn in the arctic Far East of Russia is annually open and flows to the Bering Sea
2277 during July and August, but the outlet closes by early September as lake level drops and
2278 storms move beach gravels to choke the outlet. (Brigham-Grette photo).
2279

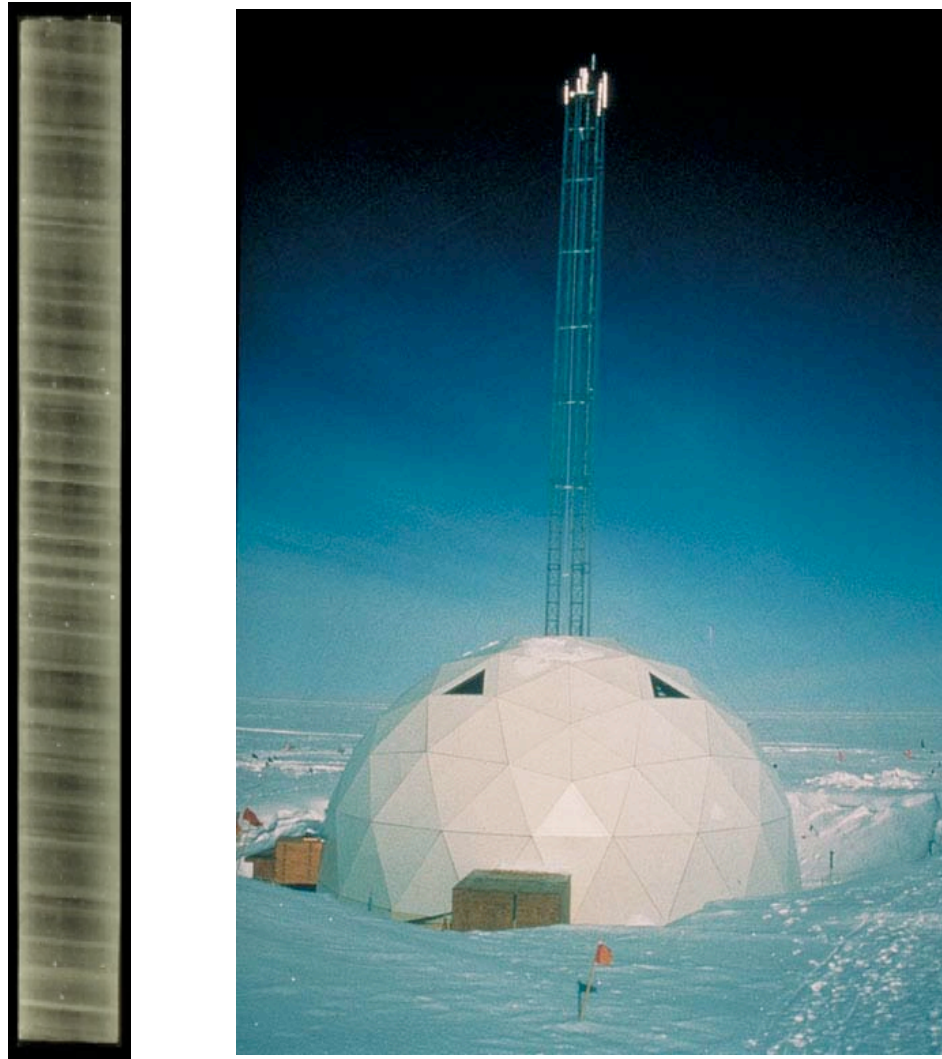
2279



2280

2281 **Figure 5.11** Locations of Arctic and sub-Arctic lakes (blue) and ice cores (green) for
2282 which oxygen isotope records documenting Holocene paleoclimate have been
2283 constructed. Map adapted from the Atlas of Canada, © 2002. Her Majesty the Queen in
2284 Right of Canada, Natural Resources Canada. / Sa Majesté la Reine du chef du Canada,
2285 Ressources naturelles Canada.

2286



a

b

Figure 5.12 a) One meter section of the Greenland Ice Core Project core from a depth of 1837 meters showing annual layers. (Source: courtesy of Eric Cravens, Assistant Curator, U.S. National Ice Core Laboratory) . **b)** Field site of Summit Station on the top of the Greenland Ice sheet (photo by Michael Morrison, GISP2 SMO, University of New Hampshire; NOAA Paleoslide Set)

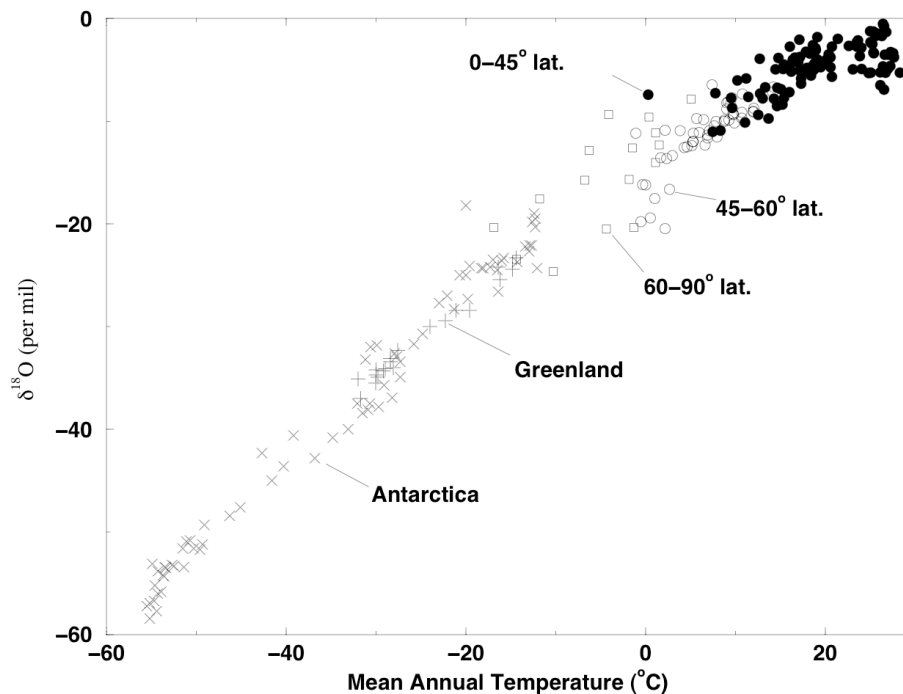
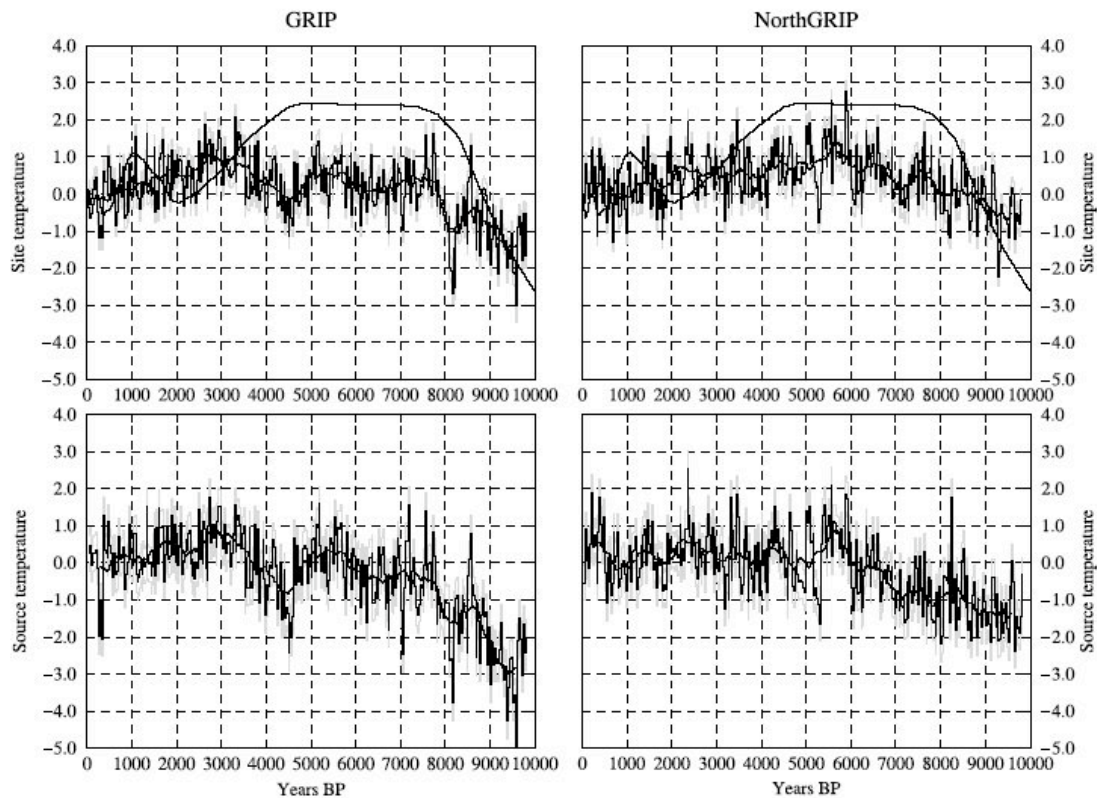


Figure 5.13 Relationship between the isotopic composition of precipitation and temperature in the colder parts of the world where ice sheets exist. Data from the International Atomic Energy Agency (IAEA) network (Fricke and O’Neil, 1999; calculated as the means of the summer and winter data of their Table 1 for all sites with complete data), and from Greenland (x; Johnsen et al., 1989) and Antarctica (+; Dahe et al., 1994). For the IAEA data, open squares are poleward of 60° latitude (but with no inland ice-sheet sites), open circles from 45° to 60°, and filled circles equatorward of 45°. About 71% of the Earth’s surface area is equatorward of 45°, where dependence of $\delta^{18}\text{O}$ on temperature is weak to nonexistent. Only 16% of Earth’s surface falls in the 45° to 60° band, with only 13% poleward of 60°. The linear array is clearly dominated by data from the ice sheets. (Source: Alley and Cuffey, 2001)

2306

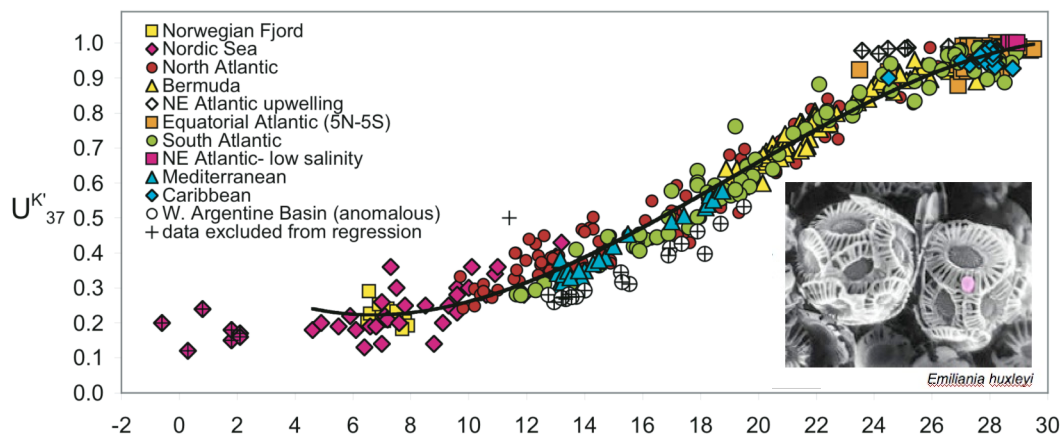


2307

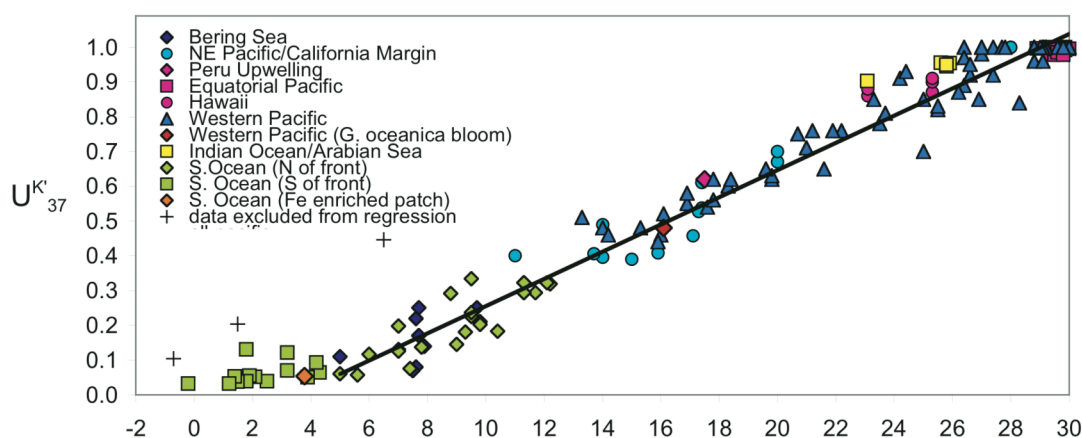
2308 **Figure 5.14** Paleotemperature estimates of site and source waters from Greenland: GRIP
2309 and NorthGrip Masson-Delmotte et al., 2005). GRIP (left) and NorthGRIP (right)
2310 site(top) and source (bottom) temperatures derived from GRIP and NorthGRIP $\delta^{18}\text{O}$ and
2311 deuterium excess corrected for seawater $\delta^{18}\text{O}$ (until 6000 BP). Shaded lines show an
2312 estimate of the uncertainties due to the tuning of the isotopic model and the analytical
2313 precision. Solid line is GRIP temperature derived from the borehole temperature profile
2314 (Dahl-Jensen et al., 1998).

2315

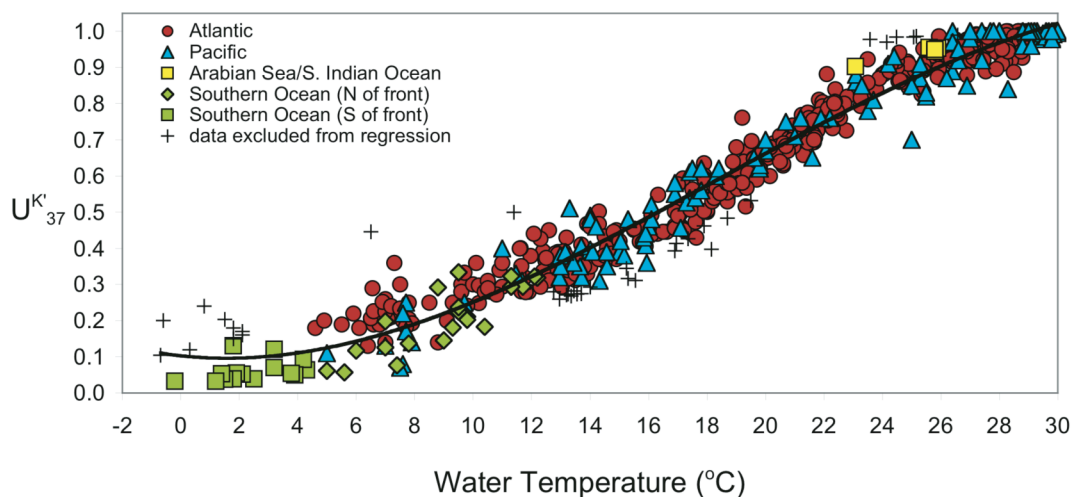
(A) Atlantic (451)



(B) Pacific (131), Indian(5) and Southern(42) Oceans



(C) Global dataset (629)

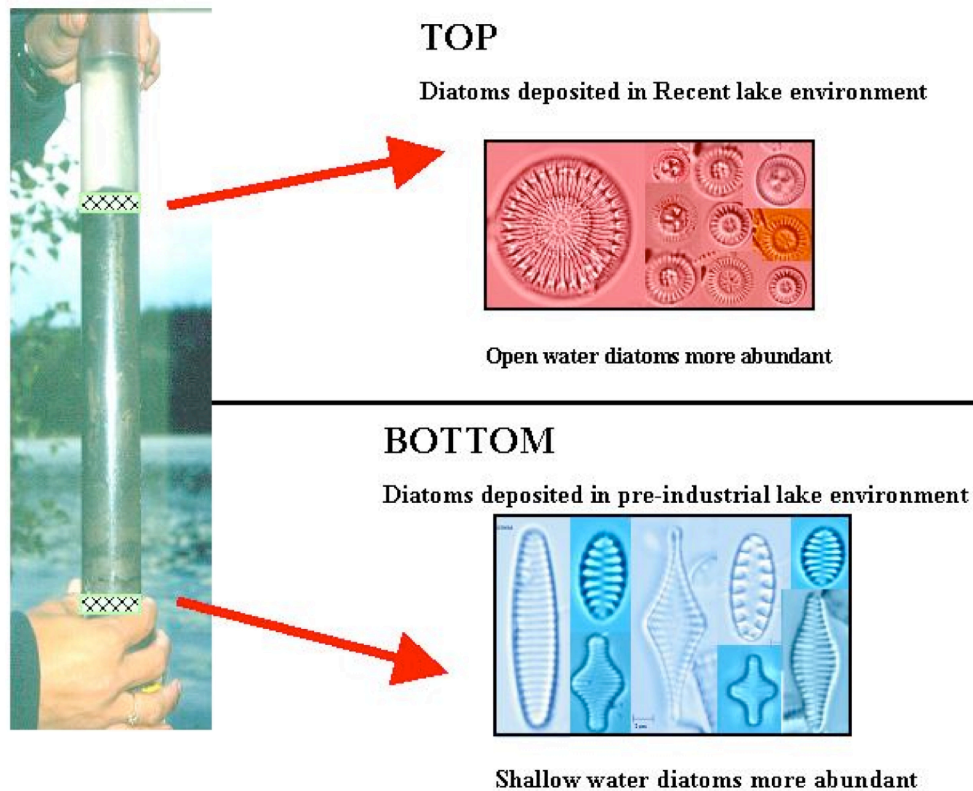


2315

2316 **Figure 5.15** Biomarker alkenone. U_{37}^K versus measured water temperature for surface
2317 mixed layer (0–30 m) samples. (a) Atlantic region. The empirical 3rd order polynomial

2318 regression for samples collected in $>4^{\circ}\text{C}$ waters, excluding outlier data from the
2319 southwest Atlantic margin and northeast Atlantic upwelling regime, is $U_{37}^{\text{K}} = 1.004 - 10$
2320 $4T_3 + 5.744 - 10 - 3T_2 - 6.207 - 10 - 2T + 0.407$ ($r^2 = 0.98$, $n = 413$). (b) Pacific, Indian, and
2321 Southern Ocean regions. The empirical linear regression of Pacific samples is $U_{37}^{\text{K}} =$
2322 $0.0391T - 0.1364$ ($r^2 = 0.97$, $n = 131$). Pacific regression does not include the Indian and
2323 Southern Ocean data. (c) Global data. The empirical 3rd order polynomial regression,
2324 excluding anomalous southwest Atlantic margin data, is $U_{37}^{\text{K}} = 5.256 - 10 - 5T_3 + 2.884$
2325 $10 - 3T_2 - 8.4933 - 10 - 3T + 9.898$ ($r^2 = 0.97$, $n = 588$). Samples excluded from the
2326 regressions are shown by crosses. (Conte et al, 2006)
2327

2327



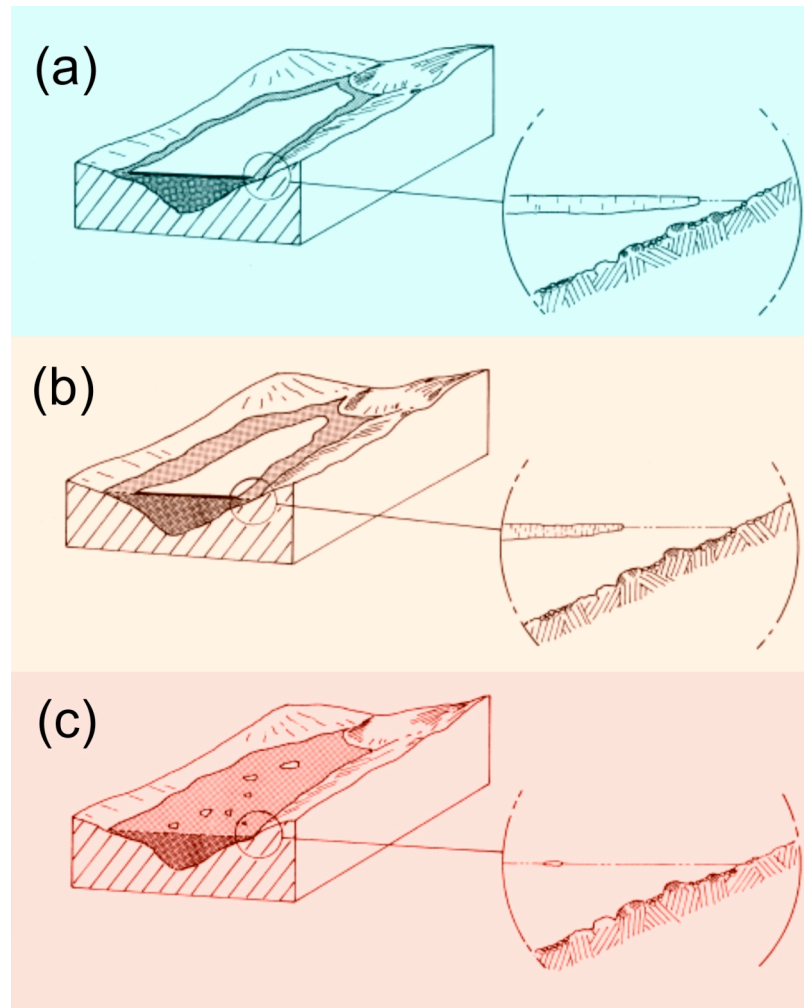
2328

2329 **Figure 5.16** Diatom assemblages reflect a variety of environmental conditions in Arctic
2330 lake systems. Transitions, especially rapid change from one assemblage to another can
2331 reflect large changes in light conditions, nutrient availability and/or temperature, for
2332 example. Biogenic silica, dominated by the silica skeletal framework constructed by
2333 diatoms, is commonly measured in lake sediments as a measure of past changes in
2334 aquatic primary productivity.

2335

2336

2336



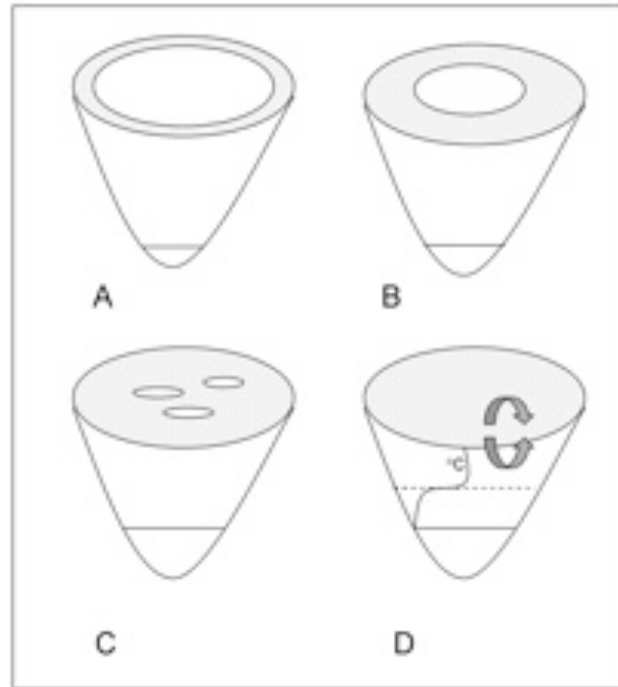
2337

2338 **Figure 5.17** Ice and snow cover often play an important role in influencing the physical,
2339 chemical, and biological characteristic of Arctic lakes. This schematic shows changing
2340 ice and snow conditions on an Arctic lake during relatively (a) cold, (b) moderate, and (c)
2341 warm conditions. During colder years, a permanent raft of ice may persist throughout the
2342 short summer, precluding the development of large populations of phytoplankton, and
2343 restricting much of the primary production to the shallow, open water moat. Many other
2344 physical, chemical and biological changes occur in lakes that are either directly or
2345 indirectly affected by snow and ice cover (see Table 1; Douglas and Smol 1999).
2346 Modified from Smol (1988).

2347

2347

2348

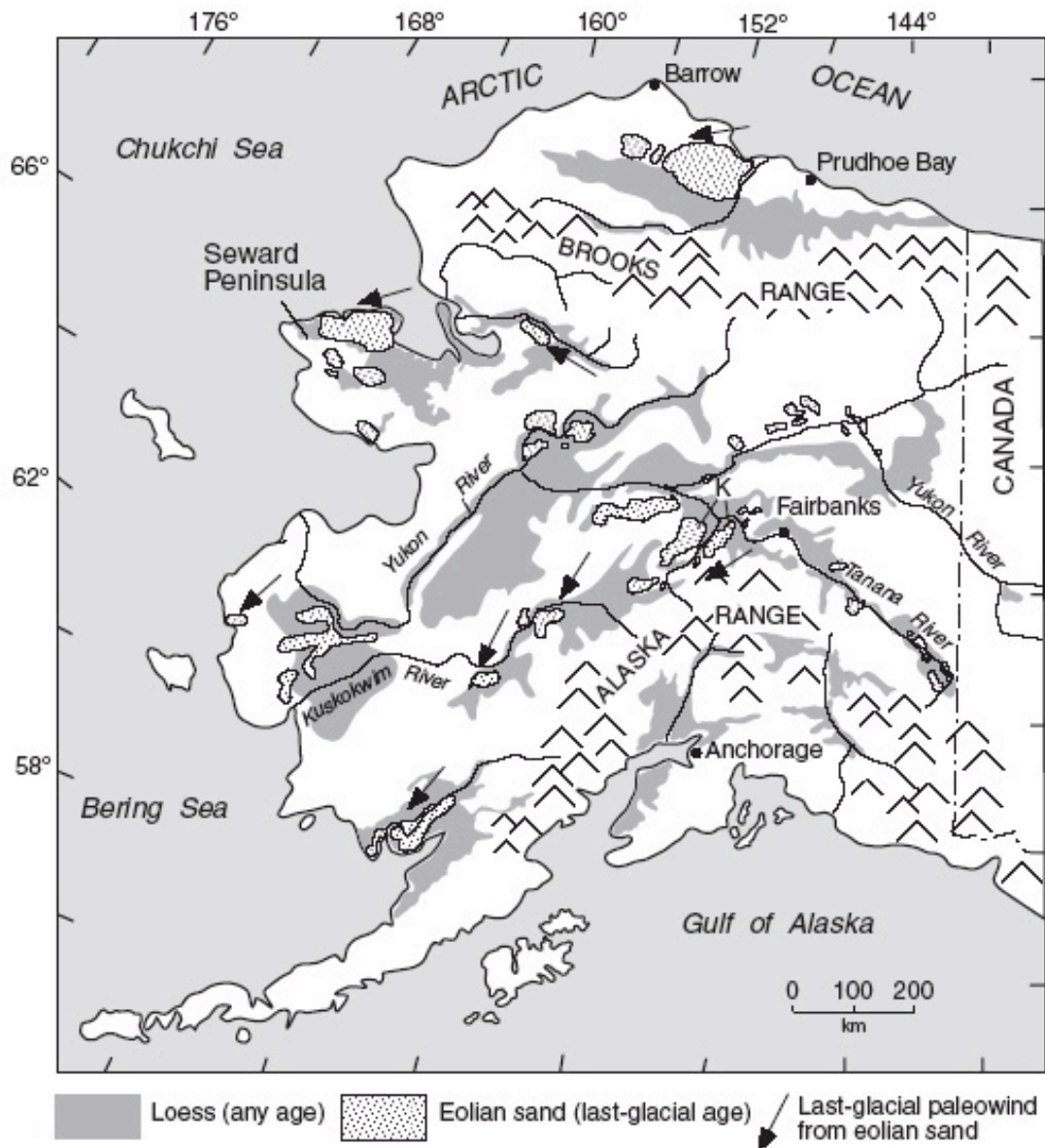


2349

2350 **Figure 5.18** Lake ice melts as it continues to warm (A – D). Eventually, in deeper lakes
2351 (vs ponds) thermal stratification may also occur (or be prolonged) during the summer
2352 months (D), further altering the limnological characteristics of the lake. Modified from
2353 Douglas (2007).

2354

2354



2355

2356 **Figure 5.19** The form and distribution of wind-blown silt (loess), wind-blown sand
2357 (dunes), and other deposits of wind-blown sediment in Alaska, have been use to infer
2358 both Holocene and last-glacial past wind directions. (Compiled from multiple sources by
2359 Muhs and Budahn, 2006).

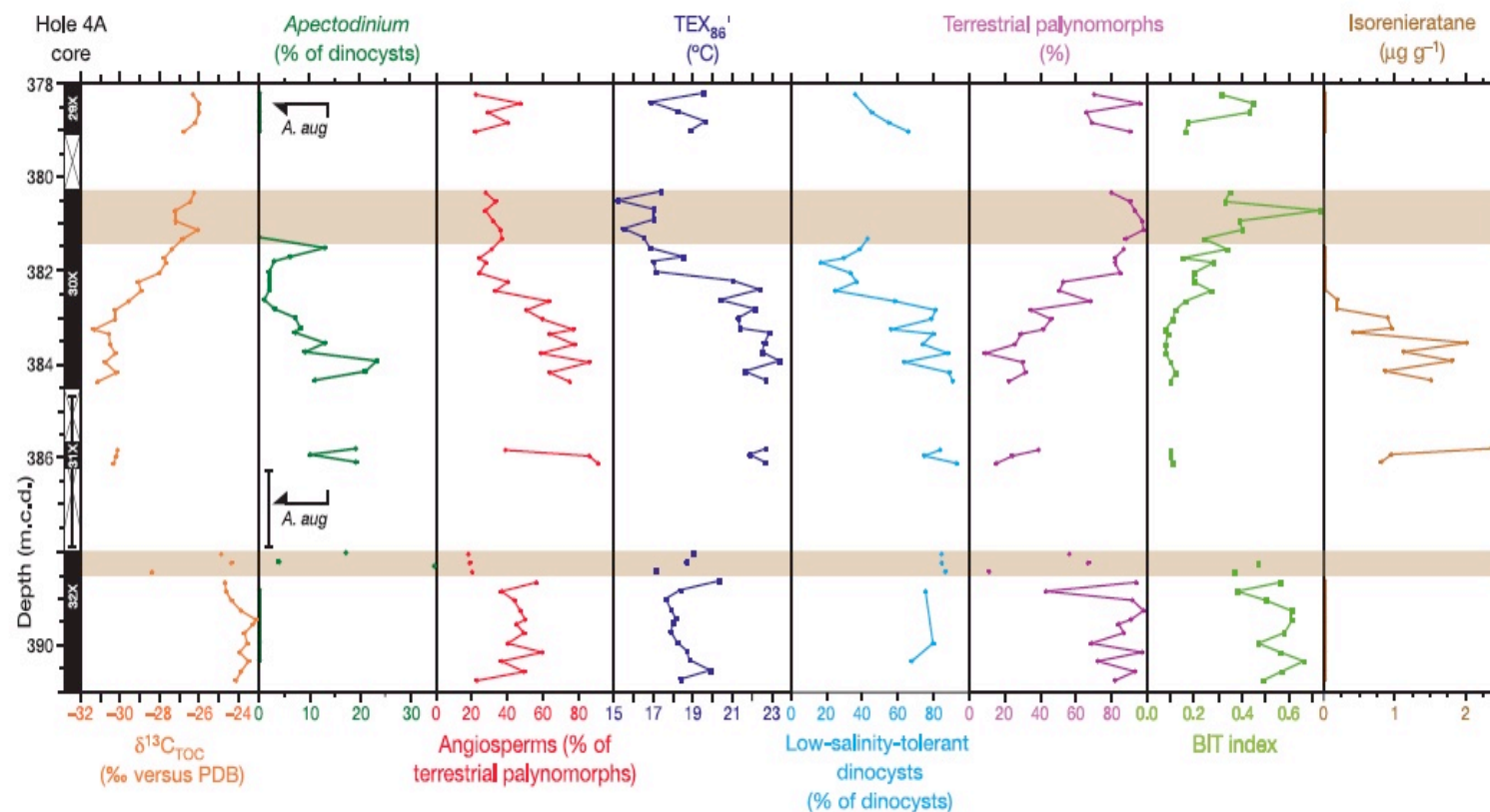
2360



2360

2361 **Figure 5.20** At this unnamed, hydrologically closed lake in the Yukon Flats Wildlife
2362 Refuge in Alaska, concentric rings of vegetation have developed progressively inward as
2363 water levels lowered due to a negative change in the lake's overall water balance. Historic
2364 Landsat imagery and air photographs indicate that these shorelines formed during the last
2365 ~40 years. (Photo by Lesleigh Anderson)

2366

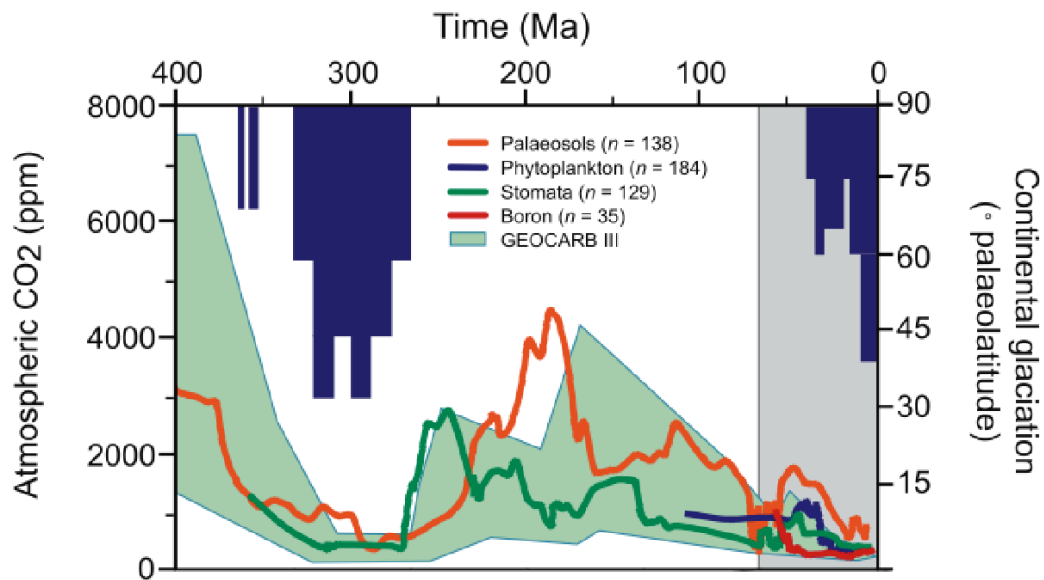


2367

2368 **Figure 5.21** Recovered sections and palynological and geochemical results across the Paleocene-Eocene Thermal Maximum ~55
2369 million yrs ago of IODP Hole 302-4A (87° 52.00' N; 136° 10.64' E; 1,288 m water depth, in the central Arctic Ocean basin). Mean
2370 annual surface water temperatures (as indicated in the TEX_{86}' column) are estimated to have reached 23°C similar to waters in the

2371 tropics today. [Error bars for Core 31X show the uncertainty of its stratigraphic position. Orange bars indicate intervals affected by
2372 drilling disturbance.] Stable carbon isotopes are expressed relative to the PeeDee Belemnite standard. Low-salinity-tolerant dinocysts
2373 comprise *Senegalinium* spp., *Cerodinium* spp., and *Polysphaeridium* spp., while *Membranosphaera* spp., *Spiniferites ramosus*
2374 complex, and *Areoligera-Glaphyrocysta* cpx. represent the typical normal marine species. Arrows and *A. aug* (second column)
2375 indicate the first and last occurrences of dinocyst *Apectodinium augustum* – a diagnostic indicator of PETM warm conditions. (Sluijs
2376 et al., 2006).

2377



2378

2379 **Figure 5.22** Atmospheric CO₂ and continental glaciation 400 Ma to present. Vertical blue
2380 bars mark the timing and palaeolatitude extent of ice sheets (after Crowley, 1998).
2381 Plotted CO₂ records represent five-point running averages from each of the four major
2382 proxies (see Royer, 2006 for details of compilation). Also plotted are the plausible ranges
2383 of CO₂ from the geochemical carbon cycle model GEOCARB III (Berner and Kothavala,
2384 2001). All data have been adjusted to the Gradstein et al. (2004) time scale. Extensive
2385 growth of continental ice sheets occurs when CO₂ is low. (source: Jansen, 2007: Figure
2386 6.1)

2387

2388

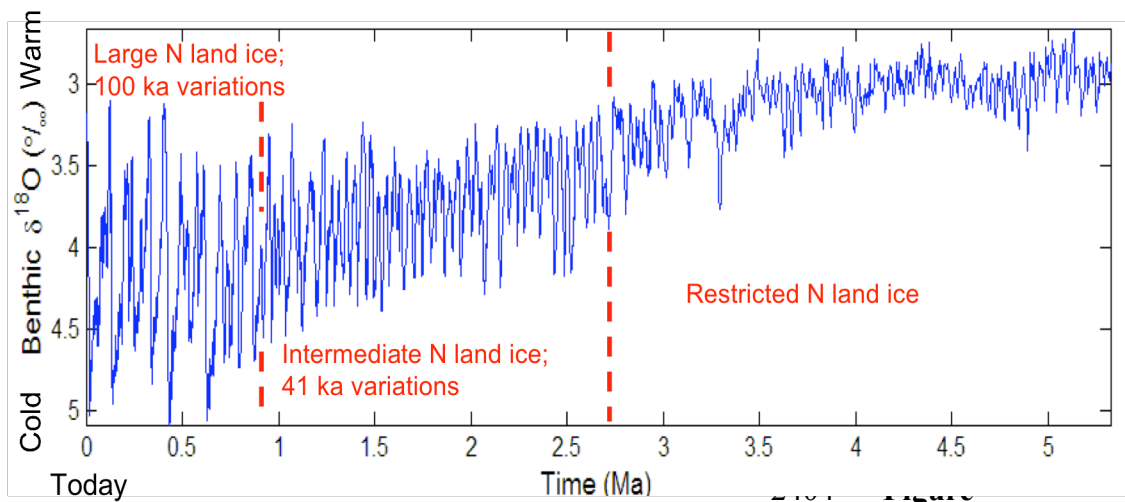


Figure 5.23 The average isotopic composition ($\delta^{18}\text{O}$) of bottom-dwelling foraminifera from a globally distributed set of 57 sediment cores covering the last 5.3 Ma (modified from Lisiecki and Raymo, 2005). The $\delta^{18}\text{O}$ is controlled primarily by global ice volume and deep-ocean temperature, with less ice and/or warmer temperatures upward. The influences of all the Milankovitch frequencies of Earth's orbital variation are present throughout, but the increase in glaciation about 2.7 Ma ago occurred with establishment of a strong 41 ka variability linked to Earth's obliquity (changes in tilt of Earth's spin axis), and the additional increase in glaciation about 1.2-0.7 Ma involved a shift to stronger 100 ka variability. Dashed lines are used because the changes seem to have been somewhat gradual. The general trend toward higher $\delta^{18}\text{O}$ that runs through this series reflects the long-term drift toward a colder Earth that began in the early Cenozoic (see Fig. 4.8).

2418



2419

2420 **Figure 5.24** (a) Greenland without ice for the last time? Dark green: boreal forest, light green: deciduous forest; brown: tundra and
2421 alpine heaths; white: ice caps. The north-south temperature gradient is constructed from a comparison between North Greenland and

2422 NW European temperatures, using standard lapse rate, and assuming precipitation distribution after the same pattern as known from
2423 the Holocene. The topographical base comes from the model by Letreguilly et al. 1991 of Greenland's sub-ice topography after
2424 isostatic recovery. (b) Upper part of the Kap København Formation, North Greenland. The sand was deposited in an estuary 2.4 Ma
2425 ago, and contains abundant well preserved leaves, seeds, twigs, and insect remains. (Photograph of S.V. Funder).

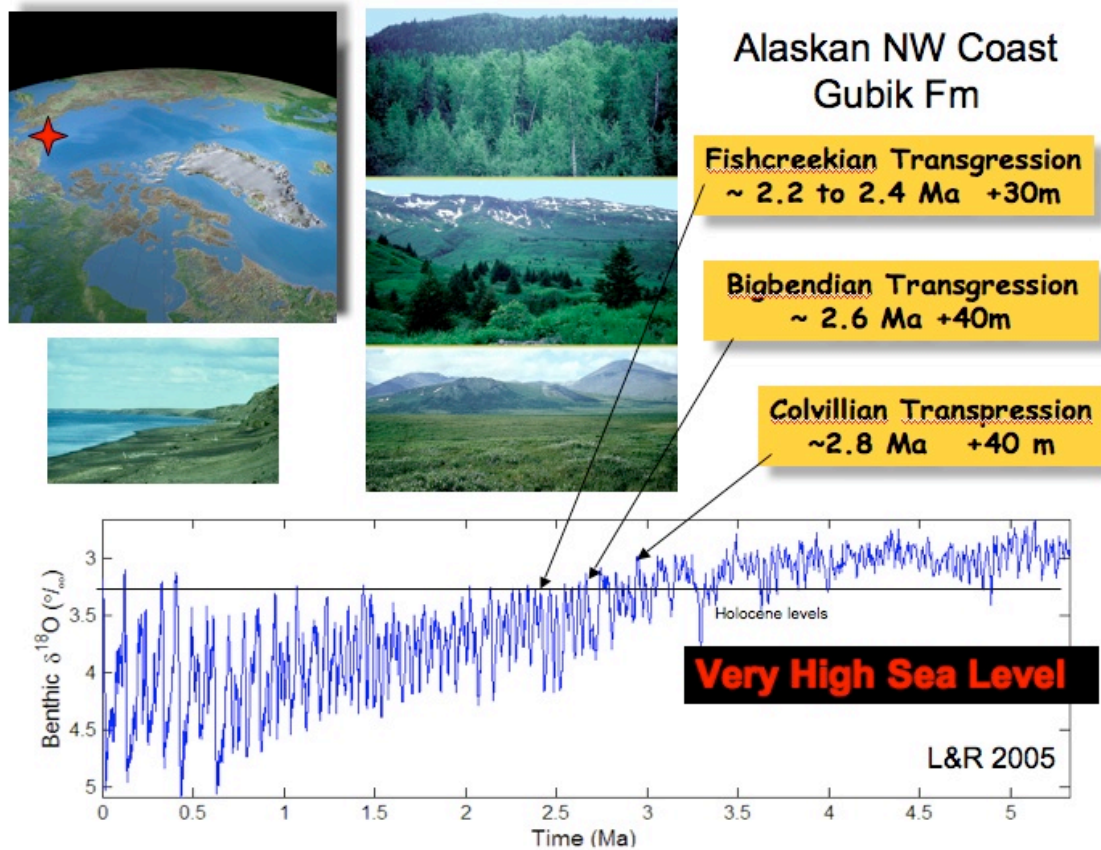


Figure 5.25 The largely marine Gubik Formation on the North Slope of Alaska contains three superposed lower units recording relative sea level as high +30-+40 m. Pollen in these same deposits suggest that borderland vegetation at each of these times was less forested with boreal forests or spruce-birch woodlands at 2.7 Ma giving way to larch and spruce forests at about 2.6 and open tundra by ca. 2.4 Ma (see photos with oldest at the top from Robert Nelson, Colby College who did the pollen work). Isotopic reference time series of Lisecki and Raymo (2005) suggests best as assignments for these sea level events (Brigham and Carter, 1992).

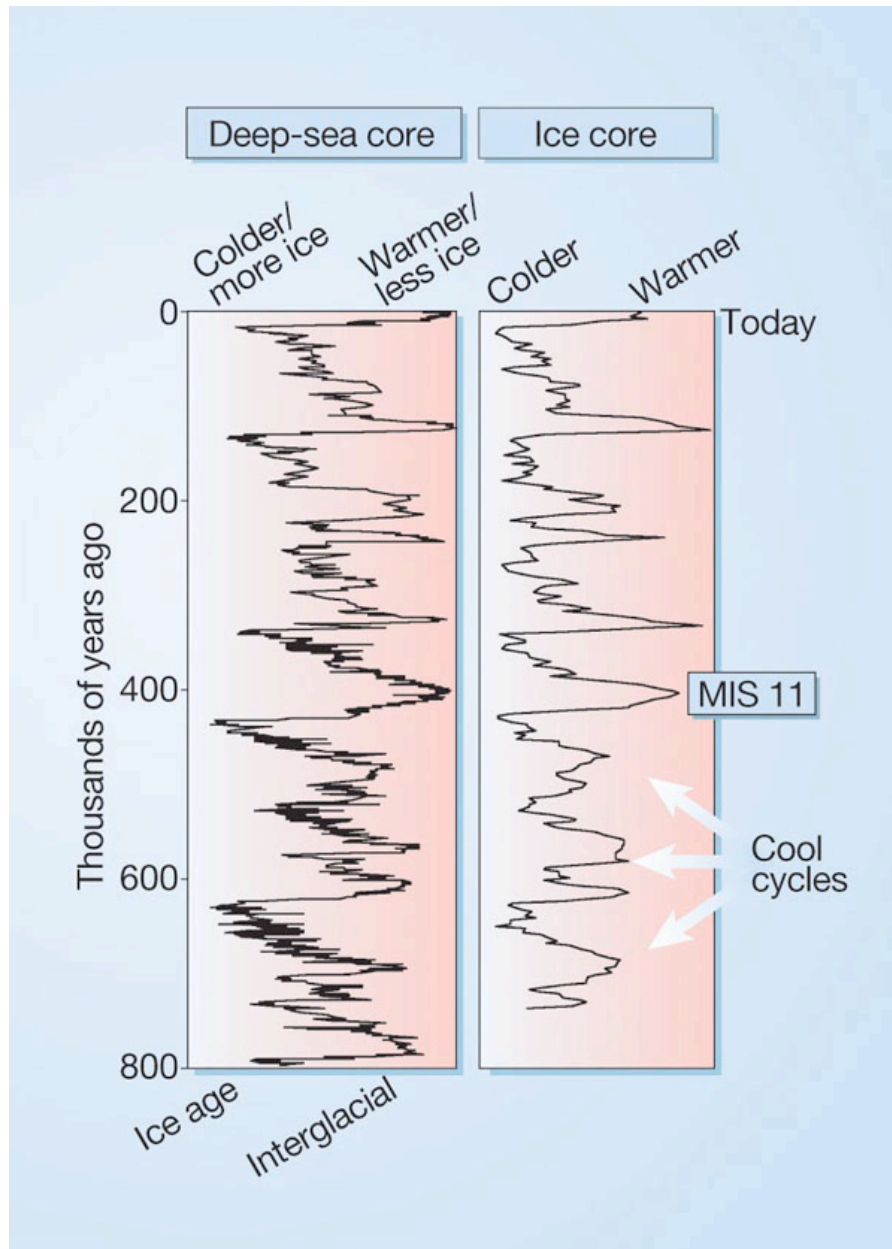
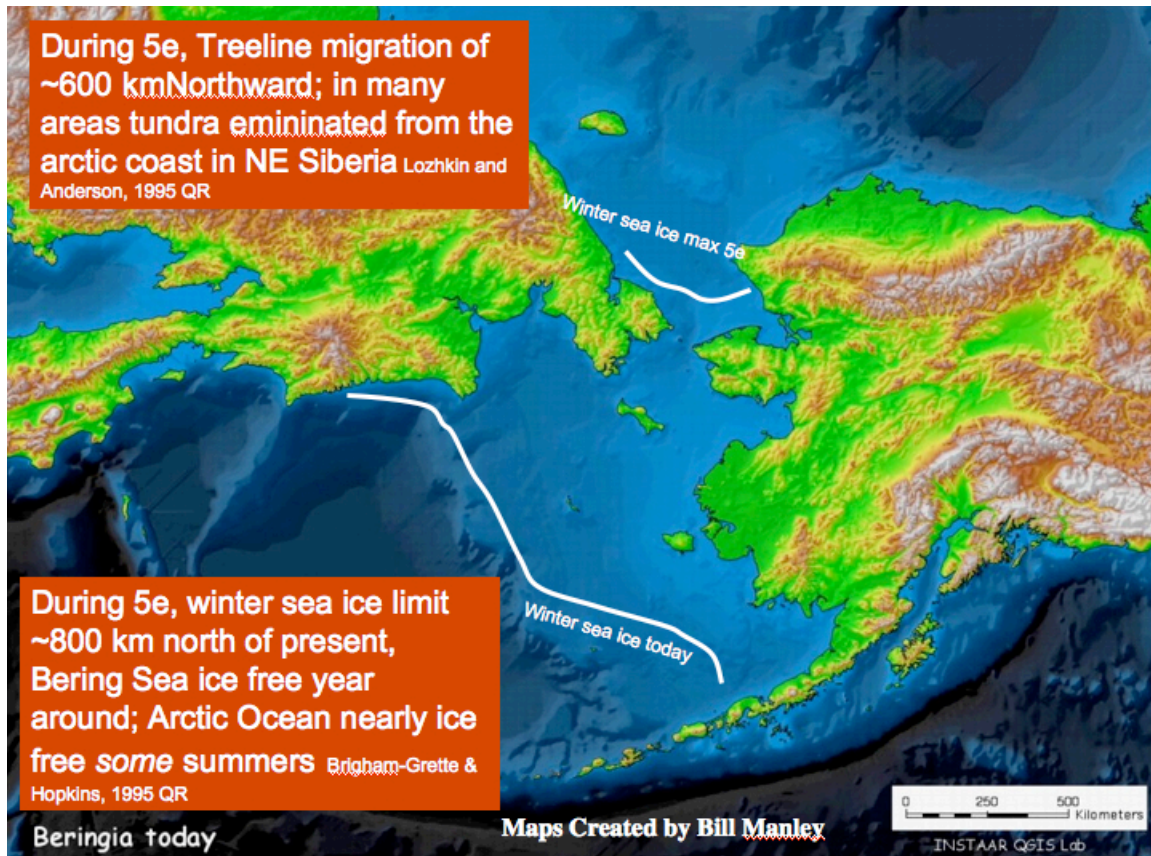


Figure 5.26 Glacial cycles over the past 800ka derived from marine-sediment and ice cores (McManus, 2004). The history of deep-ocean temperatures and global ice volume is inferred from $\delta^{18}\text{O}$ measured in bottom-dwelling foraminifera shells preserved in Atlantic Ocean sediments. Air temperatures over Antarctica are inferred from the ratio of deuterium to hydrogen in ice from central Antarctica (EPICA, 2004). Marine Isotope Stage 11 (MIS 11) is an interglacial with similar orbital parameters to the Holocene, yet lasted about twice as long as most interglacials. Note the smaller magnitude and less-

- 2444 pronounced interglacial warmth of the glacial cycles that preceded MIS 11.
2445 Interglaciations older than MIS 11 were less warm than subsequent interglaciations).

2453



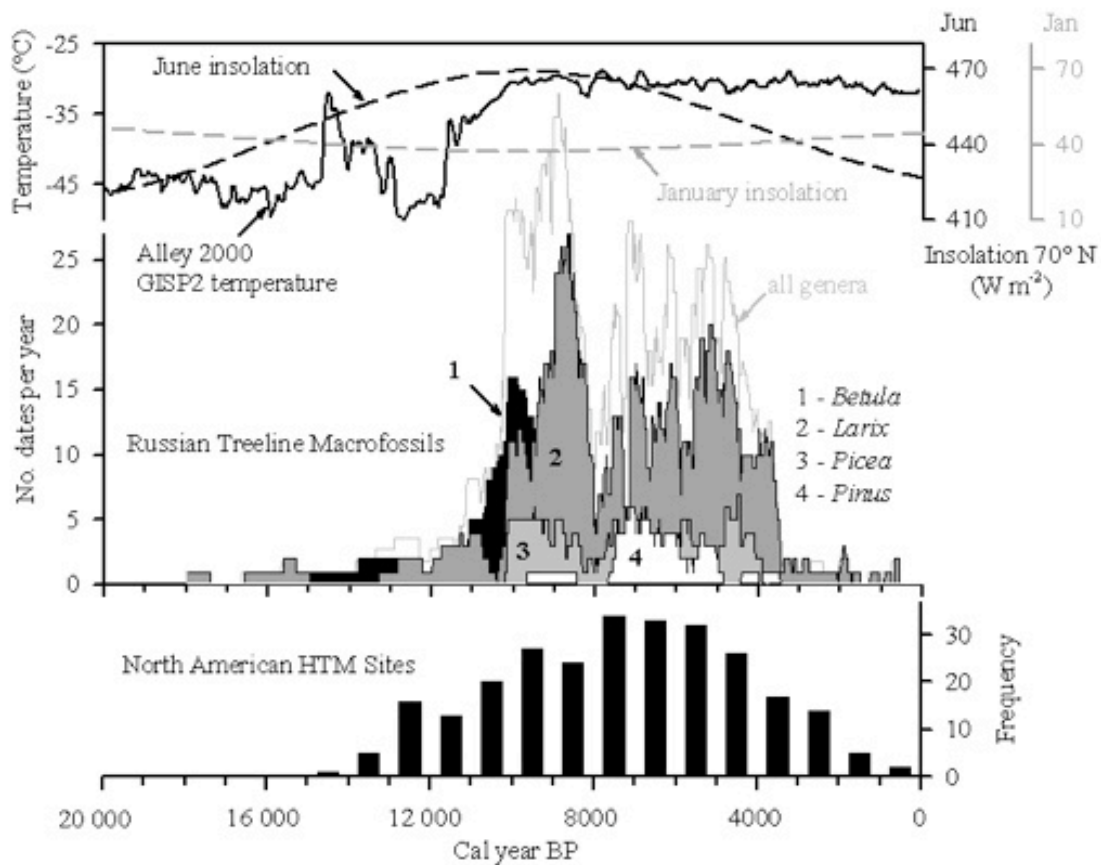
2454

2455

2456 **Figure 5.28** Fossiliferous paleoshorelines and marine sediments were used by Brigham-
2457 Grette and Hopkins (1995) to evaluate the seasonality of coastal sea ice on both sides of
2458 the Bering Strait during the Last Interglacial. The winter sea limit is estimated to have
2459 been north of the narrowest section of the strait, 800 km north of modern limits. Lozhkin
2460 and Anderson (1995) suggest from pollen data derived from Last Interglacial lake
2461 sediments that tundra was nearly eliminated from the Russian coast at this time. More
2462 open water resulted in an increase in some taxa tolerant of deeper winter snows in
2463 Chukotka during the warm interglaciation. (Map of William Manley
2464 <http://instaar.colorado.edu/QGISL/>).

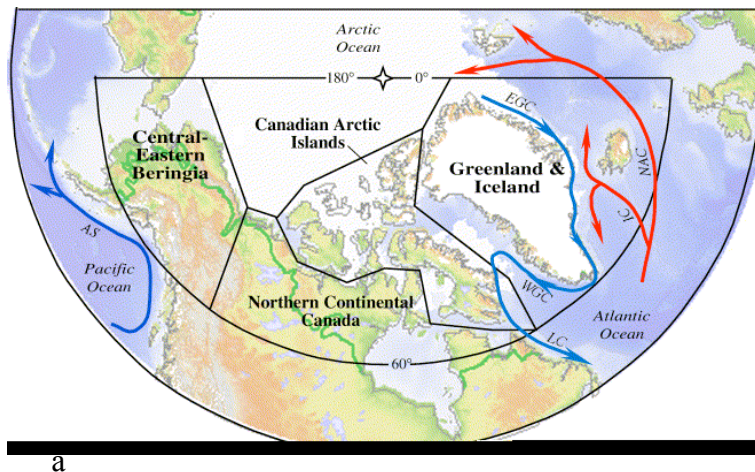
2465

2465

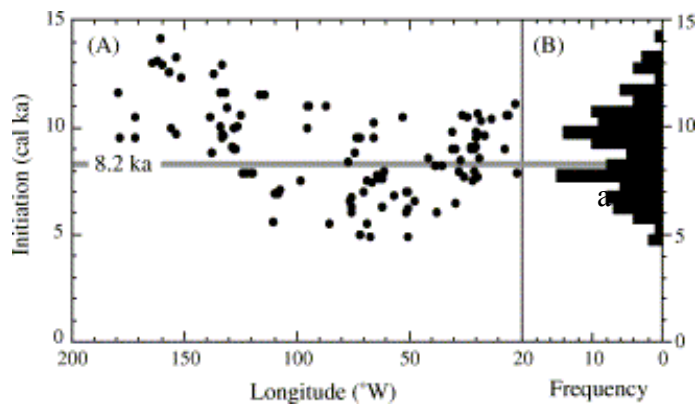


2466

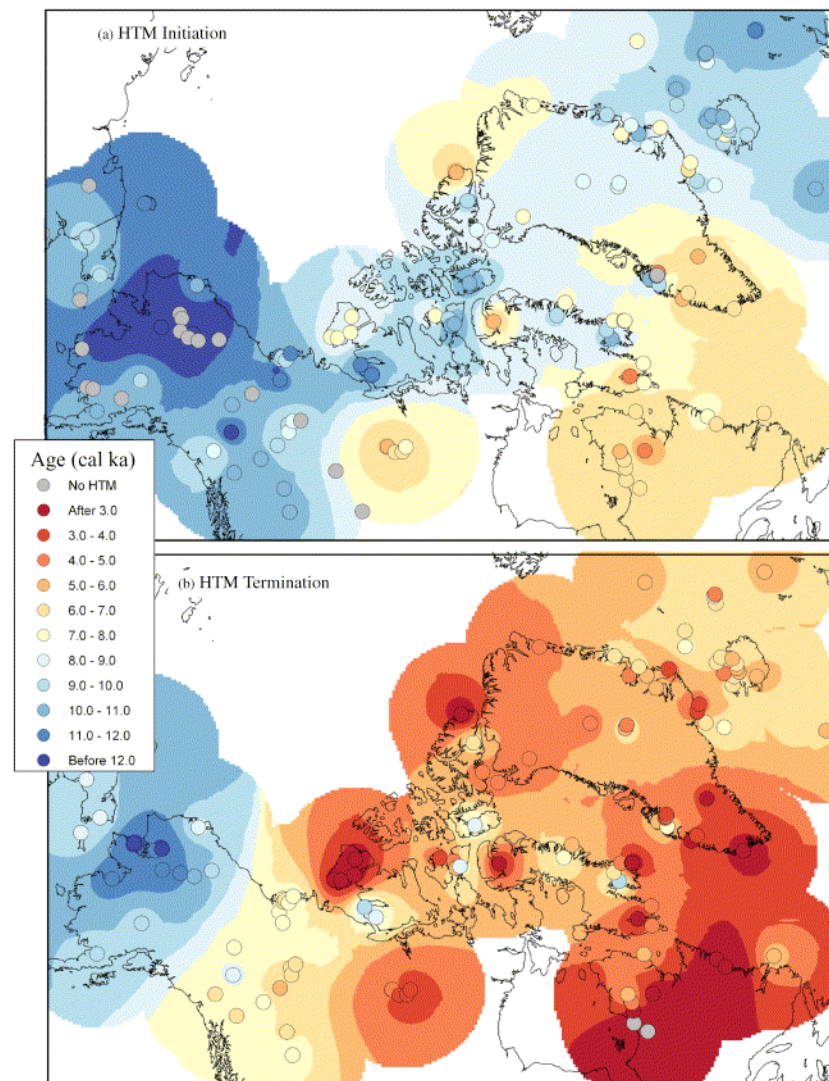
2467 **Figure 5.29** The Arctic Holocene Thermal Maximum (HTM) as expressed in a
 2468 comparison of seasonal insolation patterns at 70° N (Berger & Loutre 1991),
 2469 reconstructed Greenland air temperature from the GISP2 drilling project (Alley 2000),
 2470 the age distribution of radiocarbon-dated fossil remains of different tree genera from
 2471 north of present treeline (MacDonald et al., 2007), and the frequency of Western Arctic
 2472 sites experiencing HTM conditions.



a



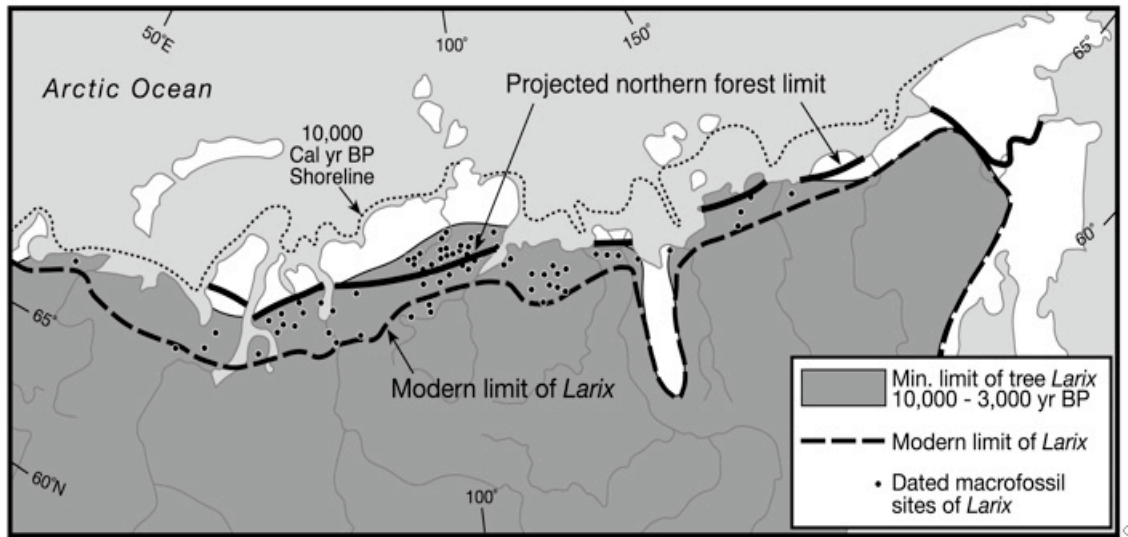
b



c

2474 **Figure. 5.30** The timing of initiation and termination of the HTM in the Western Arctic (Kaufman et al., 2004).
2475 a. Regions reviewed in Kaufman et al. 2004
2476 b. Initiation of the Holocene thermal maximum in the western Arctic. Longitudinal distribution (left) and frequency distribution
2477 (right)
2478 c. Spatio-temporal pattern of the Holocene thermal maximum (HTM) in the western Arctic. Initiation (upper) and termination (lower)
2479 of the HTM. Gray dots indicate equivocal evidence for the HTM. Dot colors indicate bracketing ages of the HTM, which are
2480 contoured using the same color scheme.
2481

2482



2483

2484

2485 **Figure. 5.31** The northward extension of larch (*Larix*) across the Eurasian Arctic during
2486 the HTM compared to present treeline larch forest distribution and anticipated (Arctic
2487 Climate Impact Assessment, 2005) northern forest limits due to climate warming
2488 (MacDonald et al., 2007).

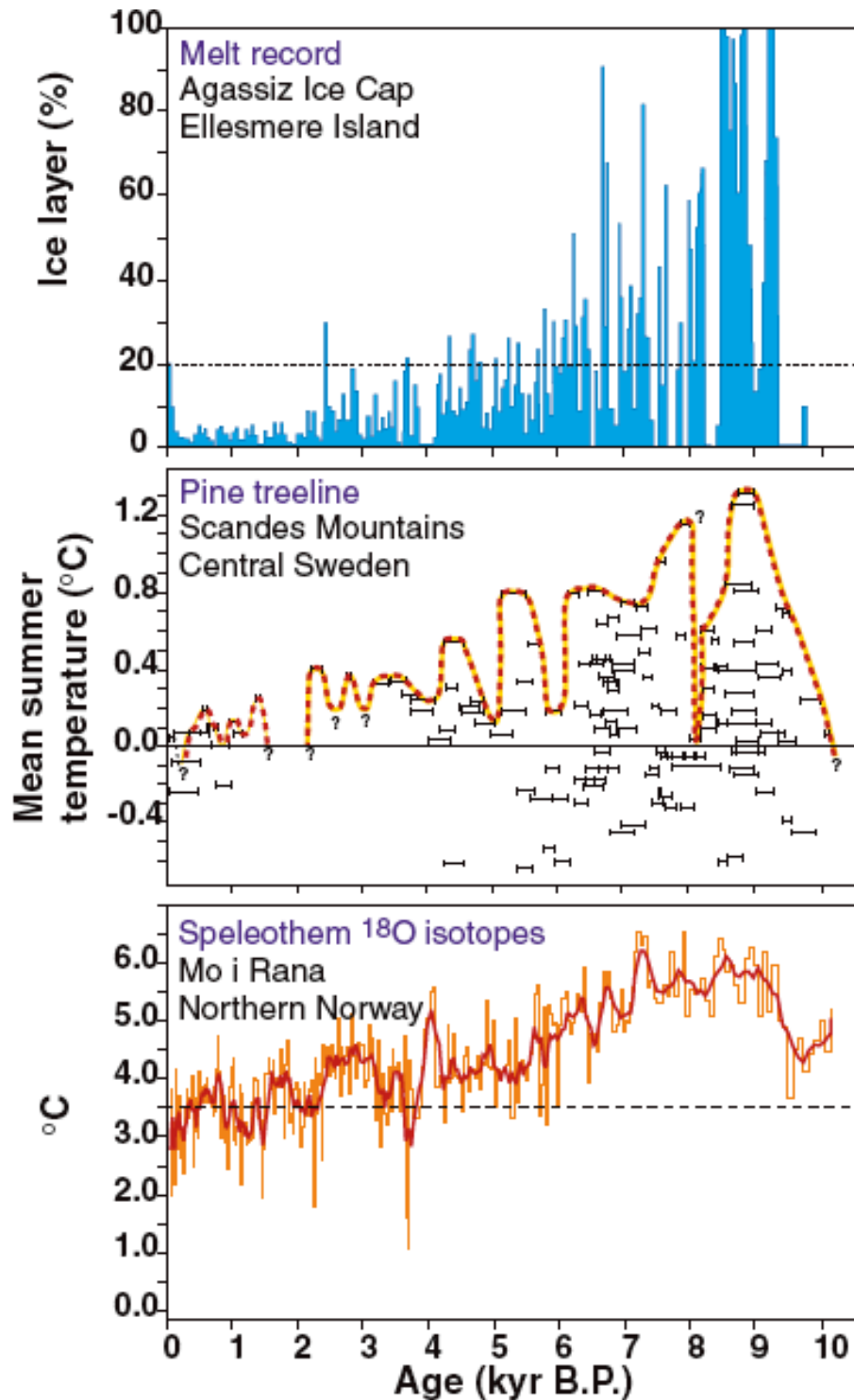
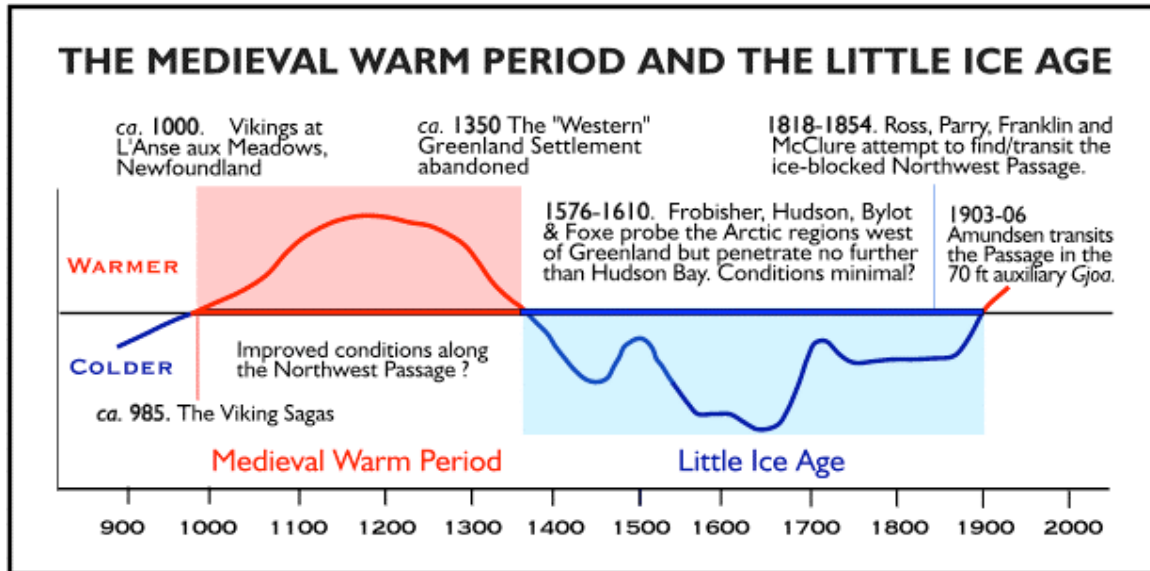


Fig. 5.32 Upper panel: The record of summer melting on the Agassiz Ice Cap, northern Ellesmere Island, Canada over the course of the Holocene. Melt indicates the fraction of each core section containing evidence of melting (from Koerner and Fisher, 1990).

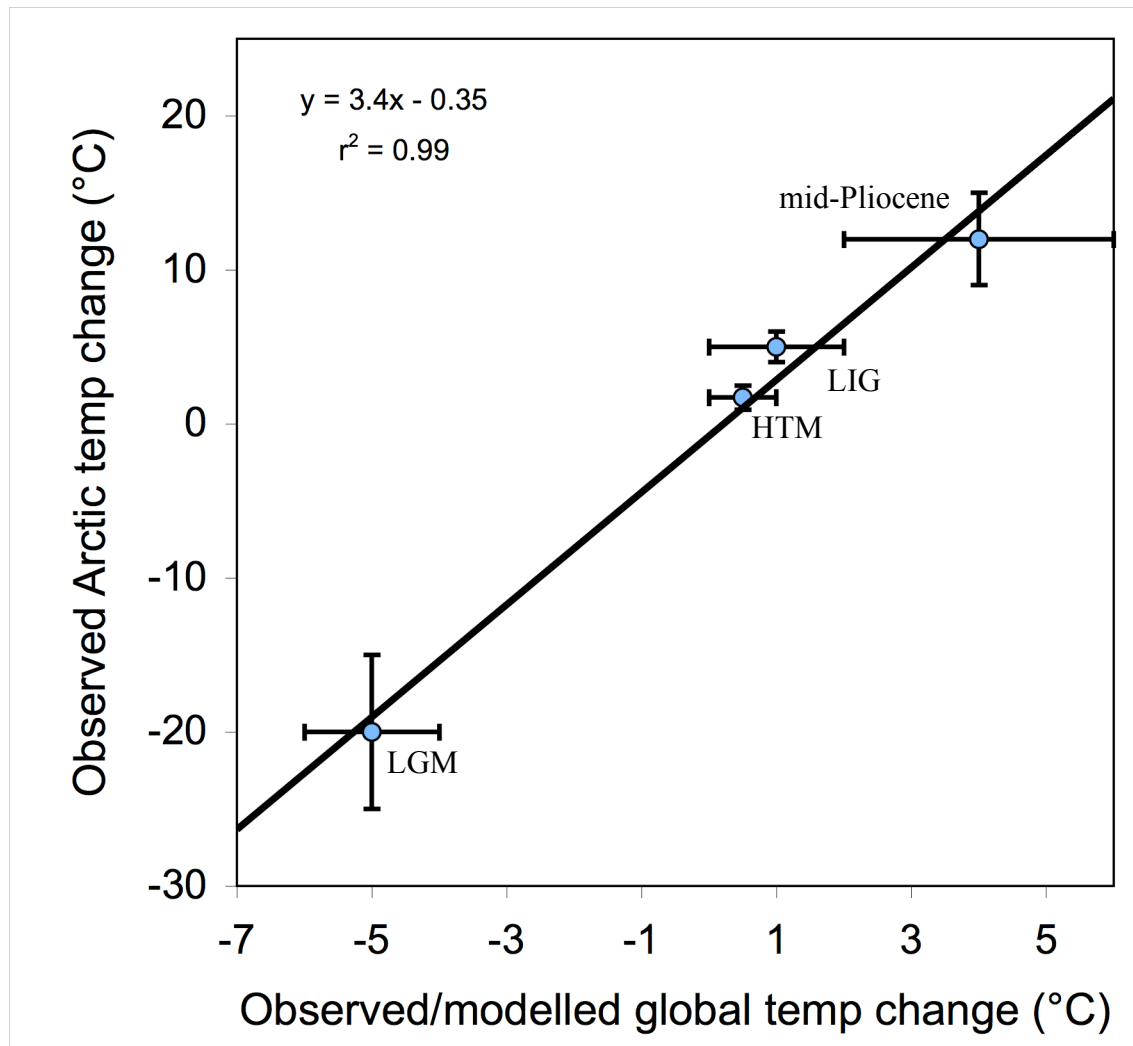
2493 Middle panel: Summer temperature anomalies estimated from the elevation of ^{14}C dated
2494 sub-fossil pine wood samples (*Pinus sylvestris* L.) in the Scandes mountains, central
2495 Sweden (black bars) relative to temperatures at the modern pine limit in the region.
2496 Upper limit of pine growth is indicated by the dashed line. Changes in temperature were
2497 estimated by assuming a lapse rate of $6\text{ }^{\circ}\text{C km}^{-1}$ (from Dahl and Nesje 1996, based on
2498 samples collected by L. Kullman and G. and J. Lundqvist). Lower panel:
2499 Paleotemperature reconstruction from oxygen isotopes in calcite sampled along the
2500 growth axis of a stalagmite from a cave at Mo i Rana, in northern Norway. Growth
2501 ceased around A.D. 1750. (from Lauritzen 1996; Lauritzen and Lundberg 1998; 2002).
2502 Figure from Bradley (2000).
2503

2503
2504



2505
2506
2507
2508
2509
2510
2511
2512

Figure 5.33 Schematic diagrams of temperature variations over the past thousand years. The dotted line nominally represents conditions near the beginning of the twentieth century. From the IPCC AR1 (Fig. 7.1; 1990). Recent reviews (e.g. Bradley et al., 2003) suggest that this curve probably is most representative of the northern North Atlantic region rather than a reflection of global temperature.



2512

2513 **Figure 5.34** Paleoclimate data quantify the magnitude of Arctic amplification. Shown
 2514 are paleoclimate estimates of Arctic summer temperature anomalies relative to recent,
 2515 and the appropriate northern-hemisphere or global summer temperature anomalies,
 2516 together with their uncertainties, for the last glacial maximum (LGM; ~20 ka ago),
 2517 Holocene thermal maximum (HTM; ~8 ka ago), last interglaciation (LIG; 130-125 ka
 2518 ago) and middle Pliocene (~3.5-3.0 Ma ago). The trend line suggests that summer
 2519 temperature changes are amplified 3 to 4 times in the Arctic. Explanation of data sources
 2520 follows for the different times considered beginning with the most recent.

2521

Holocene Thermal Maximum (HTM): Arctic $\Delta T = 1.7 \pm 0.8$ °C; NH $\Delta T = 0.5 \pm 0.3$ °C; Global $\Delta T = 0 \pm 0.5$ °C.

A recent summary of summer temperature anomalies for the western Arctic (Kaufman et al., 2004) built on earlier summaries (Kerwin et al., 1999; Cape Project Members, 2001), and is consistent with more-recent reconstructions (Kaplan and Wolfe, 2006; Flowers et al., 2007). Although the Kaufman et al. (2004) summary covered only the western half of the Arctic, the earlier summaries by Kerwin et al., (1999) and Cape Project Members (2001) indicated that similar anomalies characterized the Eastern Arctic, with all syntheses reporting the largest anomalies in the North Atlantic sector. Few data are available for the central Arctic Ocean; we assume that the circumpolar dataset provides an adequate reflection of air temperatures across the Arctic Ocean as well.

Climate models that closely match paleoclimatic data (see text) indicate that the average planetary anomaly was concentrated over the Northern Hemisphere. Braconnot et al. (2007) summarized the simulations from 10 different climate-model contributions to the PMIP2 project that compare simulated summer temperatures 6 ka ago with recent values. The global average summer temperature anomaly 6 ka ago was 0 ± 0.5 °C, whereas the Northern Hemisphere anomaly was 0.5 ± 0.3 °C. These patterns are similar to model results described by Hewitt and Mitchell (1998) and Kitoh and Murakami (2002) for 6 ka ago, and a global simulation for 9 ka (Renssen et al., 2006), that simulate little summer temperature difference outside the Arctic when compared to pre-industrial temperatures.

Last Glacial Maximum (LGM): Arctic $\Delta T = -20 \pm 5$ °C; Global and Northern Hemisphere $\Delta T = -5 \pm 1$ °C

Quantitative estimates of temperature reductions during the peak of the LGM are less widespread in the Arctic than during warm times. Ice-core borehole temperatures offer the most compelling evidence (Cuffey et al., 1995; Dahl-Jensen et al., 1998), with additional support from biological proxies in the North Pacific sector (Elias et al., 1996a), where no ice cores are available that extend back to the LGM. Because of the limited datasets for the LGM temperature reduction in the Arctic, we incorporate a large

uncertainty. The global-average temperature decrease during peak glaciations based on paleoclimate proxy data was 5 to 6 °C, with little difference between the two hemispheres (Jansen et al., 2007; Farrera et al., 1999; Braconnot et al., 2007). A similar temperature anomaly is derived from climate model simulations (Otto-Bliesner et al., 2007).

Last Interglaciation (LIG): Arctic $\Delta T = 5 \pm 1$ °C; Global and NH $\Delta T = 1 \pm 1$ °C)

A recent summary of all available quantitative reconstructions of summer temperature anomalies for the Arctic during peak LIG warmth shows a spatial pattern similar to the HTM reconstructions, with the largest anomalies in the North Atlantic sector and the smallest anomalies in the North Pacific sector, but with substantially larger anomalies (5 ± 1 °C) than during the HTM (CAPE Last Interglacial Project Members, 2006). A similar pattern of LIG summer temperature anomalies is apparent in climate model simulations (Otto-Bliesner et al., 2006). Global and Northern Hemisphere summer temperature anomalies are derived from summaries in CLIMAP Project Members (1984), Crowley (1990), Montoya et al. (2000) and Bauch and Erlenkeuser (2003).

Middle Pliocene: Arctic $\Delta T = 12 \pm 3$ °C; Global $\Delta T = 4 \pm 2$ °C)

The widespread occurrence of forests throughout the Arctic in the middle Pliocene offers a glimpse into a notably warm time in the Arctic, with essentially modern continental configurations and connections between the Arctic Ocean and the global ocean. Reconstructed Arctic temperature anomalies are available from several sites that show much warmth with no summer sea ice in the Arctic Ocean basin. These sites include the Canadian Arctic Archipelago (Dowsett et al., 1994; Elias and Matthews, 2002; Ballantyne et al., 2006), Iceland (Buchardt and Simonarson, 2003), and the North Pacific (Heusser and Morley, 1996). A global summary of mid-Pliocene biomes by Salzmann et al. (2008) concluded that Arctic mean-annual-temperature anomalies were in excess of 10 °C; some sites indicate temperature anomalies up to 15 °C. Estimates of global sea-surface temperature anomalies are from Dowsett (2007).

2582 Global reconstructions of mid Pliocene temperature anomalies from proxy data and
2583 general circulation models show modest warming across low to mid-latitudes, averaging
2584 4 ± 1 °C (Dowsett et al., 1999; Raymo et al., 1996; Sloan et al., 1996, Budyko et al.,
2585 1985; Haywood and Valdes, 2004; Jiang et al. 2005; Haywood and Valdes, 2006;
2586 Salzmann et al., 2008).
2587
2588

CHAPTER 5 REFERENCES

- Abbott**, M.B., B.P. Finney, M.E. Edwards, and K.R. Kelts, 2000: Lake-level reconstructions and paleohydrology of Birch Lake, central Alaska, based on seismic reflection profiles and core transects. *Quaternary Research*, **53**, 154-166.
- Ager**, T.A. & Brubaker, L.B. 1985: Quaternary palynology and vegetation history of Alaska. In *Pollen Records of Late-Quaternary North American Sediments*. Edited by V.M. Bryant, Jr. and R. G. Holloway. American Association of Stratigraphic Palynologists, Dallas. pp. 353-384.
- Aksu**, A.E., 1985: Planktonic foraminiferal and oxygen isotope stratigraphy of CESAR cores 102 and 103—Preliminary results. In: *Initial geological report on CESAR—The Canadian Expedition to Study the Alpha Ridge, Arctic Ocean* [Jackson, H.R., P.J. Mudie, and S.M. Blasco (eds.)]. Geological Survey of Canada Paper 84-22, pp. 115-124.
- Alfimov**, A.V. , Berman, D.I., and Sher, A.V., 2003: Tundra-steppe insect assemblages and the reconstruction of the Late Pleistocene climate in the lower reaches of the Kolyma River. *Zoologicheskii Zhurnal* **82** 281–300 (In Russian).
- Alley**, R.B., 1991: Deforming-bed origin for southern Laurentide till sheets? *Journal of Glaciology*, **37** (125), 67-76.
- Alley**, R.B., 2003: Paleoclimatic insights into future climate challenges. *Philosophical Transactions of the Royal Society of London, Series A*, **361**(1810), 1831-1849.
- Alley**, R.B. 2007: Wally was right: Predictive ability of the North Atlantic “conveyor belt” hypothesis for abrupt climate change. *Annual Review of Earth and Planetary Sciences* **35** 241-272.

- 2619 **Alley**, R.B. and S. Anandakrishnan, 1995: Variations in melt-layer frequency in the
2620 GISP2 ice core: implications for Holocene summer temperatures in central
2621 Greenland. *Annals of Glaciology*, **21**, 64-70.
2622
- 2623 **Alley**, R.B. and A.M. Agustsdottir, 2005: The 8k event: Cause and consequences of a
2624 major Holocene abrupt climate change, *Quaternary Science Reviews*, **24**, 1123 -
2625 1149.
2626
- 2627 **Alley**, R.B. and K.M. Cuffey, 2001: Oxygen- and hydrogen-isotopic ratios of water in
2628 precipitation: Beyond paleothermometry. In J.W. Valley and D. Cole, eds., Stable
2629 Isotope Geochemistry, *Reviews in Mineralogy and Geochemistry*, **43**,
2630 Mineralogical Society of America, p. 527-553
2631
- 2632 **Alley**, R.B., D.A. Meese, C.A. Shuman, A.J. Gow, K.C. Taylor, P.M. Grootes, J.W.C.
2633 White, M. Ram, E.D. Waddington, P.A. Mayewski, and G.A. Zielinski, 1993:
2634 Abrupt increase in snow accumulation at the end of the Younger Dryas event.
2635 *Nature*, **362**, 527-529.
2636
- 2637 **Alley**, R.B., C.A. Shuman, D.A. Meese, A.J. Gow, K.C. Taylor, K.M. Cuffey, J.J.
2638 Fitzpatrick, P.M. Grootes, G.A. Zielinski, M. Ram, G. Spinelli, and B. Elder,
2639 1997: Visual-stratigraphic dating of the GISP2 ice core—Basis, reproducibility,
2640 and application. *Journal of Geophysical Research*, **102**, 26,367-26,381.
2641
- 2642 **Alley**, R.B., E.J. Brook and S. Anandakrishnan, 2002: A northern lead in the orbital
2643 band: North-south phasing of ice-age events. *Quaternary Science Reviews*, **21**(1-
2644 3), 431-441
2645
- 2646 **Ammann**, Caspar M., Fortunat Joos, David S. Schimel, Bette L. Otto-Bliesner, and
2647 Robert A. Tomas, 2007: Solar influence on climate during the past millennium—
2648 Results from transient simulations with the NCAR Climate System Model.
2649 *Proceedings of the National Academy of Sciences, U.S.A.*,

www.pnas.org/cgi//doi/10.1073/pnas.0605064103

Andersen, K.K., A. Svensson, S. Johnsen, S.O. Rasmussen, M. Bigler, R. Rothlisberger, U. Ruth, M.L. Siggaard-Andersen, J.P. Steffensen, D. Dahl-Jensen, B.M. Vinther, and H.B. Clausen, 2006: The Greenland Ice Core Chronology 2005, 15–42 kyr. Part I— Constructing the time scale. *Quaternary Science Reviews*, **25, 3246-3257.**

Anderson, N.J. and M.J. Leng, 2004: Increased aridity during the early Holocene in West Greenland inferred from stable isotopes in laminated-lake sediments. *Quaternary Science Reviews* **23, 841-849.**

Anderson, L., M.B. Abbott, and B.P. Finney, 2001: Holocene climate inferred from oxygen isotope ratios in lake sediments, central Brooks Range, Alaska. *Quaternary Research*, **55, 313-321.**

Anderson, L., M.B. Abbott, B.P. Finney, and S.J. Burns, 2005: Regional atmospheric circulation change in the North Pacific during the Holocene inferred from lacustrine carbonate oxygen isotopes, Yukon Territory, Canada. *Quaternary Research*, **64, 1-35.**

Anderson, P.M. and Lozhkin, A.V., 2001: The stage 3 interstadial complex (Karginskii/middle Wisconsinan interval) of Beringia: variations in paleoenvironments and implications for paleoclimatic interpretations. *Quaternary Science Reviews*, **20 93– 125.**

Anderson, P.M., P.J. Bartlein, L.B. Brubaker, K. Gajewski, and J.C. Ritchie, 1989: Modern analogues of late Quaternary pollen spectra from the western interior of North America. *Journal of Biogeography*, **16, 573-596.**

Anderson, P.M., P.J. Bartlein, L.B. Brubaker, K. Gajewski, and J.C. Ritchie, 1991: Vegetation-pollen-climate relationships for the arcto-boreal region of North

- America and Greenland. *Journal of Biogeography*, **18** 565-582.
- Anderson**, R.K., G.H. Miller, J.P. Briner, N.A. Lifton, and S.B. DeVogel, 2008: A millennial perspective on Arctic warming from ^{14}C in quartz and plants emerging from beneath ice caps. *Geophysical Research Letters*, **35**, L01502, doi:10.1029/2007GL032057.
- Andreev**, A.A., D.M. Peteet, P.E. Tarasov, F.A. Romanenko, L.V. Filimonova, and L.D. Sulerzhitsky, 2001: Late pleistocene interstadial environment on Faddeyevskiy Island, East-Siberian Sea, Russia. *Arctic, Antarctic, and Alpine Research* **33**, 28-35.
- Andrews**, J.T., L.M. Smith, R. Preston, T. Cooper, and A.E. Jennings, 1997: Spatial and temporal patterns of iceberg rafting (IRD) along the East Greenland margin, ca. 68 N, over the last 14 cal ka. *Journal of Quaternary Science*, **12**, 1-13.
- Archer**, D., 2007: Methane hydrate stability and anthropogenic climate change. *Biogeosciences*, **4**: p. 521-544
- Arctic Climate Impact Assessment (ACIA)**, 2004: *Impacts of a Warming Arctic—Arctic Climate Impact Assessment*. Cambridge University Press, Cambridge, U.K., 1042 pp.
- Arctic Monitoring and Assessment Programme**, 1998: AMAP Assessment Report Arctic Pollution Issues. AMAP, Oslo, Norway. 871 pp.
- Astakhov**, V.I., 1995: The mode of degradation of Pleistocene permafrost in West Siberia. *Quaternary International*, **28**, 119-121.
- Backman**, J., M. Jakobsson, R. Løvlie, L. Polyak, and L.A. Febo, 2004: Is the central Arctic Ocean a sediment starved basin? *Quaternary Science Reviews*, **23**, 1435-

- 2712 1454.
2713
2714 **Backman, J.**, K. Moran, D.B. McInroy, L.A. Mayer, and the Expedition 302 scientists,
2715 2006: *Proceedings of IODP, 302*. Edinburgh (Integrated Ocean Drilling Program
2716 Management International, Inc.). doi:10.2204/iodp.proc.302.2006.
2717
2718 **Balco, G.**, Rovey, C.W. Stone, O.H., 2005a: The First Glacial Maximum in North
2719 America. *Science* **307**, 222.
2720
2721 **Balco, G.**, Stone, J.O.H, Jennings, C., 2005b: Dating Plio-Pleistocene glacial sediments
2722 using the cosmic-ray-produced radionuclides ^{10}Be and ^{26}Al . *American Journal of*
2723 *Science*, **305** 1-41.
2724
2725 **Ballantyne, A.P.**, N.L. Rybczynski, P.A. Baker, C.R. Harington, and D. White, 2006:
2726 Pliocene Arctic temperature constraints from the growth rings and isotopic
2727 composition of fossil larch. *Palaeogeography, Palaeoclimatology,*
2728 *Palaeoecology*, **242**, 188-200
2729
2730 **Barber, V.A.** and B.P. Finney, 2000: Lake Quaternary paleoclimatic reconstructions for
2731 interior Alaska based on paleolake-level data and hydrologic models. *Journal of*
2732 *Paleolimnology*, **24**, 29-41.
2733
2734 **Bard, Edouard**, 2002: Climate shocks—Abrupt changes over millennial time scales.
2735 *Physics Today*, **December**, 32-38.
2736
2737 **Barley, E.M.**, I.R. Walker, and J. Kurek, et al., 2006: A northwest North American
2738 training set—Distribution of freshwater midges in relation to air temperature and
2739 lake depth. *Journal of Paleolimnology*, **36**, 295-314.
2740
2741 **Barnekow, L.** and P. Sandgren, 2001: Palaeoclimate and tree-line changes during the
2742 Holocene based on pollen and plant macrofossil records from six lakes at different

- altitudes in northern Sweden. *Review of Palaeobotany and Palynology*, **117**, 109-118.
- Barron**, E.J., Fawcett, P.J., Pollard, D., Thompson, S., 1993: Model simulations of cretaceous climates - the role of geography and carbon-dioxide. Philosophical Transactions of the Royal Society of London Series B-Biological Sciences **341:1297** 307-315.
- Barron**, E. J., Fawcett, P. J., Peterson, W. H., Pollard, D., and Thompson, S. L., 1995: A “simulation” of mid-Cretaceous climate. *Paleoceanography*, **8** 785–798.
- Barry**, R.G., Serreze, M.C., Maslanik, J.A., Preller, R.H., 1993: The arctic sea-ice climate system - observations and modeling. *Reviews of Geophysics*, **31** (4), p. 397-422.
- Bartlein**, P.J., Anderson, K.H., Anderson, P.M., Edwards, M.E., Mock, C.J., Thompson, R.S., Webb, R.S., Webb III, T., Whitlock, C., 1998: Paleoclimate simulations for North America over the past 21,000 years: features of the simulated climate and comparisons with paleoenvironmental data. *Quaternary Science Reviews* **17**, 549–585.
- Bauch**, D., J. Carstens, and G. Wefer, 1997: Oxygen isotope composition of living *Neogloboquadrina pachyderma* (sin.) in the Arctic Ocean. *Earth and Planetary Science Letters*, **146**, 47-58.
- Bauch**, D., P. Schlosser, and R.G. Fairbanks, 1995: Freshwater balance and the sources of deep and bottom waters in the Arctic Ocean inferred from the distribution of H_2^{18}O . *Progress in Oceanography*, **35**, 53-80.
- Bauch**, H. and E.S. Kandiano, 2007: Evidence for early warming and cooling in North

- 2773 Atlantic surface waters during the last interglacial. *Paleoceanography*, **22**,
2774 PA1201, doi:10.1029/2005PA001252.
- 2775
- 2776 **Bauch**, H.A., H. Erlenkeuser, K. Fahl, R.F. Spielhagen, M.S. Weinelt, H. Andruleit, and
2777 R. Henrich, 1999: Evidence for a steeper Eemian than Holocene sea surface
2778 temperature gradient between Arctic and sub-Arctic regions. *Palaeogeography*,
2779 *Palaeoclimatology*, *Palaeoecology*, **145**, 95-117.
- 2780
- 2781 **Bauch**, H.A., H. Erlenkeuser, J.P. Helmke, and U. Struck, 2000: A paleoclimatic
2782 evaluation of marine oxygen isotope stage 11 in the high-northern Atlantic (Nordic
2783 seas). *Global and Planetary Change*, **24**, 27-39.
- 2784
- 2785 **Bauch**, H.A. and Erlenkeuser, H. 2003: Interpreting Glacial-Interglacial Changes in Ice
2786 Volume and Climate From Subarctic Deep Water Foraminiferal $\delta^{18}O$. In: Earth's
2787 Climate and Orbital Eccentricity: The Marine Isotope Stage 11 Question. Andre
2788 W. Droxler, Richard Z. Poore, and Lloyd H. Burckle (Eds) Geophysical
2789 Monograph Series **137**.
- 2790
- 2791 **Beget**, J.E., 2001: Continuous Late Quaternary proxy climate records from loess in
2792 Beringia. *Quaternary Science Reviews* 20, 499-507.
- 2793
- 2794 **Behl**, R.J., and Kennett, J.P., 1996: Brief interstadial events in the Santa Barbara Basin,
2795 NE Pacific, during the past 60 kyr. *Nature* **379** 243-246.
- 2796
- 2797 **Bennike**, O., K.P. Brodersen, E. Jeppesen, and I.R. Walker, 2004: Aquatic invertebrates
2798 and high latitude paleolimnology. In: *Long-Term Environmental Change in Arctic*
2799 *and Antarctic Lakes* [Pienitz, R., M.S.V. Douglas, and J.P. Smol (eds.)].
2800 Springer, Dordrecht. pp. 159-186.
- 2801
- 2802 **Berger**, A. and M.F. Loutre, 1991: Insolation values for the climate of the last million

- 2803 years. *Quaternary Sciences Review*, **10(4)**, 297-317.
- 2804
- 2805 **Berger**, A., Loutre, M. F. , and Laskar, J., 1992: Stability of the Astronomical
- 2806 Frequencies Over the Earth's History for Paleoclimate Studies. *Science*, **255**,
- 2807 (5044) 560-566.
- 2808
- 2809 **Berner**, R.A., and Kothavala, Z., 2001: GEOCARB III: A revised model of atmospheric
- 2810 CO₂ over Phanerozoic time. *American Journal of Science* **301(2)**, 182-204.
- 2811
- 2812 **Bice**, K.L., Birgel, D., Meyers, P.A., Dahl, K.A., Hinrichs, K.U., Norris, R.D., 2006: A
- 2813 multiple proxy and model study of Cretaceous upper ocean temperatures and
- 2814 atmospheric CO₂ concentrations. *Paleoceanography*, **21:2** PA2002.
- 2815
- 2816 **Bigelow**, N., L.B. Brubaker, M.E. Edwards, S.P. Harrison, I.C. Prentice, P.M. Anderson,
- 2817 A.A. Andreev, P.J. Bartlein, T.R. Christensen, W. Cramer, J.O. Kaplan,
- 2818 A.V. Lozhkin, N.V. Matveyeva, D.F. Murrar, A.D. McGuire, V.Y. Razzhivin,
- 2819 J.C. Ritchie, B. Smith, D.A. Walker, K. Gajewski, V. Wolf, B.H. Holmqvist, Y.
- 2820 Igarashi, K. Kremenetskii, A. Paus, M.F.J. Pisarcic, and V.S. Volkova, 2003:
- 2821 Climate change and Arctic ecosystems—1. Vegetation changes north of 55°N
- 2822 between the last glacial maximum, mid-Holocene, and present. *Journal of*
- 2823 *Geophysical Research*, **108**, doi:10.1029/2002JD002558.
- 2824
- 2825 **Bigler**, C. and R.I. Hall. 2003: Diatoms as quantitative indicators of July temperature—A
- 2826 validation attempt at century-scale with meteorological data from northern
- 2827 Sweden. *Palaeogeography, Palaeoclimatology, Palaeoecology*, **189**, 147-160.
- 2828
- 2829 **Birks**, H.H., 1991: Holocene vegetational history and climatic change in west
- 2830 Spitzbergen—Plant macrofossils from Skardtjorna, an arctic lake. *The Holocene*,
- 2831 **1**, 209–218.
- 2832
- 2833 **Birks**, H.J.B., 1998: Numerical tools in palaeolimnology—Progress, potentialities, and

- 2834 problems. *Journal of Paleolimnology*, **20**, 307-332.
- 2835
- 2836 **Björk**, G., J. Soöderkvist, P. Winsor, A. Nikolopoulos, and M. Steele, 2002: Return of
2837 the cold halocline layer to the Amundsen Basin of the Arctic Ocean—
2838 Implications for the sea ice mass balance. *Geophysical Research Letters*, **29(11)**,
2839 1513, doi:10.1029/2001GL014157.
- 2840
- 2841 **Boellstorff**, J., 1987: North American Pleistocene stages reconsidered in light of
2842 probably Pliocene-Pleistocene continental glaciation. *Science* **202**:2004365) 305-
2843 307.
- 2844
- 2845 **Bonan**, G.B., Pollard, D., Thompson, S.L., 1992: Effects of boreal forest vegetation on
2846 global climate. *Nature* **359**(6397) p.716-718.
- 2847
- 2848 **Boyd**, T.J., M. Steel, R.D. Muench, and J.T. Gunn, 2002: Partial recovery of the Arctic
2849 Ocean halocline. *Geophysical Research Letters*, **29(14)**, 1657,
2850 doi:10.1029/2001GL014047
- 2851
- 2852 **Box**, J.E., Bromwich, D.H., Veenhuis, B.A., Bai, L.S., Stroeve, J.C., Rogers, J.C.,
2853 Steffen, K., Haran, T., Wang, S.H., 2006: Greenland ice sheet surface mass
2854 balance variability (1988-2004) from calibrated polar MM5 output. *Journal of*
2855 *Climate* **19:12** 2783-2800
- 2856
- 2857 **Braconnot**, P., Otto-Bliesner, B., Harrison, S., Joussaume, FS., Peterchmitt, J.-Y., Abe-
2858 Ouchi, A., Crucifix, M., Driesschaert, E., Fichefet, Th., Hewitt, C. D., Kageyama, M.,
2859 Kitoh, A., Laine, A., Loutre, M.-F., Marti, O., Merkel, U., Ramstein, G., Valdes, P.,
2860 Weber, S. L., Yu, Y., and Zhao, Y., 2007: Results of PMIP2 coupled simulations of
2861 the Mid-Holocene and Last Glacial Maximum – Part 1: experiments and large-scale
2862 features, *Climates of the Past*, **3**, 261– 277.
- 2863
- 2864 **Bradley**, R.S., 1990: Holocene paleoclimatology of the Queen Elizabeth Islands,

- 2865 Canadian high Arctic. *Quaternary Science Reviews*, **9**, 365-384.
- 2866
- 2867 **Bradley, R. S.**, 2000: Past global changes and their significance for the future.
- 2868 *Quaternary Science Reviews* **19** 391-402.
- 2869
- 2870 **Bradley, R.S. and P.D. Jones, (eds.)**, 1992: *Climate Since AD 1500*. Routledge, London.
- 2871 677 pp.
- 2872
- 2873 **Bradley, R.S., Hughes, M.K., and Diaz, H.F.**, 2003a: Climate in Medieval Time,
- 2874 *Science*, **302**, 404 – 405 doi: 10.1126/science.1090372
- 2875
- 2876 **Bradley, R.S., K.R. Briffa, J. Cole, and T.J. Osborn**, 2003b: The climate of the last
- 2877 millennium. In: *Paleoclimate, Global Change and the Future* [Alverson, K.D.,
- 2878 R.S. Bradley, and T.F. Pedersen (eds.)]. Springer, Berlin, pp. 105-141.
- 2879
- 2880 **Brassell, S.C., G. Eglinton, I.T. Marlowe, U. Pflaumann, and M. Sarnthein**, 1986:
- 2881 Molecular stratigraphy—A new tool for climatic assessment. *Nature*, **320**, 129-
- 2882 133.
- 2883
- 2884 **Bray, P.J., Blockey, S.P.E., Coope, G.R., Dadswell, L.F., Elias, S.A., Lowe, J.J., and**
- 2885 **Pollard, A.M.**, 2006: Refining mutual climatic range (MCR) quantitative
- 2886 estimates of paleotemperature using ubiquity analysis. *Quaternary Science*
- 2887 *Reviews* **25** (15-16), 1865-1876.
- 2888
- 2889 **Brewer, S., Guiot, J., and Torre, F.**, 2007: Mid-Holocene climate change in Europe: a
- 2890 data-model comparison. *Climate of the Past* **3** 499-512.
- 2891
- 2892 **Briffa, K.R., Osborn, T.J., Schweingruber, F.H., Harris, I.C., Jones, P.D., Shiyatov,**
- 2893 **S.G., Vaganov, E.A.**, 2001: Low-frequency temperature variations from a
- 2894 northern tree ring density network. *Journal of Geophysical Research* **106**:2929–

- 2895 2941.
2896
2897 **Brigham**, J.K., 1985: Marine stratigraphy and amino acid geochronology of the Gubik
2898 Formation, western Arctic Coastal Plain, Alaska. Doctoral dissertation, University
2899 of Colorado, Boulder; U.S. Geological Survey Open-File Report 85-381. 21p.
2900
2901 **Brigham-Grette**, J. and Carter, L.D., 1992: Pliocene marine transgressions of northern
2902 Alaska— Circumarctic correlations and paleoclimate. *Arctic*, **43**(4), 74-89.
2903
2904 **Brigham-Grette**, J. and Hopkins, D.M., 1995: Emergent-marine record and paleoclimate
2905 of the last interglaciation along the northwest Alaskan coast. *Quaternary*
2906 *Research*, **43**, 154-173.
2907
2908 **Brigham-Grette**, J., Lozhkin, A.V., Anderson, P.M., and Glushkova, O.Y., 2004:
2909 Paleoenvironmental Conditions in Western Beringia Before and During the Last
2910 Glacial Maximum. IN: D. B. Madsen (editor), *Entering America: Northeast Asia*
2911 *and Beringia Before the Last Glacial Maximum*, Univ of Utah Press. Chapter 2, p.
2912 29-61.
2913
2914 **Briner**, J.P., Michelutti, N., Francis, D.R., Miller, G.H., Axford, Y., Wooller, M.J., and
2915 Wolfe, A.P. 2006: A multi-proxy lacustrine record of Holocene climate change on
2916 northeastern Baffin Island. *Quaternary Research* 65, 431-442.
2917
2918 **Brinkhuis**, H., Schouten, S., Collinson, M.E., Sluijs, A., Damsfte, J.S.S., Dickens, G.R.,
2919 Huber, M., Cronin, T.M., Onodera, J., Takahashi, K., Bujak, J.P., Stein, R., van
2920 der Burgh, J., Eldrett, J.S., Harding, I.C., Lotter, A.F., Sangiorgi, F., Cittert,
2921 H.V.V., de Leeuw, J.W., Matthiessen, J., Backman, J., Moran, K., (Expedition
2922 302 Scientists), 2006: Episodic fresh surface waters in the Eocene Arctic Ocean.
2923 *Nature*, **441** (7093) 606-609.
2924

- 2925 **Broecker, W.S.**, 2001: Was the Medieval Warm Period Global? *Science*, **291** (5508)
2926 1497-1499. DOI:10.1126/science.291.5508.1497
2927
- 2928 **Broecker, W.S. and Hemming, S.**, 2001: Climate swings come into focus. *Nature*,
2929 **294:5550** 2308-2309.
2930
- 2931 **Broecker, W.S., Peteet, D.M., Rind, D.**, 1985: Does the ocean-atmosphere system have
2932 more than one stable mode of operation. *Nature*, **315** (6014) p. 21-26.
2933
- 2934 **Brouwers, E.M.**, 1987: On *Prerygocythereis vunnieuwenhuisei* Brouwers sp.nov. In: A
2935 stereo-atlas of ostracode shells. British Micropaleontological Society, [Bate, R.H.,
2936 Home, D.J., Neale, J.W., and Siveter, D.J., [eds.)], London 14, Part 1 : 17-20.
2937
- 2938 **Brown, J. and Romanovsky, V.**, submitted. Report from the International Permafrost
2939 Association: *State of Permafrost in the First Decade of the 21st Century*.
2940 *Permafrost and Periglacial Processes* (submitted 03-26-08).
2941
- 2942 **Buchardt, B. and L.A. Simonarson**, 2003: Isotope palaeotemperatures from the Tjörnes
2943 beds in Iceland: evidence of Pliocene cooling. *Palaeogeography*,
2944 *Palaeoclimatology, Palaeoecology* **189** 71-95.
2945
- 2946 **Budyko, M.I., Ronov, A.B. and Yanshin, A.L.**, 1985: The History of the Earth's
2947 Atmosphere. Leningrad, Gidrometeoirdat. 209 pp. (In Russian; English
2948 translation: Springer, Berlin, 1987, 139 pp.
2949
- 2950 **Calkin, P.E.**, 1988: Holocene glaciation of Alaska (and adjoining Yukon Territory,
2951 Canada). *Quaternary Science Reviews*, **7**, 159-184.
2952
- 2953 **CAPE Project Members**, 2001: Holocene paleoclimate data from the Arctic: testing
2954 models of global climate change. *Quaternary Science Reviews* 20: 1275-1287.

- 2955
- 2956 **CAPE–Last Interglacial Project Members**, 2006: Last Interglacial Arctic warmth
2957 confirms polar amplification of climate change. *Quaternary Science Reviews*, **25**,
2958 1383-1400.
- 2959
- 2960 **Carter**, L.D., 1981: A Pleistocene sand sea on the Alaskan Arctic Coastal Plain, *Science*,
2961 **211** (4480) 381-383.
- 2962
- 2963 **Carter**, L.D., J. Brigham-Grette, L. Marinovich, Jr., V.L. Pease, and U.S. Hillhouse,
2964 1986: Late Cenozoic Arctic Ocean sea ice and terrestrial paleoclimate. *Geology*, **14**,
2965 675-678.
- 2966
- 2967 **Chapin**, F.S. III, M. Sturm, M.C. Serreze, J.P. Mcfadden, J.R. Key, A.H. Lloidy, and 15
2968 others, 2005: Role of land-surface changes in Arctic summer warming. *Science*,
2969 **310**, 657-660.
- 2970
- 2971 **Chapman**, M.R., N.J. Shackleton, and J.-C. Duplessy, 2000: Sea surface temperature
2972 variability during the last glacial-interglacial cycle—Assessing the magnitude and
2973 pattern of climate change in the North Atlantic. *Palaeogeography*,
2974 *Palaeoclimatology*, *Palaeoecology*, **157**, 1-25.
- 2975
- 2976 **Chapman**, W.L. and Walsh, J.E., 2007: Simulations of Arctic temperature and pressure
2977 by global coupled models. *Journal of Climate*, **20:4** p. 609-632.
- 2978
- 2979 **Clark**, P.U. and D. Pollard, 1998: Origin of the Middle Pleistocene transition by ice
2980 sheet erosion of regolith, *Paleoceanography* **13** 1–9.
- 2981
- 2982 **Clark**, P.U., Archer, D., Pollard, D., Blum, J.D., Rial, J.A., Brovkin, V., Mix, A.C.,
2983 Pisias, N.G., Roy, M., 2006: The middle Pleistocene transition:

- 2984 characteristics, mechanisms, and implications for long-term changes in
2985 atmospheric pCO₂. *Quaternary Science Reviews* **25**, 3150-3184.
2986
- 2987 **Clayden, S.L., L.C. Cwynar, G.M. MacDonald, and A.A. Velichko, 1997:** Holocene
2988 pollen and stomates from a forest-tundra site on the Taimyr Peninsula, Siberia.
2989 *Arctic and Alpine Research*, **29**, 327-333.
2990
- 2991 Climate Long-Range Investigation Mapping and Prediction (**CLIMAP**) Project
2992 Members, 1981: Seasonal reconstructions of the Earth's surface at the last glacial
2993 maximum: *Geological Society of America Map and Chart Series* MC-36, p. 1-18
2994
- 2995 Climate Long-Range Investigation Mapping and Prediction (**CLIMAP**) Project
2996 Members, 1984: The last interglacial ocean. *Quaternary Research* **21** 123-224.
2997
- 2998 **Cockford, S.J. and S.G. Frederick, 2007:** Sea ice expansion in the Bering Sea during the
2999 Neoglacial—Evidence from archeozoology. *The Holocene*, **17**, 699-706.
3000
- 3001 **Cohen, A.S., 2003:** *Paleolimnology—The history and evolution of lake systems*. Oxford
3002 University Press, Oxford, U.K., 528 pp.
3003
- 3004 **Colinvaux, P. A. 1964:** The environment of the Bering Land Bridge. *Ecological*
3005 *Monographs* **34**:297-329.
3006
- 3007 **Conte, M.H., M. Sicre, C. Rühlemann, J.C. Weber, S. Schulte, D. Schulz-Bull, and T.**
3008 **Blanz, 2006:** Global temperature calibration of the alkenone unsaturation index
3009 (UK'₃₇) in surface waters and comparison with surface sediments. *Geochemistry,*
3010 *Geophysics, Geosystems*, **7**, Q02005, doi:10.1029/2005GC001054.
3011
- 3012 **Cronin, T.M, Dwyer, G.S., Kamiyac, T., Schwedea, S. and Willarda, D. A. 2003:**
3013 Medieval Warm Period, Little Ice Age and 20th century temperature variability
3014 from Chesapeake Bay. *Global and Planetary Change*, **36**: 17-29

- Crowley, T.J.**, 1998: Significance of tectonic boundary conditions for paleoclimate simulations. In: *Tectonic Boundary Conditions for Climate Reconstructions* [Crowley, T.J., and K.C. Burke (eds.)]. Oxford University Press, New York, pp. 3-17.
- Crowley, T.J.**, 1990: Are there any satisfactory geologic analogs for a future greenhouse warming? *Journal of Climatology*, **3**: 1282- 1492.
- Crowley, T.J.**, 2000: Causes of climate change over the past 1000 years. *Science*, **289**, 270-277.
- Crowley, T.J.** and Lowery, T., 2000: How warm was the Medieval warm period? *Ambio*, **29**, 51-54.
- Crowley, T.J.**, Baum, S.K., Kim, K.Y., Hegerl, G.C., Hyde, W.T., 2003: Modeling ocean heat content changes during the last millennium. *Geophysical Research Letters* **30**:1932. doi:10.1029/2003GL017801
- Cuffey, K.M.** and G.D. Clow, 1997: Temperature, accumulation, and ice sheet elevation in central Greenland through the last deglacial transition. *Journal of Geophysical Research*, **102(C12)**, 26,383-26,396.
- Cuffey, K.M.**, G.D. Clow, R.B. Alley, M. Stuiver, E.D. Waddington, and R.W. Saltus, 1995: Large Arctic temperature change at the Wisconsin-Holocene glacial transition. *Science*, **270**, 455-458.
- D'Arrigo, R.**, Wilson, R., Jacoby, G., 2006: On the long-term context for late twentieth century warming. *Journal of Geophysical Research*, **111**, D03103, doi:10.1029/2005JD006352.

- Dahe, Q.**, Petit, J.R., Jouzel, J., Stievenard, M., 1994: Distribution of stable isotopes in surface snow along the route of the 1990 International Trans-Antarctic Expedition. *Journal of Glaciology* **40**:107–118
- Dahl, S.O.** and Nesje, A., 1996: A new approach to calculating Holocene winter precipitation by combining glacier equilibrium-line altitudes and pine-tree limits: a case stud from Hardangerjokulen, central southern Norway. *The Holocene* **6**:4 381-398. DOI: 10.1177/095968369600600401
- Dahl-Jensen, D.**, K. Mosegaard, N. Gundestrup, G.D. Clow, S.J. Johnsen, A.W. Hansen, and N. Balling, 1998: Past temperature directly from the Greenland Ice Sheet. *Science*, **282**, 268-271.
- Dansgaard, W.**, 1964: Stable isotopes in precipitation. *Tellus*, **16**, 436-468.
- Dansgaard, W.**, White, J.W.C., Johnsen, S.J., 1989: The abrupt termination of the Younger Dryas climate event. *Nature*, **339** (6225) 532-534.
- Delworth, T.L.**,and Knutson, T.R., 2000: Simulation of early 20th century global warming. *Science*, **287**:5461 2246-225
- de Vernal, A.**, C. Hillaire-Marcel, and D.A. Darby, 2005: Variability of sea ice cover in the Chukchi Sea (western Arctic Ocean) during the Holocene. *Paleoceanography*, **20**, PA4018, doi:10.1029/2005PA001157.
- Denton, G.H.**, R.B. Alley, G.C. Comer and W.S. Broecker, 2005: The role of seasonality in abrupt climate change. *Quaternary Science Reviews* **24**(10-11): 1159-1182.
- Digerfeldt, G.**, 1988: Reconstruction and regional correlation of Holocene lake-level fluctuations in Lake Bysjön, South Sweden. *Boreas*, **17**, 237-263.

- Donnadieu, Y., R. Pierrehumbert, R. Jacob, and F. Fluteau, 2006:** Modeling the primary control of paleogeography on Cretaceous climate. *Earth and Planetary Science Letters*, **248**, 426-437.
- Douglas, M.S.V. and J.P. Smol, 1994:** Limnology of high arctic ponds (Cape Herschel, Ellesmere Island, N.W.T.). *Archiv für Hydrobiologie*, **131**, 401-434.
- Douglas, M.S.V. and J.P. Smol, 1999:** Freshwater diatoms as indicators of environmental change in the High Arctic. In: *The Diatoms—Applications for the Environment and Earth Sciences* [Stoermer, E. and J.P. Smol (eds.)]. Cambridge, U.K.: Cambridge University Press. 488 p.
- Douglas, M.S.V., 2007:** Environmental change at high latitudes. In: *Geological and Environmental Applications of the Diatom—Pond Scum to Carbon Sink* [Starratt, S.W. (ed.)]. The Paleontological Society Papers, **13**, 169-179.
- Douglas, M.S.V., J.P. Smol, and W. Blake, Jr., 1994:** Marked post-18th century environmental change in high Arctic ecosystems. *Science*, **266**, 416-419.
- Douglas, M.S.V., J.P. Smol, R. Pienitz, and P. Hamilton, 2004:** Algal indicators of environmental change in arctic and antarctic lakes and ponds. In: *Long-Term Environmental Change in Arctic and Antarctic Lakes* [Pienitz, R., M.S.V. Douglas, and J.P. Smol (eds.)]. Springer, Dordrecht. pp. 117-157.
- Dowdeswell, J.A., J.O. Hagen, H. Björnsson, A.F. Glazovsky, W.D. Harrison, P. Holmlund, J. Jania, R.M. Koerner, B. Lefauconnier, C.S.L. Ommanney, and R.H. Thomas, 1997:** The mass balance of circum-Arctic glaciers and recent climate change. *Quaternary Research*, **48**, 1-14.
- Dowsett, H.J., 2007:** The PRISM Palaeoclimate Reconstruction and Pliocene Sea-

- 3107 Surface Temperature. In: *Deep-time perspectives on climate change: marrying*
3108 *the signal from computer models and biological proxies*, [Williams, M., et al.,
3109 (eds.)] The Micropalaeontological Society, Special Publication, The Geological
3110 Society, London, 459-480.
3111
- 3112 **Dowsett, H.J.** , J.A. Barron, R.Z. Poore, R.S. Thompson, T.M. Cronin, S.E. Ishman, S.E.,
3113 D.A. Willard, 1999: Middle Pliocene paleoenvironmental reconstruction:
3114 PRISM2, USGS Open File Report 99-535.
3115
- 3116 **Dowsett, H.J.**, and eight others, 1994: Joint investigations of the middle Pliocene climate
3117 I— PRISM paleoenvironmental reconstructions. *Global and Planetary Change*, **9**,
3118 169-195
3119
- 3120 **Droxler, A.W.** and Farrell, J.W., 2000: Marine Isotope Stage 11 (MIS11): new insights
3121 for a warm future. *Global and Planetary Change*, **24:1** 1-5
3122
- 3123 **Droxler, A.W.**, R.B. Alley, W.R. Howard, R.Z. Poore and L.H. Burckle. 2003: Unique
3124 and exceptionally long interglacial marine isotope stage 11: Window into Earth
3125 future climate. In Droxler, A.W., R.Z. Poore and L.H. Burckle, eds., *Earth's*
3126 *Climate and Orbital Eccentricity: The Marine Isotope Stage 11 Question*,
3127 *Geophysical Monograph* **137**, American Geophysical Union, p. 1-14.
3128
- 3129 **Duk-Rodkin, A.**, R.W. Barendregt, D.G. Froese, F. Weber, R.J. Enkin, I.R. Smith, Grant
3130 D. Zazula, P. Waters, and R. Klassen, 2004: Timing and Extent of Plio-
3131 Pleistocene glaciations in North-Western Canada and East-Central Alaska. In:
3132 *Quaternary Glaciations-Extent and Chronology, Part II, North America* [Ehlers,
3133 J. and P.L. Gibbard (eds.)]. Elsevier, New York, pp. 313-345.
3134
- 3135 **Dyke, A.S.** and J.M. Savelle, 2001: Holocene history of the Bering Sea bowhead whale
3136 (*Balaena mysticetus*) in its Beaufort Sea summer grounds off southwestern
3137 Victoria Island, western Canadian Arctic. *Quaternary Research*, **55**, 371-379.

- Dykoski**, C.A., Edwards, R.L., Cheng, H., Yuan, D., Cai, Y., Zhang, M., Lin, Y., Qing, J., An, Z., and Revenaugh, J., 2005: A high-resolution, absolute-dated Holocene and deglacial Asian monsoon record from Dongge Cave, China. *Earth and Planetary Science Letters*, **233**, 71-86.
- Edwards**, M.E., N.H. Bigelow, B.P. Finney, and W.R. Eisner, 2000: Records of aquatic pollen and sediment properties as indicators of late-Quaternary Alaskan lake levels. *Journal of Paleolimnology*, **24**, 55-68.
- Elias**, S.A. and Matthews, J.V. Jr., 2002: Arctic North American seasonal temperatures in the Pliocene and Early Pleistocene, based on mutual climatic range analysis of fossil beetle assemblages, *Canadian Journal of Earth Sciences*, **39**, 911-920.
- Elias**, S.A., 2007: Beetle records—Late Pleistocene North America. In: *Encyclopedia of Quaternary Science* [Elias, S.A. (ed.)]. Elsevier, Amsterdam, pp. 222-236.
- Elias**, S.A., J.T. Andrews, and K.H. Anderson, 1999: New insights on the climatic constraints on the beetle fauna of coastal Alaska derived from the mutual climatic range method of paleoclimate reconstruction. *Arctic, Antarctic, and Alpine Research*, **31**, 94-98.
- Elias**, S.A., K. Anderson, and J.T. and Andrews, 1996a : Late Wisconsin climate in the northeastern United States and southeastern Canada, reconstructed from fossil beetle assemblages. *Journal of Quaternary Science*, **11**, 417-421.
- Ellis**, J.M., and Calkin, P.E., 1984: Chronology of Holocene glaciation, central Brooks Range, Alaska. *Geological Society of America Bulletin*, **95**, 897-912.
- Epstein**, S., H. Buchsbaum, H. Lowenstam, and H.C. Urey, 1953: Revised carbonate-water isotopic temperature scale. *Geological Society of America Bulletin*, **64**,

- 3169 1315-1325.
- 3170
- 3171 **Erez, J.** and B. Luz, 1982: Temperature control of oxygen-isotope fractionation of
3172 cultured planktonic foraminifera. *Nature*, **297**, 220-222.
- 3173
- 3174 **Eronen, M.**, Zetterberg, P., Briffa, K.R., Lindholm, M., Meriläinen, J., Timonen, M.,
3175 2002: The supra-long Scots pine tree-ring record for Finnish Lapland: Part 1,
3176 chronology construction and initial inferences. *The Holocene*, **12(6)** 673-680.
- 3177
- 3178 **Esper, J.**, Cook, E.R., Schweingruber, F.H., 2002: Low-frequency signals in long tree-
3179 ring chronologies for reconstructing past temperature variability. *Science*
3180 **295**:2250–2253.
- 3181
- 3182 **Fairbanks, R.G.**, 1989: A 17,000-year glacio-eustatic sea level record—Influence of
3183 glacial melting rates on the Younger Dryas event and deep-ocean circulation.
3184 *Nature*, **343**, 612-616.
- 3185
- 3186 **Farrera, I.** , Harrison, S. P., Prentice, I. C., Ramstein, G., Guiot, J., Bartlein, P. J.,
3187 Bonnelle, R. Bush, M. Cramer, W. von Grafenstein, U., Holmgren, K.,
3188 Hooghiemstra, H., Hope, G., Jolly, D., Lauritzen, S.-E., Ono, Y., Pinot, S., Stute,
3189 M., Yu, G., 1999: Tropical climates at the Last Glacial Maximum: a new
3190 synthesis of terrestrial palaeoclimate data. I. Vegetation, lake-levels and
3191 geochemistry. *Climate Dynamics* **15**, 823-856.
- 3192
- 3193 **Finney, B.**, K. Rühland, J.P. Smol, and M.-A. Fallu, 2004: Paleolimnology of the North
3194 American subarctic. In: *Long-Term Environmental Change in Arctic and*
3195 *Antarctic Lakes* [Pienitz, R., M.S.V. Douglas, and J.P. Smol (eds.)]. Springer,
3196 Dordrecht. pp. 269-318.
- 3197
- 3198 **Fisher, D.A.**, 1979: Comparison of 100,000 years of oxygen isotope and insoluble
3199 impurity profiles from the Devon Island and Camp Century ice cores. *Quaternary*

- 3200 *Research*, **11**, 299-304.
- 3201
- 3202 **Fisher**, D.A. and R.M. Koerner, Holocene ice core climate history, a multi-variable
3203 approach. 2003: In: *Global Change in the Holocene*, [A. Mackay, R. Battarbee, J.
3204 Birks and F. Oldfield, (eds.)] Arnold, London pp. 281–293.
- 3205
- 3206 **Fisher**, D.A., C. Wake, K. Kreutz, K. Yalcin, E. Steig, P. Mayewski, L. Anderson, J.
3207 Aheng, S. Rupper, C. Zdanowicz, M. Demuth, M. Waskiewicz, D. Dahl-Jensen,
3208 K. Goto-Azuma, J.B. Bourgeois, R.M. Koerner, J. Sekerka, E. Osterberg, M.B.
3209 Abbott, B.P. Finney, and S.J. Burns, 2004: Stable isotope records from Mount
3210 Logan, Eclipse ice cores and nearby Jellybean Lake. Water cycle of the North
3211 Pacific over 2000 years and over five vertical kilometres—Sudden shift and
3212 tropical connections. *Geographie physique et Quaternaire*, **58**, 9033-9048.
- 3213
- 3214 **Fisher**, D.A., R.M. Koerner, J.C. Bourgeois, G. Zielinski, C. Wake, C.U. Hammer, H.B.
3215 Clausen, N. Gundestrup, S. Johnsen, K. Goto- Azuma, T. Hondoh, E. Blake, and
3216 M. Gerasimoff, 1998: Penny Ice Cap cores, Baffin Island, Canada, and the
3217 Wisconsinan Foxe Dome connection—Two states of Hudson Bay ice cover.
3218 *Science*, **279**, 692-695.
- 3219
- 3220 **Flowers**, G.E., Björnsson, H., Geirsdóttir, Á., Miller, G.H., Black, J.L., and Clarke,
3221 G.K.C., **in press**: Holocene climate conditions and glacier variation in central
3222 Iceland from physical modelling and empirical evidence. *Quaternary Science*
3223 *Reviews*.
- 3224
- 3225 **Francis**, J.E., 1988: A 50-million-year-old fossil forest from Strathcona Fiord, Ellesmere
3226 Island, Arctic Canada—Evidence for a warm polar climate. *Arctic*, **41(4)**, 314-318.
- 3227
- 3228 **Fricke**, H.C., O’Neil, J.R., 1999: The correlation between $^{18}\text{O}/^{16}\text{O}$ ratios of meteoric
3229 water and surface temperature: its use in investigating terrestrial climate change

- 3230 over geologic time. *Earth and Planetary Science Letters* **170**:181–196
- 3231
- 3232 **Fronval, T. & Jansen, E., 1997:** Eemian and early Weichselian (140- 60 ka)
- 3233 paleoceanography and paleoclimate in the Nordic seas with comparisons to
- 3234 Holocene conditions. *Paleoceanography* **12**: 443-462.
- 3235
- 3236 **Funder, S., 1989:** Quaternary geology of East Greenland. In: *Quaternary Geology of*
- 3237 *Canada and Greenland* [Fulton, R.J. (ed.)]. Geological Society of America
- 3238 Decade of North American Geology vol. K1, pp. 756-763.
- 3239
- 3240 **Funder, S., O. Bennike, J. Böcher, C. Israelson, K.S. Petersen, and L.A. Simonarson,**
- 3241 **2001:** Late Pliocene Greenland—The Kap Kobenhavn Formation in North
- 3242 Greenland. *Bulletin of the Geological Society of Denmark*, **48**, 117-134.
- 3243
- 3244 **Funder, S., I. Demidov, and Y. Yelovicheva, 2002:** Hydrography and mollusc faunas of
- 3245 the Baltic and the White Sea-North Sea seaway in the Eemian. *Palaeogeography,*
- 3246 *Palaeoclimatology, Palaeoecology*, **184**, 275-304.
- 3247
- 3248 **Fyles, J.G., L. Marinovich Jr., J.V. Mathews Jr., and R. Barendregt, 1991:** Unique
- 3249 mollusc find in the Beaufort Formation (Pliocene) Meighen Island, Arctic Canada. In:
- 3250 *Current Research, Part B, Geological Survey of Canada, Paper 91-1B*, pp. 461-468.
- 3251
- 3252 **Gajewski, K. and G.M. MacDonald, 2004:** Palynology of North American Arctic Lakes.
- 3253 In: *Long Term Environmental Change in Arctic and Antarctic Lakes* [R. Pienitz,
- 3254 M.S.V. Douglas and J.P. Smol (eds.)]. Springer, Netherlands, p. 89-116.
- 3255
- 3256 **Gard, G., 1986:** Calcareous nannofossil biostratigraphy north of 80° latitude in the
- 3257 eastern Arctic Ocean. *Boreas*, **15**, 217-229.
- 3258
- 3259 **Gard, G., 1987:** Late Quaternary calcareous nannofossil biostratigraphy and

- 3260 sedimentation patterns—Fram Strait, Arctica. *Paleoceanography*, **2**, 219-229.
- 3261
- 3262 **Gard, G.**, 1993: Late Quaternary coccoliths at the North Pole—Evidence of ice-free
- 3263 conditions and rapid sedimentation in the central Arctic Ocean. *Geology*, **21**, 227-
- 3264 230.
- 3265
- 3266 **Geirsdottir, A.**, Miller, G.H., Axford, Y. and Olafsdottir, S., in press, Holocene and
- 3267 latest Pleistocene climate and glacier fluctuations in Iceland. *Quaternary Science*
- 3268 *Reviews*.
- 3269
- 3270 **Gervais, B.R.**, G.M. MacDonald, J.A. Snyder, and C.V. Kremenetski, 2002: *Pinus*
- 3271 *sylvestris* treeline development and movement on the Kola Peninsula of Russia—
- 3272 Pollen and stomate evidence. *Journal of Ecology*, **90**, 627-638.
- 3273
- 3274 **Goetcheus, V.G.**, and Birks, H.H. 2001: Full-glacial upland tundra vegetation preserved
- 3275 under tephra in the Beringia National Park, Seward Peninsula, Alaska.
- 3276 *Quaternary Science Reviews*, **20** (1-3): 135-147.
- 3277
- 3278 **Goetz, S.J.**, M.C. Mack, K.R. Gurney, J.T. Randerson, and R.A. Houghton, 2007:
- 3279 Ecosystem responses to recent climate change and fire disturbance at northern
- 3280 high latitudes—Observations and model results contrasting northern Eurasia and
- 3281 North America. *Environmental Research Letters*, **2**, 045031, doi:10.1088/1748-
- 3282 9326/2/4/045031
- 3283
- 3284 **Goodfriend, G.A.**, Brigham-Grette, J., Miller, G.H., 1996: Enhanced age resolution of
- 3285 the marine quaternary record in the Arctic using aspartic acid racemization dating
- 3286 of bivalve shells. *Quaternary Research* **45**: 176–187
- 3287
- 3288 **Goosse, H.**, H. Renssen, A. Timmermann, and R.A. Bradley, 2005: Internal and forced
- 3289 climate variability during the last millennium—A model-data comparison using
- 3290 ensemble simulations. *Quaternary Science Reviews*, **24**, 1345-1360.

- Gradstein**, F.M., Ogg, J.G., and Smith, A.G. (eds.), 2004: *A Geologic Time Scale*. Cambridge University Press, Cambridge, 589 pp.
- Grice**, K., W.C.M. Klein Breteler, S. Schoten, V. Grossi, J.W. de Leeuw, and J.S. Sinninge Damste, 1998: Effects of zooplankton herbivory on biomarker proxy records. *Paleoceanography*, **13**, 686-693.
- Grootes**, P.M., Stuiver, M., White, J.W.C., Johnsen, S., and Jouzel, J., 1993: Comparison of oxygen isotope records from the GISP2 and GRIP Greenland Ice cores. *Nature* **366**, 522-555.
- Grove**, J.M., 1988: *The Little Ice Age*. Methuen, London, 498 pp.
- Grudd**, H., K.R. Briffa, W. Karlén, T.S. Bartholin, P.D. Jones, and B. Kromer, 2002: A 7400-year tree-ring chronology in northern Swedish Lapland—Natural climatic variability expressed on annual to millennial timescales. *The Holocene*, **12**, 657-666.
- Gudina**, V.D. Kryukov, L.K. Levchuk and L.A. Sudkov, 1983: Upper-Pleistocene sediments in north-eastern Taimyr, *Bulletin of Commission on Quaternary Researches* **52**, 90–97 (in Russian).
- Haeberli**, W., Cheng, G.D., Gorbunov, A.P. Harris, S.A., 1993: Mountain permafrost and climatic change. *Permafrost and Periglacial Processes*, **4(2)** 165-174
- Hammarlund**, D., L. Barnekow, H.J.B. Birks, B. Buchardt, and T.W.D. Edwards, 2002: Holocene changes in atmospheric circulation recorded in the oxygen-isotope stratigraphy of lacustrine carbonates from northern Sweden. *The Holocene*, **12**, 339-351.

- Hannon**, G.E. and M.J. Gaillard, 1997: The plant-macrofossil record of past lake-level changes. *Journal of Paleolimnology*, **18**, 15-28.
- Harrison**, S. P., Jolly, D., Laarif, F., Abe-Ouchi, A., Dong, B., Herterich, K., Hewitt, C., Joussaume, S., Kutzbach, J. E., Mitchell, J., de Noblet, N., and Valdes, P., 1998: Intercomparison of simulated global vegetation distributions in response to 6 kyr BP orbital forcing. *Journal of Climate* **11**, 2721-2742.
- Harrison**, S. P., Kutzbach, J. E., Prentice, I. C., Behling, P. J., and Sykes, M. T., 1995: The response of northern hemisphere extratropical climate and vegetation to orbitally induced changes in insolation during the last interglaciation. *Quaternary Research* **43**(2), 174-184.
- Harrison**, S., Braconnot, P., Hewitt, C., and Stouffer, R. J., 2002: Fourth International Workshop of the Palaeoclimate Modelling Inter- comparison Project (PMIP): Launching PMIP Phase II., *EOS* **83**, 447-447.
- Haywood**, A.M. and Valdes, P.J., 2004: Modeling Pliocene warmth: contribution of atmosphere, oceans and cryosphere. *Earth and Planetary Science Letters* **218** 363-377.
- Haywood**, A.M. and Valdes, P.J., 2006: Vegetation cover in a warmer world simulated using a dynamic global vegetation model for the Mid-Pliocene. *Palaeogeography, Palaeoclimatology, Palaeoecology* **237**, 412-427.
- Haywood**, A.M., P. Dekens, A.C. Ravelo, and M. Williams, 2005: Warmer tropics during the mid-Pliocene? Evidence from alkenone paleothermometry and a fully coupled ocean-atmosphere GCM. *Geochemistry, Geophysics, Geosystems*, **6**, Q03010, doi:10.1029/2004GC000799
- Helmke**, J.P. and Bauch, H.A., 2003: Comparison of glacial and interglacial conditions

- 3353 between the polar and subpolar North Atlantic region over the last five climatic
3354 cycles. *Paleoceanograph* **18:2** 1036, doi:10.1029/2002PA000794, 2003
3355
- 3356 **Henrich** R. and K.-H. Baumann, 1994: Evolution of the Norwegian current and the
3357 Scandinavian ice sheets during the past 2.6 m.y.: evidence from ODP Leg 104
3358 biogenic carbonate and terrigenous records. *Palaeogeography,*
3359 *Palaeoclimatology, Palaeoecology* **108** 75–94.
3360
- 3361 **Herbert**, T.D., 2003: *Alkenone paleotemperature determinations*. In: *Treatise in Marine*
3362 *Geochemistry* [Elderfield, H. and K.K. Turekian (eds.)]. Elsevier, Amsterdam, p.
3363 391-432.
3364
- 3365 **Heusser**, L. and Morley, J., 1996: Pliocene climate of Japan and environs between 4.8
3366 and 2.8 Ma: a joint pollen and marine faunal study. *Marine Micropaleontology*
3367 **27:1/4** 6-106
3368
- 3369 **Hewitt**, C.D. and J.F.B. Mitchell, 1998: A Fully Coupled GCM Simulation of the
3370 Climate of the Mid-Holocene, *Geophysical. Research. Letters* **25**, 361-364.
3371
- 3372 **Hoffmann**, G., M. Werner, and M. Heimann, 1998: Water isotope module of the
3373 ECHAM atmospheric general circulation model—A study on timescales from
3374 days to several years. *Journal of Geophysical Research*, **103**, 16,871-16,896.
3375
- 3376 **Holland**, M.M. and C.M. Bitz, 2003: Polar amplification of climate change in coupled
3377 models. *Climate Dynamics*, **21**, 221-232.
3378
- 3379 **Holland**, M.H., C.M., Bitz, and B. Tremblay, 2006a: Future abrupt reductions in the
3380 summer Arctic sea ice. *Geophysical Research Letters*, **33**, L23503,
3381 doi:10.1029/2006GL028024.
3382

- 3383 **Huber, C.**, M. Leuenberger, R. Spahni, J. Flückiger, J. Schwander, T. F. Stocker, S.
3384 Johnsen, A. Landals, and J. Jouzel, 2006: Isotope calibrated Greenland
3385 temperature record over Marine Isotope Stage 3 and its relation to CH₄. *Earth*
3386 *and Planetary Science Letters*, **243**, 504-519.
- 3387
- 3388 **Hughen, K.**, J. Overpeck, R.F. Anderson, K.M. and Williams, 1996: The potential for
3389 palaeoclimate records from varved Arctic lake sediments: Baffin Island, Eastern
3390 Canadian Arctic. In: *Lacustrine Environments. Palaeoclimatology and*
3391 *Palaeoceanography from Laminated Sediments* [Kemp, A.E.S. (ed.)], Geological
3392 Society, London, Special Publications 116, pp. 57-71.
- 3393
- 3394 **Hughes, M.K.** and H.F. Diaz, 1994: Was there a 'Medieval Warm Period' and if so,
3395 where and when? *Journal of Climatic Change*, **265**, 109-142.
- 3396
- 3397 **Hyvärinen, H.**, 1976: Flandrian pollen deposition rates and tree-line history in northern
3398 Fennoscandia. *Boreas* **5:3** 163-175.
- 3399
- 3400 **Ilyashuk, E.A.**, B.P. Ilyashuk, D. Hammarlund, and I. Larocque, 2005: Holocene climatic
3401 and environmental changes inferred from midge records (Diptera: Chironomidae,
3402 Chaoboridae, Ceratopogonidae) at Lake Berkut, southern Kola Peninsula, Russia.
3403 *Holocene*, **15**, 897-914.
- 3404
- 3405 **Imbrie, J.**, and N.G. Kipp, 1971: A new micropaleontological method for Quantitative
3406 Paleoclimatology: Application to a late Pleistocene Caribbean Core, In: *The Late*
3407 *Cenozoic Glacial Ages*. [K.K. Turekian, (ed.)], Yale Univ. Press, New Haven,
3408 CT, pp. 71-181.
- 3409
- 3410 **Imbrie, J.**, A. Berger, E.A. Boyle, S.C. Clemens, A. Duffy, W.R. Howard, G. Kukla, J.
3411 Kutzbach, D.G. Martinson, A. McIntyre, A.C. Mix, B. Molino, J.J. Morley, L.C.
3412 Peterson, N.G. Pisias, W.L. Prell, M.E. Raymo, N.J. Shackleton, and J.R.

- 3413 Toggweiler. 1993: On the structure and origin of major glaciation cycles. 2. The
3414 100,000-year cycle. *Paleoceanography*, **8**, 699-735.
3415
- 3416 **IPCC**, 1990: *Climate Change: The IPCC scientific assessment* [J.T. Houghton, G.J.
3417 Jenkins, and J.J. Ephraums, eds.], Cambridge University Press, Cambridge.
3418
- 3419 **IPCC**, 2007: Summary for Policymakers. In: *Climate Change 2007: The Physical*
3420 *Science Basis. Contribution of Working Group I to the Fourth Assessment Report*
3421 *of the Intergovernmental Panel on Climate Change* [Solomon, S., D. Qin, M.
3422 Manning, Z. Chen, M. Marquis, K.B. Averyt, M. Tignor and H.L. Miller (eds.)].
3423 Cambridge University Press, Cambridge, United Kingdom and New York, NY,
3424 USA. 996 pp.
3425
- 3426 **Iversen J.** 1944 *Viscum, Hedera and Ilex* as climatic indicators. A contribution to the
3427 study of past-glacial temperature climate. *Geol. Fören. Förhandl.* **66**:463–483.
3428
- 3429 **Jakobsson, M.**, and Macnab, R., 2006: A comparison between GEBCO sheet 5.17 and
3430 the International Bathymetric Chart of the Arctic Ocean (IBCAO) version 1.0.
3431 *Marine Geophysical Researches* , **27** (1), 35-48.
3432
- 3433 **Jakobsson, M.**, R. Løvlie, H. Al-Hanbali, E. Arnold, J. Backman, and M. Mörrth, 2000:
3434 Manganese color cycles in Arctic Ocean sediments constrain Pleistocene
3435 chronology. *Geology*, **28**, 23-26.
3436
- 3437 **Jansen, E.**, Bleil, E., Henrich, R., Kringstad, L., Slettemark, B., 1988:
3438 Paleoenvironmental changes in the Norwegian Sea and the northeast atlantic
3439 during the last 2.8 m.y.: deep sea drilling project/ocean drilling program sites 610,
3440 642, 643 and 644. *Paleoceanography* **3** 563–581.
3441
- 3442 **Jansen, E.**, J. Overpeck, K.R. Briffa, J.-C. Duplessy, F. Joos, V. Masson-Delmotte, D.
3443 Olago, B. Otto-Bliesner, W.R. Peltier, S. Rahmstorf, R. Ramesh, D. Raynaud, D.

- 3444 Rind, O. Solomina, R. Villalba, and D. Zhang, 2007: Palaeoclimate. In: *Climate*
3445 *Change 2007—The Physical Science Basis. Contribution of Working Group I to*
3446 *the Fourth Assessment Report of the Intergovernmental Panel on Climate Change*
3447 [Solomon, S., D. Qin, M. Manning, Z. Chen, M. Marquis, K.B. Averyt, M.
3448 Tignor, and H.L. Miller (eds.)]. Cambridge University Press, Cambridge, U.K.,
3449 and New York.
- 3450
- 3451 **Jenkyns, H.C.**, A. Forster, S. Schouten, and J.S. Sinninghe Damsté, 2004: High
3452 temperatures in the Late Cretaceous Arctic Ocean. *Nature*, **432(7019)**, 888-892.
3453
- 3454 **Jennings, A.**, K. Knudsen, M. Hald, C. Hansen, and J. Andrews, 2002: A mid-Holocene
3455 shift in Arctic sea-ice variability on the East Greenland Shelf. *The Holocene*, **12**,
3456 49-58.
3457
- 3458 **Jiang D.**, H. Wang, Z. Ding, X. Lang, H. Drange, 2005: Modeling the middle Pliocene
3459 climate with a global atmospheric general circulation model, *Journal of*
3460 *Geophysical Research* 110, D14107, doi:10.1029/2004JD005639.
3461
- 3462 **Johnsen, S.**, H. Clausen, W. Dansgaard, K. Fuhrer, N. Gundestrup, C. Hammer, P.
3463 Iversen, J. Jouzel, B. Stauffer, and J. Steffensen, 1992: Irregular glacial
3464 interstadials recorded in a new Greenland ice core. *Nature*, **359**, 311-313.
3465
- 3466 **Johnsen, S.J.**, D. Dahl-Jensen, W. Dansgaard, and N. Gundestrup, 1995: Greenland
3467 palaeotemperatures derived from GRIP bore hole temperature and ice core isotope
3468 profiles. *Tellus*, **47B**, 624-629.
3469
- 3470 **Johnsen, S.J.**, W. Dansgaard, and J.W.C. White, 1989: The origin of Arctic precipitation
3471 under present and glacial conditions. *Tellus*, **41B**, 452-468.
3472
- 3473 **Jones, P.D.**, Briffa, K.R., Barnett, T.P., Tett, S.F.B., 1998: High-resolution
3474 palaeoclimatic records for the last millennium: interpretation, integration and

3475 comparison with General Circulation Model control-run temperatures. *Holocene*
3476 **8**:455–471.
3477
3478 **Jouzel, J.** , V. Masson-Delmotte, O. Cattani, G. Dreyfus, S. Falourd, G. Hoffmann, B.
3479 Minster, J. Nouet, J. M. Barnola, J. Chappellaz, H. Fischer, J. C. Gallet, S. Johnsen,
3480 M. Leuenberger, L. Loulergue, D. Luethi, H. Oerter, F. Parrenin, G. Raisbeck, D.
3481 Raynaud, A. Schilt, J. Schwander, E. Selmo, R. Souchez, R. Spahni, B. Stauffer, J. P.
3482 Steffensen, B. Stenni, T. F. Stocker, J. L. Tison, M. Werner, and E. W. Wolff, 2007:
3483 Orbital and Millennial Antarctic Climate Variability over the Past 800,000 Years.
3484 *Science* **317**, 793-796, DOI: 10.1126/science.1141038
3485
3486 **Jouzel, J.**, R.B. Alley, K.M. Cuffey, W. Dansgaard, P. Grootes, G. Hoffmann, S.J.
3487 Johnsen, R.D. Koster, D. Peel, C.A. Shuman, M. Stievenard, M. Stuiver, and J.
3488 White, 1997: Validity of the temperature reconstruction from water isotopes in ice
3489 cores. *Journal of Geophysical Research*, **102**, 26471-26487.
3490
3491 **Joynt, E.H. III** and A.P. Wolfe, 2001: Paleoenvironmental inference models from
3492 sediment diatom assemblages in Baffin Island lakes (Nunavut, Canada) and
3493 reconstruction of summer water temperature. *Canadian Journal of Fisheries and*
3494 *Aquatic Sciences*, **58**, 1222-1243.
3495
3496 **Kaakinen, A.** and M. Eronen, 2000: Holocene pollen stratigraphy indicating climatic and
3497 tree-line changes derived from a peat section at Ortino, in the Pechora lowland,
3498 northern Russia. *The Holocene*, **10**, 611-620.
3499
3500 **Kageyama, M.**, Peyron, O., Pinot, S., Tarasov, P., Guiot, J., Joussaume, S. & Ramstein,
3501 G., 2001: The Last Glacial Maximum climate over Europe and western
3502 Siberia: a PMIP comparison between models and data. *Climate Dynamics*, **17**,
3503 23–43.
3504

- Kandiano**, E.S. and H.A. Bauch, 2007: Phase relationship and surface water mass change in the Northeast Atlantic during Marine Isotope Stage 11 (MIS11). *Quaternary Research*, **68:3** 445-455
- Kaplan**, J.O., N.H. Bigelow, P.J. Bartlein, T.R. Christiansen, W. Cramer, S.P. Harrison, N.V. Matveyeva, A.D. McGuire, D.F. Murray, I.C. Prentice, V.Y. Razzhivin, B. Smith, D.A. Walker, P.M. Anderson, A.A. Andreev, L.B. Brubaker, M.E. Edwards, A.V. Lozhkin, and J.C. Ritchie, 2003: Climate change and arctic ecosystems II—Modeling paleodata-model comparisons, and future projections. *Journal of Geophysical Research*, **108(D19)**, Article 8171. doi:10.1029/2002JD002559.
- Kaplan**, M.R. & A.P. Wolfe, 2006: Spatial and temporal variability of Holocene temperature trends in the North Atlantic sector. *Quaternary Research* **65**: 223-231.
- Kapsner**, W.R., R.B. Alley, C.A. Shuman, S. Anandakrishnan, and P.M. Grootes, 1995: Dominant influence of atmospheric circulation on snow accumulation in Greenland over the past 18,000 years. *Nature*, **373**, 52-54.
- Karlén**, W., 1988: Scandinavian glacial and climate fluctuations during the Holocene. *Quaternary Science Reviews*, **7**, 199-209.
- Kaspar**, F., Kühl, N., Cubasch, U. and Litt, T., 2005: A model-data-comparison of European temperatures in the Eemian interglacial, *Geophysical Research Letters*, **32**: L11703, doi:10.1029/2005GL022456.
- Kaufman**, D.S. and J. Brigham-Grette, 1993: Aminostratigraphic correlations and paleotemperature implications, Pliocene-Pleistocene high sea level deposits, northwestern Alaska. *Quaternary Science Reviews*, **12**, 21-33.

- Kaufman**, D.S., T.A. Ager, N.J. Anderson, P.M. Anderson, J.T. Andrew, P.J. Bartlein, L.B. Brubaker, L.L. Coats, L.C. Cwynar, M.L. Duvall, A.S. Dyke, M.E. Edwards, W.R. Eisner, K. Gajewski, A. Geirsdóttir, F.S. Hu, A.E. Jennings, M.R. Kaplan, M.W. Kerwin, A.V. Lozhkin, G.M. MacDonald, G.H. Miller, C.J. Mock, W.W. Oswald, B.L. Otto-Bliesver, D.F. Porinchu, K. Ruüland, J.P. Smol, E.J. Steig, and B.B. Wolfe, 2004: Holocene thermal maximum in the western Arctic (0–180°W). *Quaternary Science Reviews*, **23**, 529-560.
- Kellogg**, T.B., 1977: Paleoclimatology and paleo-oceanography of the Norwegian and Greenland seas: the last 450,000 years, *Marine Micropaleontology* **2** 235–249.
- Kerwin**, M., J.T. Overpeck, R.S. Webb, A. DeVernal, D.H. Rind and R.J. Healy, 1999: The role of oceanic forcing in mid-Holocene northern hemisphere climatic change. *Paleoceanography* **14**, 200-210.
- Kirk-Davidov**, D.B., Schrag, D.P., Anderson, J.G., 2002: On the feedback of stratospheric clouds on polar climate. *Geophysical Research Letters* **29**:11, 1556.
- Kitoh**, A., and S. Murakami, 2002: Tropical Pacific Climate at the mid-Holocene and the Last Glacial Maximum simulated by a coupled ocean-atmosphere general circulation model, *Paleoceanography* **17**: 1-13
- Knutson**, T.R., Delworth, T.L., Dixon, K.W., Held, I.M., Lu, J., Ramaswamy, V., Schwarzkopf, M.D., Stenchikov, G., Stouffer, R.J., 2006: Assessment of twentieth-century regional surface temperature trends using the GFDL CM2 coupled models. *Journal of Climate*, **19**:9, 1624-1651.
- Koç**, N. and E. Jansen, 1994: Response of the high-latitude Northern Hemisphere to climate forcing—Evidence from the Nordic Seas. *Geology*, **22**, 523-526.
- Koç**, N., E. Jansen, and H. Haflidason, 1993: Paleoceanographic reconstruction of

- 3567 surface ocean conditions in the Greenland, Iceland and Norwegian Seas through
3568 the last 14 ka based on diatoms. *Quaternary Science Reviews*, **12**, 115-140.
3569
- 3570 **Koerner**, R.M., 2005: Mass Balance of glaciers in the Queen Elizabeth Islands, Nunavut,
3571 Canada. *Annals of Glaciology* **42:1** 417-423.
3572
- 3573 **Koerner**, R.M. and D.A. Fisher, 1990: A record of Holocene summer climate from a
3574 Canadian high-Arctic ice core. *Nature*, **343**, 630-631.
3575
- 3576 **Korhola**, A., H. Olander, and T. Blom, 2000: Cladoceran and chironomid assemblages as
3577 quantitative indicators of water depth in sub-Arctic Fennoscandian lakes. *Journal*
3578 *of Paleolimnology*, **24**, 43-54.
3579
- 3580 **Korty**, R.L., Emanuel, K.A., Scott, J.R. 2008: Tropical cyclone-induced upper-ocean
3581 mixing and climate: Application to equable climates. *Journal of Climate*, **21** (4),
3582 638-654.
3583
- 3584 **Kremenetski**, C.V., L.D. Sulerzhitsky, and R. Hantemirov, 1998: Holocene history of the
3585 northern range limits of some trees and shrubs in Russia. *Arctic and Alpine*
3586 *Research*, **30**, 317-333.
3587
- 3588 **Kukla**, G.J., 2000: The last interglacial. *Science* **287**, 987-988.
3589
- 3590 **Kump**, L.R. and D. Pollard, 2008: Amplification of Cretaceous Warmth by Biological
3591 Cloud Feedbacks. *Science* **11**, (5873), 195. DOI: 10.1126/science.1153883.
3592
- 3593 **Kvenvolden**, K.A., 1988: Methane hydrate—a major reservoir of carbon in the shallow
3594 geosphere? *Chemical Geology* **71**, 41-51.
3595
- 3596 **Kvenvolden**, K.A., 1993: A primer on gas hydrates. In: Howel, D.G., Editor, The Future
3597 of Energy Gases. Professional Paper- **1570**, U.S. Geological Survey, p. 279-291.
3598

- Lamb**, H.H., 1977: *Climate History and the Future. Climate—Past, Present and Future*. Metheun, London, vol. 2, 835 pp.
- Lambeck**, K., Yokoyama, Y., and Purcell, T., 2002: Into and out of the Last Glacial Maximum: sea-level change during oxygen isotope stages 3 and 2. *Quaternary Science Reviews*, **21**, 343-360
- Larocque**, I. and R.I. Hall, 2004: Holocene temperature estimates and chironomid community composition in the Abisko Valley, northern Sweden. *Quaternary Science Reviews*, **23**, 2453-2465.
- Lauritzen**, S.-E., 1996: Calibration of speleothem stable isotopes against historical records: a Holocene temperature curve for north Norway?. In: *Climatic Change: the Karst Record* [Lauritzen, S.-E. (Ed.)] Vol. 2 Karst Waters Institute Special Publication, Charles Town, West Virginia, pp. 78–80.
- Lauritzen**, S.E. and Lundberg, J., 1998: Rapid temperature variations and volcanic events during the Holocene from a Norwegian speleothem record. Past Global Changes and their Significance for the Future. Volume of Abstracts, IGBP-PAGES, Bern 00, p. 88.
- Lemke**, P., J. Ren, R.B. Alley, I. Allison, J. Carrasco, G. Flato, Y. Fujii, G. Kaser, P. Mote, R.H. Thomas, and T. Zhang, 2007: Observations: Changes in Snow, Ice and Frozen Ground. In: *Climate Change 2007: The Physical Science Basis. Contribution of Working Group I to the Fourth Assessment Report of the Intergovernmental Panel on Climate Change* [Solomon, S., D. Qin, M. Manning, Z. Chen, M. Marquis, K.B. Averyt, M. Tignor and H.L. Miller (eds.)]. Cambridge University Press, Cambridge and New York, 996 pp.
- Leng**, M.J. and J.D. Marshall, 2004: Palaeoclimate interpretation of stable isotope data from lake sediment archives. *Quaternary Science Reviews*, **23**, 811-831.

- Levac**, E., A. de Vernal, and W.J. Blake, 2001: Sea-surface conditions in northernmost Baffin Bay during the Holocene—Palynological evidence. *Journal of Quaternary Science*, **16**, 353-363.
- Levy**, L.B., D.S. Kaufman, and A. Werner, 2003: Holocene glacier fluctuations, Waskey Lake, northeastern Ahklun Mountains, southwestern Alaska. *Holocene*, **14**, 185-193.
- Ling**, F., and Zhang, T.J., 2007: Modeled impacts of changes in tundra snow thickness on ground thermal regime and heat flow to the atmosphere in Northernmost Alaska. *Global and Planetary Change* **57**:(3-4) p. 235-246.
- Lisiecki**, L.E. and M.E. Raymo, 2005: A Pliocene-Pleistocene stack of 57 globally distributed benthic $\delta^{18}\text{O}$ records. *Paleoceanography*, **20**, PA1003, doi:10.1029/2004PA001071.
- Lisiecki**, L.E. and M.E. Raymo, 2007: Plio-Pleistocene climate evolution—Trends and transitions in glacial cycle dynamics. *Quaternary Science Reviews*, **26**, 56-69.
- Loutre**, M.F., 2003: Clues from MIS 11 to predict the future climate – a modeling point of view. *Earth and Planetary Science Letters*, **212**(1-2) 213-224
- Lozhkin**, A.V. and P.M. Anderson, 1995: The last interglaciation of northeast Siberia. *Quaternary Research*, **43**, 147-158.
- Lozhkin**, A.V. and Anderson, P.M., 1996: A late Quaternary pollen record from Elikchan 4 Lake, northeast Siberia. *Geology of the Pacific Ocean*, **12**, 6-9-616.

- 3659 **Lozhkin, A.V.,** P.M. Anderson, W.R. Eisner, L.G. Ravako, D.M. Hopkins, L.B.
3660 Brubaker, P.A. Colinvaux, and M.C. Miller, 1993: Late Quaternary lacustrine
3661 pollen records from southwestern Beringia. *Quaternary Research* **9**, 314-324.
3662
- 3663 **Lozhkin, A.V.,** Anderson, P. M., Matrosova, T. V., Minyuk, P. S., 2007: The pollen
3664 record from El'gygytyn Lake: implications for vegetation and climate histories
3665 of northern Chukotka since the late middle Pleistocene. *Journal of*
3666 *Paleolimnology* **37:1** 135-153
3667
- 3668 **Lubinski, D.J.,** S.L. Forman, and G.H. Miller, 1999: Holocene glacier and climate
3669 fluctuations on Franz Josef Land, Arctic Russia, 80°N. *Quaternary Science*
3670 *Reviews*, **18**, 85-108.
3671
- 3672 **MacDonald, G.J.,** 1990: Role of methane clathrates in past and future climates.
3673 *Climatic Change*, **16(3)** 247-281.
3674
- 3675 **MacDonald, G.M.,** Edwards, T., Moser, K. , and Pienitz, R., 1993: Rapid response of
3676 treeline vegetation and lakes to past climate warming. *Nature*, **361**, 243-246.
3677
- 3678 **MacDonald, G.M.,** Gervais, B.R., Snyder, J.A., Tarasov, G.A., and Borisova, O.K.,
3679 2000b: Radiocarbon dated *Pinus sylvestris* L. wood from beyond treeline on the
3680 Kola Peninsula, Russia. *The Holocene*, **10**, 143-147.
3681
- 3682 **MacDonald, G.M.,** Kremenetski, K.V., and Beilman, D.W., 2007: Climate change and
3683 the northern Russian treeline zone. *Philosophical Transactions of the Royal*
3684 *Society B*, doi:10.1098/rstb.2007.2200.
3685
- 3686 **MacDonald, G.M.,** Velichko, A.A. , Kremenetski, C.V., Borisova, O.K. , Goleva, A.A. ,
3687 Andreev, A.A. , Cwynar, L.C. , Riding, R.T. , Forman, S.L. , Edwards, T.W.D. ,
3688 Aravena, R. , Hammarlund, D. , Szeicz, J.M. , and Gattaulin, V.N. , 2000a:
3689 Holocene treeline history and climate change across northern Eurasia. *Quaternary*

- 3690 *Research*, **53**, 302-311.
- 3691
- 3692 **Macdonald**, R.W. and J.M. Bowers, 1996: Contaminants in the arctic marine
3693 environment: priorities for protection. *ICES Journal of Marine Science* **53**: 537-
3694 563
- 3695
- 3696 **McManus**, J.F., 2004: A great grand-daddy of ice cores. *Nature* **429**, 611-612.
- 3697
- 3698 **Manabe**, S. and R.J. Stouffer, 1980: Sensitivity of a global climate model to an increase
3699 of CO₂ in the atmosphere. *Journal of Geophysical Research*, **85(C10)**, 5529-5554.
- 3700
- 3701 **Mann**, M. E., Bradley, R. S. and M. K. Hughes, 1998: Global-scale temperature
3702 patterns and climate forcing over the past six centuries. *Nature* **392**, 779– 787.
- 3703
- 3704 **Mann**, D.H., Peteet, D.M., Reanier, R.E., and Kunz, M.L., 2002: Responses of an arctic
3705 landscape to Late glacial and early Holocene climatic changes: The importance of
3706 moisture: *Quaternary Science Reviews*, **21**, 997–1021, doi: 10.1016/S0277-
3707 3791(01)00116-0.
- 3708
- 3709 **Mann**, M.E., and Jones, P.D., 2003: Global surface temperatures over the past two
3710 millennia. *Geophysical Research Letters*, **30**:15, 1820,
3711 doi:10.1029/2003GL017814
- 3712
- 3713 **Marchant**, D. R., and G. H. Denton, 1996: Miocene and Pliocene paleoclimate of the
3714 Dry Valleys region, southern Victoria Land: A geomorphological approach,
3715 *Marine Micropaleontology* **27** 253– 271.
- 3716
- 3717 **Marincovitch**, L. Jr. and Gladenkov, A.Y., 2000: New evidence for the age of Bering
3718 Strait. *Quaternary Science Reviews* **20** (1-3) 329-335
- 3719
- 3720 **Marlowe** IT, Green JC, Neal AC, Brassell SC, Eglinton G, Course PA, 1984: Long-chain

- 3721 (N-C37-C39) alkenones in the prymnesiophyceae - distribution of alkenones and
3722 other lipids and their taxonomic significance. *British Phycological Journal* **19:3**
3723 203-216
3724
- 3725 **Marotzke, J.**, 2000: Abrupt climate change and thermohaline circulation—Mechanisms
3726 and predictability. *Proceedings of the National Academy of Sciences, U.S.A.*,
3727 **97(4)**, 1347-1350.
3728
- 3729 **Marshall, S.J.**, Clark, P.U., 2002: Basal temperature evolution of North American ice
3730 sheets and implications for the 100-kyr cycle. *Geophysical Research Letters*, **29**
3731 (24) Article Number: 2214.
3732
- 3733 **Martinson, D.G.** and M. Steele, 2001: Future of the Arctic sea ice cover—Implications
3734 of an Antarctic analog. *Geophysical Research Letters*, **28**, 307-310.
3735
- 3736 **Masson-Delmotte, V.**, J. Jouzel, A. Landais, M. Stievenard, S.J. Johnsen, J.W.C. White,
3737 M.A. Werner, A. Sveinbjornsdottir, and K. Fuhrer, 2005: GRIP deuterium excess
3738 reveals rapid and orbital-scale changes in Greenland moisture origin. *Science*,
3739 **309**, 118-121
3740
- 3741 **Mathieu, R.**, D. Pollard, J.E. Cole, J.W.C. White, R.S. Webb, and S.L. Thompson, 2002:
3742 Simulation of stable water isotope variations by the GENESIS GCM for modern
3743 conditions. *Journal of Geophysical Research*, **107**, doi:10.1029/2001JD900255.
3744
- 3745 **Matthews, J.V., Jr.**, C.E. Schweger, and J. Janssens, 1990: The last (Koy-Yukon)
3746 interglaciation in the northern Yukon—Evidence from unit 4 at Chijee's Bluff,
3747 Bluefish Basin. *Geographie physique et Quaternaire*, **44**, 341-362.
3748
- 3749 **Mayewski, P.A.**, L.D., Meeker, M.S. Twickler, S.I. Whitlow, Q. Yang, W.B. Lyons, and
3750 M. Prentice, 1997: Major features and forcing of high-latitude Northern
3751 Hemisphere atmospheric circulation using a 110,000-year-long glaciochemical

- series. *Journal of Geophysical Research*, **102**, 26,345-26,366.
- McGhee**, R., 2004: The last imaginary place; a human history of the Arctic world. Key Porter, Ontario, 296 pp.
- McKenna**, M.C., 1980. Eocene paleolatitude, climate and mammals of Ellesmere Island, *Paleogeography, Paleoclimatology and Paleoecology*, **30**, 349-362.
- McLaughlin**, F., E. Carmack, R. Macdonald, A. J. Weaver, and J. Smith, 2002: The Canada Basin, 1989–1995—Upstream events and far-field effects of the Barents Sea. *Journal of Geophysical Research*, **107**(C7), 3082, doi:10.1029/2001JC000904.
- Meehl**, G.A., T.F. Stocker, W.D. Collins, P. Friedlingstein, A.T. Gaye, J.M. Gregory, A. Kitoh, R. Knutti, J.M. Murphy, A. Noda, S.C.B. Raper, I.G. Watterson, A.J. Weaver and Z.-C. Zhao, 2007: Global Climate Projections. In: *Climate Change 2007: The Physical Science Basis. Contribution of Working Group I to the Fourth Assessment Report of the Intergovernmental Panel on Climate Change* [Solomon, S., D. Qin, M. Manning, Z. Chen, M. Marquis, K.B. Averyt, M. Tignor and H.L. Miller (eds.)]. Cambridge University Press, Cambridge, United Kingdom and New York, NY, USA. pp. 747-845.
- Meeker**, L.D. and P.A. Mayewski, 2002: A 1400-year high-resolution record of atmospheric circulation over the North Atlantic and Asia. *Holocene*, **12**, 257-266.
- Meier**, M.F., M.B. Dyurgerov, U. K. Rick, S. O'Neel, W. T. Pfeffer, R. S. Anderson, S. P. Anderson, A. F. Glazovsky, 2007: Glaciers Dominate Eustatic Sea-Level Rise in the 21st Century. *Science* **317**:5841, 1064 – 1067 doi: 10.1126/science.1143906
- Miller**, G.H., A.P. Wolfe, J.P. Briner, P.E. Sauer, and A. Nesje, 2005: Holocene glaciation and climate evolution of Baffin Island, Arctic Canada. *Quaternary*

- 3783 *Science Reviews*, **24**, 1703-1721.
- 3784
- 3785 **Moberg**, A., Sonechkin, D.M., Holmgren, K., Datsenko, N.M., Karlen, W., 2005:
- 3786 Highly variable northern hemisphere temperatures reconstructed from low- and
- 3787 high-resolution proxy data. *Nature*, **433**:613–617.
- 3788
- 3789 **Montoya**, M. von Storch, H., and Crowley, T.J. 2000: Climate Simulation for 125 kyr
- 3790 BP with a Coupled Ocean–Atmosphere General Circulation Model. *Journal of*
- 3791 *Climate* **13**, 1057–1072.
- 3792
- 3793 **Moran**, K., J. Backman, H. Brinkhuis, S.C. Clemens, T. Cronin, G.R. Dickens, F.
- 3794 Eynaud, J. Gattacceca, M. Jakobsson, R.W. Jordan, M. Kaminski, J. King, N.
- 3795 Koc, A. Krylov, N. Martinez, J. Matthiessen, D. McInroy, T.C. Moore, J.
- 3796 Onodera, M. O'Regan, H. Palike, B. Rea, D. Rio, T. Sakamoto, D.C. Smith, R.
- 3797 Stein, K. St. John, I. Suto, N. Suzuki, K. Takahashi, M. Watanabe, M. Yamamoto,
- 3798 J. Farrell, M. Frank, P. Kubik, W. Jokat and Y. Kristoffersen, 2006: The Cenozoic
- 3799 palaeoenvironment of the Arctic Ocean. *Nature*, **441**, 601-605.
- 3800
- 3801 **Morison**, J., Aagaard, K., Steele, M., 2000: Recent environmental changes in the arctic,
- 3802 *Arctic*, **53** (4), p. 359-371.
- 3803
- 3804 **Muhs**, D.R. and Budahn, J.R., 2006: Geochemical evidence for the origin of late
- 3805 Quaternary loess in central Alaska, *Canadian Journal of Earth Science* **43**, 323-
- 3806 337
- 3807
- 3808 **Muller**, P.J., G. Kirst, G. Ruhland, I. von Storch, and A. Rossell-Mele, 1998: Calibration
- 3809 of the alkenone paleotemperature index U₃₇ based on core-tops from the
- 3810 eastern South Atlantic and the global ocean (60°N–60°S). *Geochimica et*
- 3811 *Cosmochimica Acta*, **62**, 1757-1772.
- 3812

- National Research Council**, 2006: Surface Temperature Reconstructions for the Last 2,000 Years. National Academies Press, Washington, DC. 160pp.
- Naurzbaev**, M.M., E.A. Vaganov, O.V. Sidorova, and F.H. Schweingruber, 2002: Summer temperatures in eastern Taimyr inferred from a 2427-year late-Holocene tree-ring chronology and earlier floating series. *The Holocene*, **12**, 727-736.
- Nelson**, R.E., and Carter, L.D. 1991. Preliminary interpretation of vegetation and paleoclimate in northern Alaska during the late Pliocene Colvillian marine transgression. In: *Geologic studies in Alaska* [Bradley, D.C., and Ford, A.B., (eds.)] U.S.Geological Survey Bulletin 1999, pp. 219-222.
- Nesje**, A. , Matthews, J.A., Dahl, S.O., Berrisford, M.S. and C. Andersson, 2001: Holocene glacier fluctuations of Flatebreen and winter precipitation changes in the Jostedalbreen region, western Norway, based on glaciolacustrine records. *The Holocene* **11** 267–280.
- Nesje**, A., J. Bakke, S.O. Dahl, O. Lie, and J.A. Matthews, 2008: Norwegian mountain glaciers in the past, present and future. *Global and Planetary Change*, **60**, 10-27.
- Nørgaard-Pedersen**, N., N. Mikkelsen, and Y. Kristoffersen, 2007b: Arctic Ocean record of last two glacial-interglacial cycles off North Greenland/Ellesmere Island—Implications for glacial history. *Marine Geology*, **244(2007)**, 93-108.
- Nørgaard-Pedersen**, N., N. Mikkelsen, S.J. Lassen, Y. Kristoffersen, and E. Sheldon, 2007a: Reduced sea ice concentrations in the Arctic Ocean during the last interglacial period revealed by sediment cores off northern Greenland. *Paleoceanography*, **22**, PA1218. doi:10.1029/2006PA001283.
- Nørgaard-Pedersen**, N., R.F. Spielhagen, H. Erlenkeuser, P.M. Grootes, J. Heinemeier,

- 3843 and J. Knies, 2003: The Arctic Ocean during the Last Glacial Maximum—
3844 Atlantic and polar domains of surface water mass distribution and ice cover.
3845 *Paleoceanography*, **18**, 8-1 to 8-19.
3846
- 3847 **Nørgaard-Pedersen**, N., R.F. Spielhagen, J. Thiede, and H. Kassens, 1998: Central
3848 Arctic surface ocean environment during the past 80,000 years.
3849 *Paleoceanography*, **13**, 193-204.
3850
- 3851 **Nürnberg**, D., Tiedemann, R., 2004: Environmental changes in the Sea of Okhotsk
3852 during the last 1.1 million years. *Paleoceanography* **19**, PA4011.
- 3853 **O'Brien**, S.R., Mayewski, P.A., Meeker, L.D., Meese, D.A., Twickler, M.S., Whitlow,
3854 S.I., 1995: Complexity of Holocene climate as reconstructed from a Greenland ice
3855 core. *Science* **270**, 1962-1964.
3856
- 3857 **Obata**, A., 2007: Climate-carbon cycle model response to freshwater discharge
3858 into the North Atlantic. *Journal of Climate* **20:24** p. 5962-5976.
3859
- 3860 **Ogilvie**, A. E. J., and Jónsson, T., 2001: "Little Ice Age" Research: A Perspective from
3861 Iceland. *Climate Change* **48**, 9-52.
3862
- 3863 **Ogilvie**, A.E.J. and Jónsdóttir, I. 2000. Sea ice, climate and Icelandic fisheries in
3864 historical times, *Arctic* **53** (4), 383-394.
3865
- 3866 **Ohkouchi**, N., T.I. Eglinton, L.D. Keigwin, and J.M. Hayes, 2002: Spatial and temporal
3867 offsets between proxy records in a sediment drift. *Science*, **298**, 1224-1227.
3868
- 3869 **Oswald**, W.W., Brubaker, L.B., Anderson, P.M., 1999, Late Quaternary vegetational
3870 history of the Howard Pass area, northwestern Alaska, *Canadian Journal of*
3871 *Botany* **77** (4): 570-581
3872

- 3873 **Oswald, W.W., L.B. Brubaker, F.S. Hu, and G.W. Kling, 2003: Holocene pollen records**
3874 **from the central Arctic Foothills, northern Alaska—Testing the role of substrate**
3875 **in the response of tundra to climate change. *Journal of Ecology*, **91**, 1034-1048**
3876
- 3877 **Otto-Bliesner, B.L., Hewitt, C.D., Marchitto, T.M., Brady, E., Abe-Ouchi, A., Crucifix,**
3878 **M., Murakami, S. and Weber, S.L., 2007: Last Glacial Maximum ocean**
3879 **thermohaline circulation: PMIP2model inter-comparisons and data constraints.**
3880 ***Geophysical Research Letters*, **34**: L12706, doi:10.1029/2007GL029475.**
3881
- 3882 **Otto-Bliesner, B.L., S.J. Marshall, J.T. Overpeck, G.H. Miller, A. Hu, and CAPE Last**
3883 **Interglacial Project members, 2006, Simulating Arctic climate warmth and icefield**
3884 **retreat in the Last Interglaciation. *Science*, **311**, 1751-1753. DOI:**
3885 **10.1126/science.1120808**
3886
- 3887 **Overpeck, J., K. Hughen, D. Hardy, R. Bradley, R. Case, M. Douglas, B. Finney, K.**
3888 **Gajewski, C. Jacoby, A. Jennings, S. Lamoureux, A. Lasca, G. MacDonald, J.**
3889 **Moore, M. Retelle, S. Smith, A. Wolfe, and G. Zielinski, 1997: Arctic**
3890 **environmental change of the last four centuries. *Science*, **278**, 1251-1256.**
3891
- 3892 **Pagani, M., Caldeira, K., Archer, D. Zachos, J.C., 2006: An Ancient Carbon Mystery.**
3893 ***Science* **314**: 1556 – 1557 DOI: 10.1126/science.1136110**
3894
- 3895 **Peterson, B.J., J. McClelland, R. Murry, R.M. Holmes, J.E. Walsh, and K. Aagaard,**
3896 **2006: Trajectory shifts in the Arctic and subarctic freshwater cycle. *Science*, **313**,**
3897 **1061-1066.**
3898
- 3899 **Peterson, B.J., R.M. Holmes, J.W. McClelland, C.J. Vorosmarty, R.B. Lammers, A.I.**
3900 **Shiklomanov, I.A. Shiklomanov, and S. Rahmstorf, 2002: Increasing river**
3901 **discharge to the Arctic Ocean. *Science*, **298**, 2171-2173.**

- Pienitz**, R. and Smol, J.P., 1993: Diatom assemblages and their relationship to environmental variables in lakes from the boreal forest-tundra ecotone near Yellowknife, Northwest-Territories, Canada. *Hydrobiologia* **269** 391-404.
- Pienitz**, R., M.S.V. Douglas, and J.P. Smol (eds.), 2004: *Long-Term Environmental Change in Arctic and Antarctic Lakes*. Dordrecht, Germany: Springer, 579 pp.
- Pienitz**, R., Smol, J.P., Last, W.M., Leavitt, P.R., Cumming, B.F., 2000: Multi-proxy Holocene palaeoclimatic record from a saline lake in the Canadian Subarctic. *The Holocene* **10:6** No. 6, 673-686 DOI: 10.1191/09596830094935
- Pierrehumbert**, R.T., H. Brogniez, and R. Roca, 2007: On the relative humidity of the atmosphere. In: *The Global Circulation of the Atmosphere* [Schneider, T. and A. Sobel (eds.)]. Princeton University Press, Princeton, New Jersey, pp.143-185.
- Peixoto**, J.P. and A.H. Oort, 1992: *Physics of Climate*. American Institute of Physics, New York, 520 pp.
- Pinot**, S., Ramstein, G., Harrison, S. P., Prentice, I. C., Guiot, J., Stute. M. & Joussaume, S., 1999: Tropical paleoclimates of the Last Glacial Maximum: comparison of Paleoclimate Modelling Intercomparison Project (PMIP) simulations and paleodata. *Climate Dynamics*,. **15**, 857–874.
- Pisaric**, M. F. J., MacDonald, G. M., Velichko, A. A., Cwynar, L. C., 2001: The late-glacial and post-glacial vegetation history of the northwestern limits of Beringia, from pollen, stomates and tree stump evidence. *Quaternary Science Reviews* **20**: 235–245.
- Pollard**, D. & Thompson, S. L., 1997: Climate and ice-sheet mass balance at the Last Glacial Maximum from the GENESIS Version 2 global climate model.

- 3933 *Quaternary Science Reviews*, **16**, 841–864
- 3934
- 3935 **Polyak, L.**, W.B. Curry, D.A. Darby, J. Bischof, and T.M. Cronin, 2004: Contrasting
- 3936 glacial/interglacial regimes in the western Arctic Ocean as exemplified by a
- 3937 sedimentary record from the Mendeleev Ridge. *Palaeogeography,*
- 3938 *Palaeoclimatology, Palaeoecology*, **203**, 73-93.
- 3939
- 3940 **Porter, S.C.** and G.H. Denton, 1967: Chronology of neoglaciation. *American Journal of*
- 3941 *Science*, **165**, 177-210.
- 3942
- 3943 **Poulsen, C.J.**, Barron, E.J., Peterson, W.H., Wilson, P.A., 1999: A reinterpretation of
- 3944 mid-Cretaceous shallow marine temperatures through model-data comparison.
- 3945 *Paleoceanography* **14:6** 679-697
- 3946
- 3947 **Prahl, F.G.**, G.J. de Lange, M. Lyle, and M.A. Sparrow, 1989: Post-depositional stability
- 3948 of long-chain alkenones under contrasting redox conditions. *Nature*, **341**, 434-
- 3949 437.
- 3950
- 3951 **Prahl, F.G.**, L.A. Muelhausen, and D.L. Zahnle, 1988: Further evaluation of long-chain
- 3952 alkenones as indicators of paleoceanographic conditions. *Geochimica et*
- 3953 *Cosmochimica Acta*, **52**, 2303-2310.
- 3954
- 3955 **Prentice, I.C.** and T. Webb III, 1998: BIOME 6000—Reconstructing global mid-
- 3956 Holocene vegetation patterns from palaeoecological records. *Journal of*
- 3957 *Biogeography*, **25**, 997-1005.
- 3958
- 3959 **Rahmstorf, S.**, 1996: On the freshwater forcing and transport of the Atlantic
- 3960 thermohaline circulation. *Climate Dynamics*, **12**, 799-811
- 3961
- 3962 **Rahmstorf, S.**, 2002: Ocean circulation and climate during the past 120,000 years.

- 3963 *Nature*, **419**, 207-214.
- 3964
- 3965 **Rasmussen**, S.O., K.K. Andersen, A.M. Svensson, J.P. Steffensen, B.M. Vinther, H.B.
- 3966 Clausen, M.L. Siggaard-Andersen, S.J. Johnsen, L.B. Larsen, D. Dahl-Jensen, M.
- 3967 Bigler, R. Rothlisberger, H. Fischer, K. Goto-Azuma, M.E. Hansson, and U.
- 3968 Ruth, 2006: A new Greenland ice core chronology for the last glacial termination.
- 3969 *Journal of Geophysical Research*, **111**, D061202, doi:10.1029/2005JD006079.
- 3970
- 3971 **Raymo**, M.E., 1994: The initiation of northern hemisphere glaciation. *Annual Review of*
- 3972 *Earth and Planetary Sciences* **22** 353-383.
- 3973 doi:10.1146/annurev.earth.22.050194.002033
- 3974
- 3975 **Raymo**, M.E., B. Grant, M. Horowitz, and G.H. Rau, 1996: Mid-Pliocene warmth—
- 3976 Stronger greenhouse and stronger conveyor. *Marine Micropaleontology*, **27**, 313-
- 3977 326.
- 3978
- 3979 **Raymo**, M.E., Lisiecki, L.E., Nisancioglu, K.H., 2006: Plio-Pleistocene ice volume,
- 3980 Antarctic climate, and the global $\delta^{18}\text{O}$ record. *Science* **313**, 492-495.
- 3981
- 3982 **Raymo**, M.E., Oppo, D.W., and Curry, W., 1997: The mid-Pleistocene climate transition:
- 3983 A deep sea carbon isotopic perspective: *Paleoceanography*, **12** 546-559.
- 3984
- 3985 **Renssen**, H., Driesschaert, E., Loutre, M.F. and Fichet, T., 2006: On the importance of
- 3986 initial conditions for simulations of the Mid-Holocene climate. *Climate of the*
- 3987 *Past* **2**, 91–97.
- 3988
- 3989 **Renssen**, H., H. Goosse, T. Fichet, V. Brovkin, E. Driesschaert, and F. Wolk, 2005:
- 3990 Simulating the Holocene climate evolution at northern high latitudes using a
- 3991 coupled atmosphere–sea ice–ocean–vegetation model. *Climate Dynamics*, **24**, 23-
- 3992 43.
- 3993

- Reyes, A.V., G.C. Wiles, D.J. Smith, D.J. Barclay, S. Allen, S. Jackson, S. Larocque, S. Laxton, D. Lewis, P.E. Calkin, and J.J. Clauge, 2006:** Expansion of alpine glaciers in Pacific North America in the first millennium A.D. *Geology*, **34**, 57-60.
- Rignot, E. and R.H. Thomas, 2002:** Mass balance of polar ice sheets. *Science* **297**, 1502-1506.
- Rigor, I.G. and J.M. Wallace, 2004:** Variations in the age of Arctic sea-ice and summer sea-ice extent. *Geophysical Research Letters*, **31**, L09401, doi:10.1029/2004GL019492.
- Rimbu, N., Lohmann, G. and Grosfeld, K., 2007:** Northern Hemisphere atmospheric blocking in ice core accumulation records from northern Greenland. *Geophysical Research Letters*, **34**: L09704, doi:10.1029/2006GL029175.
- Ritchie, J.C., 1984:** *Past and Present Vegetation of the Far Northwest of Canada*. University of Toronto Press, Toronto. 251 p.
- Ritchie, J.C., L.C. Cwynar, and R.W. Spear, 1983:** Evidence from northwest Canada for an early Holocene Milankovitch thermal maximum. *Nature* **305** 126-128.
- Rivers, A.R., and Lynch, A.H., 2004:** On the influence of land cover on early Holocene climate in northern latitudes. *Journal of Geophysical Research-Atmospheres* **109**:D21 Article Number: D21114.
- Roe, G.H., Allen, M.R., 1999:** A comparison of competing explanations for the 100,000-yr ice age cycle. *Geophysical Research Letters*, **26** (15), 2259-2262.
- Rosell-Mele, A. and P. Comes, 1999:** Evidence for a warm Last Glacial Maximum in the Nordic sea or an example of shortcomings in Uk37^İ and Uk37 to estimate low sea

- surface temperature? *Paleoceanography*, **14**, 770-776.
- Rosell-Mele**, A., G. Eglinton, U. Pflaumann, and M. Sarnthein, 1995: Atlantic core top calibration of the Uk37 index as a sea-surface temperature indicator. *Geochimica et Cosmochimica Acta*, **59**, 3099-3107.
- Royer**, D.L., 2006: CO₂-forced climate thresholds during the Phanerozoic. *Geochimica et Cosmochimica Acta*, **70** (23) 5665-5675.
- Royer**, D.L., R.A. Berner, and J. Park, 2007: Climate sensitivity constrained by CO₂ concentrations over the past 420 million years. *Nature*, **446**, 530-532.
- Ruddiman**, W. F.: 2003: Insolation, Ice Sheets and Greenhouse Gases. *Quaternary Science Reviews* **22**, 1597.
- Ruddiman**, W.F., Shackleton, N.J. and McIntyre, A., 1986: North Atlantic sea-surface temperatures for the last 1.1 million years. In: *North Atlantic Paleoceanography* [Summerhayes, C.P. and Shackleton, N.J. (eds.)], Geological Society of London, Special Publication, **21**, 155–173.
- Rudels**, B., L.G. Anderson, E.P. Jones, and G. Kattner, 1996: Formation and evolution of the surface mixed layer and halocline of the Arctic Ocean. *Journal of Geophysical Research*, **101**, 8807-8821.
- Rühland**, K., A. Priesnitz, and J.P. Smol, 2003: Evidence for recent environmental changes in 50 lakes the across Canadian Arctic treeline. *Arctic, Antarctic, and Alpine Research*, **35**, 110–23.
- Salvigsen**, O., S.L. Forman, and G.H. Miller, 1992: Thermophilous mollusks on Svalbard during the Holocene and their paleoclimatic implications. *Polar Research*, **11**, 1-10.

- Salzmann**, U., Haywood, A.M., Lunt, D.J., Valdes, P.J., Hill, D.J. 2008: A new global biome reconstruction and data-model comparison for the Middle Pliocene. *Global Ecology and Biogeography* **17**:432–447.
- Sauer**, P.E., G.H. Miller, and J.T. Overpeck, 2001: Oxygen isotope ratios of organic matter in Arctic lakes as a paleoclimate proxy—Field and laboratory investigations. *Journal of Paleolimnology*, **25**, 43-64.
- Schauer**, U., B. Rudels, E.P. Jones, L.G. Anderson, R.D. Muench, G. Björk, J.H. Swift, V. Ivanov, and A.-M. Larsson, 2002: Confluence and redistribution of Atlantic water in the Nansen, Amundsen and Makarov basins. *Annals of Geophysics*, **20**, 257- 273.
- Schindler**, D.W. and J.P. Smol, 2006: Cumulative effects of climate warming and other human activities on freshwaters of Arctic and subarctic North America. *Ambio*, **35**, 160-68.
- Schlosser**, P., B. Ekwurzel, S. Khatiwala, B. Newton, W. Maslowski, and S. Pfirman, 2000: Tracer studies of the Arctic freshwater budget. In: *The Freshwater Budget of the Arctic Ocean* [Lewis, E.L. (ed.)]. Kluwer Academic Publishers, Norwell, Mass. pp. 453- 478.
- Schlosser**, P., R. Newton, B. Ekwurzel, S. Khatiwala, R. Mortlock, and R. Fairbanks, 2002: Decrease of river runoff in the upper waters of the Eurasian Basin, Arctic Ocean, between 1991 and 1996—Evidence from $d^{18}O$ data. *Geophysical Research Letters*, **29(9)**, 1289, doi:10.1029/ 2001GL013135.
- Schmittner**, A., 2005: Decline of the marine ecosystem caused by a reduction in the Atlantic overturning circulation. *Nature*, **434**, 628-33.

- 4087 **Schouten, S., E.C. Hopmans, and J.S.S. Damsté, 2004:** The effect of maturity and
4088 depositional redox conditions on archaeal tetraether lipid
4089 palaeothermometry. *Organic Geochemistry*, **35(5)**, 567-571
4090
- 4091 **Schulz, H., von Rad, U., and Erlenkeuser, H., 1998:** Correlation between Arabian Sea
4092 and Greenland climate oscillations of the past 110,000 year: *Nature*, **393** 54-57.
4093
- 4094 **Scott, D.B., P.J. Mudie, V. Baki, K.D. MacKinnon, and F.E. Cole, 1989:** Biostratigraphy
4095 and late Cenozoic paleoceanography of the Arctic Ocean—Foraminiferal,
4096 lithostratigraphic, and isotopic evidence. *Geological Society of America Bulletin*,
4097 **101**, 260-277.
4098
- 4099 **Seager, R., Battisti, D.S., Yin, J., Gordon, N., Naik, N., Clement, A.C., Cane, M.A.,**
4100 **2002:** Is the Gulf Stream responsible for Europe's mild winters? *Quarterly*
4101 *Journal of the Royal Meteorological Society* **128:586** p. 2563-2586
4102
- 4103 **Seppä, H., 1996:** Post-glacial dynamics of vegetation and tree-lines in the far north of
4104 Fennoscandia. *Fennia*, **174**, 1-96.
4105
- 4106 **Seppä, H. and H.J.B. Birks, 2001:** July mean temperature and annual precipitation trends
4107 during the Holocene in the Fennoscandian tree-line area—Pollen-based climate
4108 reconstructions. *The Holocene*, **11**, 527-539.
4109
- 4110 **Seppä, H. and H.J.B. Birks, 2002:** Holocene climate reconstructions from the
4111 Fennoscandian tree-line area based on pollen data from Toskaljavri. *Quaternary*
4112 *Research*, **57**, 191-199.
4113
- 4114 **Seppä, H. and Hammarlund, D., 2000:** Pollen-stratigraphical evidence of Holocene
4115 hydrological change in northern Fennoscandia supported by independent isotopic
4116 data. *Journal of Paleolimnology* **24:1** 69-79

- 4117
4118 **Seppä, H., H.J.B. Birks, A. Odland, A. Poska, and S. Veski, 2004:** A modern pollen-
4119 climate calibration set from northern Europe—Developing and testing a tool for
4120 palaeoclimatological reconstructions. *Journal of Biogeography*, **31**, 251-267.
4121
4122 **Seppä, H., L.C. Cwynar, and G.M. MacDonald, 2003:** Post-glacial vegetation
4123 reconstruction and a possible 8200 cal. Yr BP event from the low arctic of
4124 continental Nunavut, Canada. *Journal of Quaternary Science*, **18**, 621-629.
4125
4126 **Serreze, M.C. and J.A. Francis, 2006:** The Arctic amplification debate. *Climatic Change*,
4127 **76**, 241-264.
4128
4129 **Serreze, M.C., A.P. Barrett, A.J. Slater, M. Steele, J. Zhang, and K.E. Trenberth, 2007a:**
4130 The large-scale energy budget of the Arctic. *Journal of Geophysical Research*,
4131 **112**, D11122, doi:10.1029/2006JD008230.
4132
4133 **Serreze, M.C., Barrett, A.P., Slater, A.G., Woodgate, R.A., Aagaard, K., Lammers, R.B.,**
4134 **Steele, M., Moritz, R., Meredith, M., Lee, C.M., 2006:** The large-scale freshwater
4135 cycle of the Arctic, *Journal of Geophysical Research-Oceans*, **111**: C11 C11010
4136
4137 **Serreze, M.C., M.M. Holland, and J. Stroeve, 2007b:** Perspectives on the Arctic's
4138 shrinking sea ice cover. *Science*, **315**, 1533-1536.
4139
4140 **Severinghaus, J.P., and E.J. Brook, 1999:** Abrupt climate change at the end of the last
4141 glacial period inferred from trapped air in polar ice. *Science*, **286**, 930-934.
4142
4143 **Severinghaus, J.P., T. Sowers, E.J. Brook, R.B. Alley and M.L. Bender. 1998:** Timing
4144 of abrupt climate change at the end of the Younger Dryas interval from thermally
4145 fractionated gases in polar ice. *Nature*, **391**(6663), 141-146.
4146

Sewall, J.O. and L.C. Sloan, 2004: Disappearing Arctic sea ice reduces available water in the American west. *Geophysical Research Letters*, **31**, doi:10.1029/2003GL019133.

Sewall, J.O., Sloan, L.C., 2001: Equable Paleogene climates: The result of a stable, positive Arctic Oscillation? *Geophysical Research Letters*, **28** (19) 3693-3695.

Shackleton, N.J., 1967: Oxygen isotope analyses and paleotemperatures reassessed. *Nature*, **215**, 15-17.

Shackleton, N.J., 1974: Attainment of isotopic equilibrium between ocean water and the benthonic foraminifera genus *Uvigerina*—Isotopic changes in the ocean during the last glacial. *Coll. Int. du CNRS*, **219**, 203-209.

Shellito, C. J., Sloan, L.C., and M. Huber, 2003: Climate model sensitivity to atmospheric CO₂ levels in the early-middle Paleogene. *Palaeogeography, Palaeoclimatology, Palaeoecology*, **193**, 113-123.

Shindell, D.T., G.A. Schmidt, M.E. Mann, D. Rind, and A. Waple, 2001: Solar forcing of regional climate change during the Maunder Minimum. *Science*, **294**, 2149-2152.

Schneider, K.B. and Faro, B., 1975: Effects of sea ice on sea otters (*Enhydra lutris*). *Journal of Mammalogy* **56** 91-101.

Shuman, C.A., R.B. Alley, S. Anandakrishnan, J.W.C. White, P.M. Grootes and C.R. Stearns, 1995: Temperature and accumulation at the Greenland Summit: comparison of high-resolution isotope profiles and satellite passive microwave brightness temperature trends. *Journal of Geophysical Research* 100(D5), 9165-9177.

- 4177 **Siegenthaler**, U., Stocker, T.F., Monnin, E., Lüthi, E., Schwander, J., Stauffer, B.,
4178 Raynaud, D., Barnola, J.M., Fischer, H., Masson-Delmotte, V., Jouzel, J., 2005:
4179 Stable carbon cycle–climate relationship during the late Pleistocene. *Science* **310**
4180 1313 – 1317. doi: 10.1126/science.1120130
4181
- 4182 **Sloan**, L.C., and Barron, E.J., 1992: A comparison of eocene climate model results to
4183 quantified paleoclimatic interpretations. *Palaeogeography, Palaeoclimatology,*
4184 *Palaeoecology* **93**(3-4) 183-202
4185
- 4186 **Sloan**, L.C., and Pollard, D., 1998: Polar stratospheric clouds: A high latitude warming
4187 mechanism in an ancient greenhouse world. *Geophysical Research Letters* **25**:18
4188 3517-3520.
4189
- 4190 **Sloan**, L., Crowley, T.J. and Pollard, D., 1996: Modeling of middle Pliocene climate
4191 with the NCAR GENESIS general circulation model, *Marine Micropaleontology*
4192 27, pp. 51–61.
4193
- 4194 **Sluijs**, A., Rohl, U., Schouten, S., Brumsack, H.J., Sangiorgi, F., Damste, J.S.S.,
4195 Brinkhuis, H., 2008: Arctic late Paleocene-early Eocene paleoenvironments with
4196 special emphasis on the Paleocene-Eocene thermal maximum (Lomonosov Ridge,
4197 Integrated Ocean Drilling Program Expedition 302). *Paleoceanography*, **23** (1),
4198 PA1S11.
4199
- 4200 **Sluijs**, A., S. Schouten, M. Pagani, M. Woltering, H. Brinkhuis, J.S.S. Damste, G.R.
4201 Dickens, M. Huber, G.J. Reichert, R. Stein, J. Matthiessen, L.J. Lourens, N.
4202 Pedentchouk, J. Backman and K. Moran, 2006: Subtropical arctic ocean temperatures
4203 during the Palaeocene/Eocene thermal maximum. *Nature*, **441**, 610-613.
4204
- 4205 **Smith**, L.C., MacDonald, G.M., Velichko, A.A., Beilman, D.W., Borisova, O.K., Frey,
4206 K.E., Kremenetski, K.V., Sheng, Y., 2004: Siberian peatlands a net carbon sink
4207 and global methane source since the early Holocene. *Science* **303**:5656 353-356

- 4208
- 4209 **Smol, J.P.**, 1988: Paleoclimate proxy data from freshwater Arctic diatoms. *Internationale*
4210 *Vereinigung für Limnologie*, **23**, 837-44.
- 4211
- 4212 **Smol, J.P.**, 2008: Pollution of lakes and rivers—A paleoenvironmental perspective,
4213 Blackwell Publishing, Oxford, U.K., 2nd ed., 280 p.
- 4214
- 4215 **Smol, J.P.** and B.F. Cumming, 2000: Tracking long-term changes in climate using algal
4216 indicators in lake sediments. *Journal of Phycology*, **36**, 986-1011.
- 4217
- 4218 **Smol, J.P.** and M.S.V. Douglas, 2007a: From controversy to consensus—Making the
4219 case for recent climatic change in the Arctic using lake sediments. *Frontiers in*
4220 *Ecology and the Environment*, **5**, 466-474
- 4221
- 4222 **Smol, J.P.** and M.S.V. Douglas, 2007b: Crossing the final ecological threshold in high
4223 Arctic ponds. *Proceedings of the National Academy of Sciences, U.S.A.*, **104**,
4224 12,395-12,397.
- 4225
- 4226 **Solovieva, N.**, P.E. Tarasov, and G.M. MacDonald, 2005: Quantitative reconstruction of
4227 Holocene climate from the Chuna Lake pollen record, Kola Peninsula, northwest
4228 Russia. *The Holocene*, **15**, 141-148.
- 4229
- 4230 **Sorvari, S.**, and Korhola, A., 1998: Recent diatom assemblage changes in subarctic Lake
4231 Saanajarvi, NW Finnish Lapland, and their paleoenvironmental implications.
4232 *Journal of Paleolimnology* **20:3** 205-215
- 4233
- 4234 **Sorvari, S.**, A. Korhola, and R. Thompson, 2002: Lake diatom response to recent Arctic
4235 warming in Finnish Lapland. *Global Change Biology*, **8**, 171-181.
- 4236

- Sowers**, T., Bender, M., Raynaud, D., 1989: Elemental and isotopic composition of occluded O₂ and N₂ in polar ice. *Journal of Geophysical Research-Atmospheres*, **94:D4** 5137-5150.
- Spencer**, M.K., R.B. Alley and J.J. Fitzpatrick, 2006: Developing a bubble number-density paleoclimatic indicator for glacier ice. *Journal of Glaciology* **52**(178), 358-364.
- Spielhagen**, R.F. and H. Erlenkeuser, 1994: Stable oxygen and carbon isotopes in planktic foraminifers from Arctic Ocean surface sediments—Reflection of the low salinity surface water layer. *Marine Geology*, **119(3/4)**, 227-250.
- Spielhagen**, R.F., G. Bonani, A. Eisenhauer, M. Frank, T. Frederichs, H. Kassens, P.W. Kubik, N. Nørgaard-Pedersen, N. R. Nowaczyk, A. Mangini, S. Schäper, R. Stein, J. Thiede, R. Tiedemann, and M. Wahsner, 1997: Arctic Ocean evidence for late Quaternary initiation of northern Eurasian ice sheets. *Geology*, **25(9)**, 783-786.
- Spielhagen**, R.F., H. Erlenkeuser, and C. Siebert, 2005: History of freshwater runoff across the Laptev Sea (Arctic) during the last deglaciation. *Global and Planetary Change*, **48(1-3)**, 187-207.
- Spielhagen**, R.F., K-H Baumann, H. Erlenkeuser, N.R. Nowaczyk, N. Nørgaard-Pedersen, C. Vogt, and D. Weiel, 2004: Arctic Ocean deep-sea record of northern Eurasian ice sheet history. *Quaternary Science Reviews*, **23(11-13)**, 1455-1483.
- Stanton-Frazee**, C. , D.A. Warnke, K. Venz, D.A. Hodell, 1999: The stage 11 problem as seen from ODP site 982, in: *Marine Oxygen Isotope Stage 11 and Associated Terrestrial Records*, [R.Z. Poore, L. Burckle, A. Droxler, W.E. McNulty (Eds.),] U.S. Geological Survey Open-file Report 99-312, 1999, p. 75.
- Steele**, M. and T. Boyd, 1998: Retreat of the cold halocline layer in the Arctic Ocean.

Journal of Geophysical Research, **103**, 10,419-10,435.

Stein, R., S.I. Nam, C. Schubert, C. Vogt, D. Fütterer, and J. Heinemeier, 1994: The last deglaciation event in the eastern central Arctic Ocean. *Science*, **264**, 692-696.

Stötter, J., M. Wastl, C. Caseldine, and T. Häberle, 1999: Holocene palaeoclimatic reconstruction in Northern Iceland—Approaches and results. *Quaternary Science Reviews*, **18**, 457-474.

Stroeve, J., Serreze, M., Drobot, S., Gearheard, S., Holland, M., Maslanik, J., Meier, W., Scambos, T., 2008: Arctic Sea Ice Extent Plummets in 2007: *EOS*, Transactions, American Geophysical Union **89**(2), 8 January, 13-14.

Sturm, M., Douglas, T., Racine, C., and Liston, G.E., 2005: Changing Snow and shrub conditions affect albedo with global implications. *Journal of Geophysical Research* **110**, G01004, doi:10.1029/2005JG000013.

Svendsen, J.I. and J. Mangerud, 1997: Holocene glacial and climatic variations on Spitsbergen, Svalbard. *The Holocene*, **7**, 45-57.

Teece, M.A., J.M. Getliff, J.W. Leftley, R.J. Parkes, and J.R. Maxwell, 1998: Microbial degradation of the marine prymnesiophyte *Emiliana huxleyi* under oxic and anoxic conditions as a model for early diagenesis—Long chain alkenones, alkenones and alkyl alkenoates. *Organic Geochemistry*, **29**, 863-880.

Thomas, D.J., Zachos, J.C., Bralower, T.J., Thomas, E., Bohaty, S., 2002: Warming the fuel for the fire: Evidence for the thermal dissociation of methane hydrate during the Paleocene-Eocene thermal maximum. *Geology*, **30**(12) 1067-1070.

Thomsen, C., D.E. Schulz-Bull, G. Petrick, and J.C. Duinker, 1998: Seasonal variability of the long-chain alkenone flux and the effect on the Uk37 index in the

- 4299 Norwegian Sea. *Organic Geochemistry*, **28**, 311-323.
- 4300
- 4301 **Troitsky**, S.L., 1964: Osnoviye zakonomernosti izmeneniya sostava fauny po
4302 razrezam morskikh meshmorenykh sloev ust-eniseyskoy vpadiny i nishne-
4303 pechorskoy depressii. *Akademia NAUK SSSR, Trudy instituta geologii i*
4304 *geofiziki* **9** 48–65 (in Russian).
- 4305
- 4306 **Vassiljev**, J., 1998: The simulated response of lakes to changes in annual and seasonal
4307 precipitation—Implication for Holocene lake-level changes in northern Europe.
4308 *Climate Dynamics*, **14**, 791-801.
- 4309
- 4310 **Vassiljev**, J., S.P. Harrison, and J. Guiot, 1998: Simulating the Holocene lake-level
4311 record of Lake Bysjon, southern Sweden. *Quaternary Research*, **49**, 62-71.
- 4312
- 4313 **Velichko**, A.A., A.A. Andreev, and V.A. Klimanov, 1997: Climate and vegetation
4314 dynamics in the tundra and forest zone during the Late Glacial and Holocene.
4315 *Quaternary International*, **41/42**, 71-96.
- 4316
- 4317 **Vinther**, B.M., H.B. Clausen, S.J. Johnsen, S.O. Rasmussen, K.K. Andersen, S.L.
4318 Buchardt, D. Dahl-Jensen, I.K. Seierstad, M.L. Siggaard-Andersen, J.P.
4319 Steffensen, A. Svensson, J. Olsen, and J. Heinemeier, 2006: A synchronized
4320 dating of three Greenland ice cores throughout the Holocene. *Journal of*
4321 *Geophysical Research*, **111**, D13102, doi:10.1029/2005JD006921.
- 4322
- 4323 **Vörösmarty**, C.J., L.D. Hinzman, B.J. Peterson, D.H. Bromwich, L.C. Hamilton,
4324 J. Morison, V.E. Romanovsky, M. Sturm, and R.S. Webb. 2001: The Hydrologic
4325 Cycle and its Role in Arctic and Global Environmental Change: A Rationale and
4326 Strategy for Synthesis Study. Fairbanks, Alaska: Arctic Research Consortium of
4327 the U.S., 84 pp.
- 4328

- Vörösmarty**, C., Hinzman, L. Pundsack, J., 2008: Introduction to special section on Changes in the Arctic Freshwater System: Identification, Attribution, and Impacts at Local and Global Scales. *Journal of Geophysical Research-Biogeosciences*. **113**(G1) Article Number: G01S91.
- Wang**, Y.J., et al., 2001: A high-resolution absolute-dated late Pleistocene monsoon record from Hulu Cave, China. *Science*, **294**, 2345–2348.
- Weaver**, A.J., C.M. Bitz, A.F. Fanning, and M.M. Holland, 1999: Thermohaline circulation—High latitude phenomena and the difference between the Pacific and Atlantic. *Annual Review of Earth and Planetary Sciences*, **27**, 231-285.
- Weckström**, J., A. Korhola, P. Erästö, and L. Holmström, 2006: Temperature patterns over the past eight centuries in northern Fennoscandia inferred from sedimentary diatoms. *Quaternary Research*, **66**, 78-86.
- Weijers**, J.W.H., S. Schouten, O.C. Spaargaren, and J.S.S. Damsté, 2006: Occurrence and distribution of tetraether membrane lipids in solid—Implications for the use of the TEX₈₆ proxy and the BIT index. *Organic Geochemistry*, **37**(12), 1680-1693.
- Weijers**, J.W.H., Schouten, S., Sluijs, A., Brinkhuis, H., Damste, J.S.S., 2007: Warm arctic continents during the Palaeocene-Eocene thermal maximum. *Earth and Planetary Science Letters*, **261** (1-2) 230-238.
- Werner**, M., U. Mikolajewicz, M. Heimann, and G. Hoffmann, 2000: Borehole versus isotope temperatures on Greenland—Seasonality does matter. *Geophysical Research Letters*, **27**, 723-726.

- Whitlock**, C. and M.R. Dawson, 1990: Pollen and vertebrates of the early Neogene Haughton Formation, Devon Island, Arctic Canada. *Arctic*, **43(4)**, 324-330.
- Wiles**, G.C., Barclay, D.J., Calkin, P.E., Lowell, T.V., 2008: Century to millennial-scale temperature variations for the last two thousand years indicated from glacial geologic records of Southern Alaska. *Global and Planetary Change*, **60**, 15–125.
- Williams**, C..J., Johnson, A.H., LePage, B.A., Vann D.R. and T. Sweda. 2003: Reconstruction of Tertiary Metasequoia Forests II. Structure, Biomass and Productivity of Eocene Floodplain Forests in the Canadian Arctic, *Paleobiology*, **29**, 271-292.
- Wohlfahrt**, J., S.P. Harrison, and P. Braconnot, 2004: Synergistic feedbacks between ocean and vegetation on mid- and high-latitude climates during the Holocene. *Climate Dynamics*, **22**, 223-238.
- Wohlfarth**, B., G. Lemdahl, S. Olsson, T. Persson, I. Snowball, J. Ising, and V. Jones, 1995: Early Holocene environment on Bjornoya (Svalbard) inferred from multidisciplinary lake sediment studies. *Polar Research*, **14**, 253-275.
- Wooller**, M.J., Francis, D., Fogel, M.L., Miller, G.H., Walker, I.R., Wolfe, A.P., 2004: Quantitative paleotemperature estimates from delta O-18 of chironomid head capsules preserved in arctic lake sediments. *Journal of Paleolimnology* **31:3** 267-274
- Wuchter**, C., S. Schouten, M.J.L. Coolen, and J.S.S. Damsté, 2005: Temperature-dependent variation in the distribution of tetraether membrane lipids of marine Crenarchaeota— Implications for TEX86 paleothermometry. *Paleoceanography*, **19(4)**, Art. No. PA4028

- 4388 **Zachos**, J.C., Dickens, G.R., Zeebe, R.E., 2008: An early Cenozoic perspective on
4389 greenhouse warming and carbon-cycle dynamics. *Nature*, **451** (7176), 279-283.
4390
- 4391 **Zachos**, Z., P. Pagani, L. Sloan, E. Thomas, and K. Billups, 2001: Trends, rhythms, and
4392 aberrations in global climate 65 Ma to present. *Science*, **292**, 686-693.
4393
- 4394 **Zazula** G.D., D.G.Froese, C.E. Schweger, R.W. Mathewes, A.B. Beaudoin, A.M. Telka,
4395 C.R. Harington, and J.A. Westgate, 2003: Ice-age steppe vegetation in east
4396 Beringia - tiny plant fossils indicate how this frozen region once sustained huge
4397 herds of mammals. *Nature* **423**: 603-603.
4398